JIMMA UNIVERSITY

JIMMA INSTITUTE OF TECHNOLOGY

SCHOOL OF CHEMICAL ENGINEERING

MSC PROGRAM IN PROCESS ENGINEERING

Green Synthesis, Characterization, and Application of Teff Straw-Assisted ZnO Nanoparticle for Removal of Methylene Blue Dye from Textile Industry Wastewater

By

Getachew Legesse

A Thesis Submitted to Jimma University Institute of Technology, School of Chemical Engineering in Partial Fulfillment of the Requirements for Degree of Master of Science in Chemical Engineering (Process Engineering)

November 2021

Jimma, Ethiopia

JIMMA UNIVERSITY

JIMMA INSTITUTE OF TECHNOLOGY

SCHOOL OF CHEMICAL ENGINEERING

This is to certify that the thesis prepared by Getachew Legesse, entitled: **"Green Synthesis, Characterization, and Application of Teff Straw-Assisted ZnO Nanoparticle for Removal of Methylene Blue Dye from Textile Industry Wastewater "** is submitted in partial fulfillment of the requirement for the degree of Master of Science in Chemical (Process Engineering) complies with the regulations of the university and meets the accepted standards concerning originality and quality.

Approved by the Examining Board:

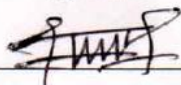Abdisa Jabesa (PhD)   30/12/2021

External Examiner   Signature   Date

Tafere Aga (Msc)   1/04/2022

Internal Examiner   Signature   Date

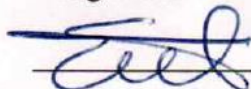Dereje Tadesse (Ass. Prof.)

Advisor   Signature   Date

Mr. Ketema Beyecha (Msc)

Chair, Process Engineering   Signature   Date

Ermias Girma (Ass. Prof.)

School dean   Signature   Date

DECLARATION

I hereby declare that thesis entitled **"Green Synthesis, Characterization, and Application of Teff Straw-Assisted ZnO Nanoparticle for Removal of Methylene Blue Dye from Textile Industry Wastewater"** is my original work, with the guidance of my advisors, and it has not been presented for a degree in Jimma University or any other University and all sources of materials that used for the proposed thesis have been duly acknowledged.

Submitted by:

Getachew Legesse   _____   _____

                                              Signature   Date

Approved by:

Dereje Tadesse (Ass. Prof.)   _____   _____

Advisor   Signature   Date

Ms. Meron Asteraye (Msc)   _____   _____

Co-advisor   Signature   Date

Ketema Beyecha (Msc)   _____   _____

Program coordinator   Signature   Date

ACKNOWLEDGEMENTS

First of all, I would like to thank the Almighty God for protection and guidance in all ways throughout my work. Secondly, I would like to thank my main advisor Dereje Tadesse (assistant professor) for his guidance and advice, understanding of attitudes and constructive suggestions, continuous support, as well as his great patience during my thesis study, and also, I would like to thank my co-advisor Ms. Meron Astraye for her generous help and suggestions, talent advice and comments on this work. I would like to convey my heartfelt gratitude to Mr. Ermias Girma, Dean School of Chemical Engineering, for his assistance, essential comments, and unending encouragement, as well as Mr. Samuel Gesesse for providing me with the drive to complete this study.Also,my thanks goes to both of Mr. Surafel Mustafa and Mr. Gadissa tokumma for their convinent advice and support. Words cannot explain how grateful I am to Mr. Firomsa B, Mr. Dafar Getahun, Mr. Bediru Miressa, Mr. Tsegay Markosi, Mr. Endariyas Adane, and Mr. Mohammed Nuri, for their laboratory technical assistance on my study. Because of their generosity, I was able to do this thesis. My thanks also go to my friends and everyone else who has contributed to the successful completion of this study. Next, I would like to express my gratitude to the administrative and laboratory technician members in the Jimma Institute of Technology (School of Chemical Engineering, School of Materials Science and Engineering, School of Civil and Environmental Engineering, Jimma University main campus lab technicians especially Mr. Dembelash Fiqiru) and Mettu University staffs, Chemistry Department Head and laboratory technicians). It is their kind help and support that made my study successful. At last, but not least, I would like to thank my family for their advice, tremendous support, and enormous understanding in all my life and work. Finally, special thanks go to my wife Zewiditu Tola who support me in both moral and economical contribution, initiation, and to all other my friends for being the source of my positive energy that enabled me to succeed.

ABSTRACT

Contamination of water resources by methylene blue dye has become a source of environmental concern because of its toxicity thus causing significant harm to human organs and having an impact on aquatic lives. Although Zinc Oxide nanoparticles synthesized by chemical and physical methods have been developed for the removal of methylene blue dye wastewater by adsorption method, Zinc Oxide nanoparticles lose reactivity towards the adsorbate, posing toxicity to the environment, instability, and agglomeration problematic. Hence, surface modified; green synthesized Zinc Oxide nanoparticles are alternative adsorbent, which form stable and alleviate agglomeration in the Zinc Oxide nanoparticles synthesis for methylene blue dye removal are required. The emphasis of this thesis is on the green synthesis, characterization, and application of Zinc oxide teff straw assisted nanoparticles for the removal of methylene blue dye from textile wastewater.Teff straw-assisted Zinc Oxide nanoparticles were synthesized by reduction of Zinc nitrate hexahydrate solution using neem leaf extract as a capping agent. The physicochemical properties of Teff straw assisted Zinc Oxide nanoparticles were characterized using, X-ray diffraction and Fourier transform-infrared spectroscopy, analysis confirmed that the surface of Zinc oxide nanoparticles was efficiently functionalized. The X-ray diffraction analysis revealed the presence of Zinc oxide in the synthesized Teff straw-assisted Zinc Oxide nanoparticles with an average crystalline size of 27.196 nm. Series adsorption experiments were conducted to examine the removal efficiency of methylene blue dye on Teff straw-assisted Zinc Oxide nanoparticles and the effect of various adsorption parameters from Textile Wastewaters. It was found that pH, the dose of Teff straw assisted Zinc Oxide nanoparticles, contact time and initial concentration affects the removal of methylene blue dye. A response surface methodology with the central composite design was used for the optimization of removal efficiency of methylene blue dye onto the adsorbent's surface. The optimal conditions selected using the design tool were 6.904 pH, 68.489 mg/L initial methylene blue dye concentration,0.265 g dosage of Teff straw assisted Zinc Oxide nanoparticles, and 77.873 min contact time providing a predicted value of 99.769 % removal efficiency and this was adequately fit into the Freundlich isotherm model with correlation coefficient of 0.99. Also, the water quality parameters in real textile wastewater were determined and its removal efficiency was 92.5%.

Keywords: *ZnO NPs, Green synthesis, Neem leaf,Teff straw, and Removal of MBD.*

TABLE OF CONTENTS

LIST OF TABLES

LIST OF FIGURES

LIST OF ABBREVIATIONS

A. Indica	Azadirachta indica
BOD	Biological oxygen demand
CNTs	Carbon nanotubes
COD	Chemical oxygen demand
Conc.	Concentration
DOE	Design of Experiment
FTIR	Fourier transform infrared spectroscopy
FWHM	Full width at half maximum [radians]
G	Graphene
GO	Graphene oxide
MNP	Metal nanoparticle
MB	Methylene blue
MBD	Methylene blue dye
MONPS	Metal oxide nanoparticles
NP	Nanoparticle
NPS	Nanoparticles
NM	Nanomaterial
RSM	Response surface methodology
SEM	Scanning electron microscope

TDS   Total Dissolved solution

TS   Total solid

TSS   Total suspended solid

TWW   Textile wastewater

TSP   Teff straw powder

WHO   World health organization

XRD   X-ray Diffractometer

ZnO NP   Zinc oxide nanoparticle

ZnO-TSA   Teff Straw Assisted Zinc oxide Nanoparticle

1. INTRODUCTION

1.1. Background

Water, which makes up two-thirds of the earth's surface, is the most basic ingredient for all life forms (Goutam et al., 2020). Contamination of water resources has increased as a result of wastewater discharged directly into the water without sufficient treatment as industry and urbanization have progressed (Gayathri et al., 2019). Environmental pollution caused by colored effluents is threatening to the world (Ahmadi et al., 2020). Textiles, rubber, paper, plastic, cosmetics, and others produce colored organic effluent (Gayathri et al., 2019). Textile industries processes are among the nearly all industries that discharge colored wastewater including dye that becomes a major environmental alarm (Mohammad Razi et al., 2017).

 As revealed by Oyewo et al. (2020), Methylene blue is the most widely used dye in the textile and printing sectors. Methylene Blue ($C_{16}H_{18}N_3CLS$) is a cationic dye that's commonly used to color cotton, wool, and silk (Moawed et al., 2019). In the chemical industry, it's also utilized as a stabilizer and an indicator. As a result, these companies' effluents include a high quantity of MB, rendering water unsuitable for both industrial and home usage (Oyewo et al., 2020). This is because MB, even at trace levels, has a considerable impact on aquatic life's photosynthetic activity. It could potentially cause significant harm to human organs, including the reproductive system, kidneys, central nervous system, brain, and liver (Rajabi et al., 2017). MB can also cause eye burns, breathing difficulties, convulsions, tachycardia, skin irritation, and vomiting, nausea, anemia, hypertension, diarrhea, and mental confusion when exposed for lengthy periods (Basnet et al., 2018). As a result, wastewater discharges containing traces of MB dye must be treated to avoid all of the hazards it causes (Basnet et al., 2018).

The World Health Organization (WHO) recommends that coloring chemicals in drinking water be limited to 1 mg L^{-1} (Sharifi & Wood., 2018). As a result, effective and functional equipment to extract MB from wastewaters is urgently needed (Seyed Hassan Sharifi & Wood, 2018). The textile industry discharged effluents into receiving water might be hazardous to marine life, and sunlight transmission is reduced through colored water. Particularly when even 1.0 mg L^{-1} of concentration of dye in water supply could be unsuitable for human intake (Getasew et al., 2019).

Different procedures, including biological, chemical, and physical processes, could be used to remove MB from wastewater. Some of these approaches have drawbacks, such as limited performance, MB non-biodegradability, and secondary waste formation, all of which cause disposal issues (Oyewo et al., 2020). Because of its simplicity, low cost, and high efficiency in removing color and other impurities, the adsorption method is frequently utilized (Ahmadi et al., 2020).

The use of nanoparticles in adsorption techniques is getting attention, and it's a potential method for removing color from textile wastewater (Yashni et al., 2020). Because of their higher surface-to-volume ratio than other adsorbents, nanoparticles have been shown to have a significant potential for adsorbing organic chemicals, particularly colors, from wastewater and sewage tanks (Ahmadi et al., 2020).

Adsorption of hazardous dyes by metal oxide nanoparticles has shown considerable promise. (Rath et al., 2019). Because of their great surface area and thermal and chemical stability, a variety of inorganic metal oxides may be useful adsorbents (Shokry et al., 2014). Because of its nontoxicity, long-term stability, affordable cost, biocompatibility, and powerful antibacterial properties against microbes often found in water, zinc oxide nanoparticle (ZnO NP) has gotten a lot of interest for water treatment (Gu et al., 2020). Chemical, physical, and biological techniques, for example, take less time to synthesize vast amounts of metal nanoparticles, but they require hazardous compounds as capping agents to ensure stability, resulting in environmental toxicity (Nithya & Kalyanasundharam, 2019). Sol-gel techniques, co-precipitation, laser vaporization, microemulsion, and ball milling are some of the physiochemical approaches that can be used to make ZnO nanoparticles (NPS). The expensive cost of equipment, the wide-area required for equipment setup, and the added usage of capping agents, stabilizers, and hazardous chemicals are all common drawbacks of these preparation procedures (N.K.Sankaranarayanan, 2021).

As a result, there is an increasing need to develop clean, non-toxic, and environmentally friendly nanoparticle synthesis procedures. Some of the distinct advantages that biological synthesis protocols have over traditional physical and chemical methods are as follows (Herlekar et al., 2014): Because no toxic chemicals are used, the method is clean and environmentally friendly; the active biological component, such as an enzyme, acts as a reducing and capping agent,

lowering the overall cost of the synthesis process; Even during large-scale production, small nanoparticles can be produced. External experimental conditions such as high energy and pressure are not required, resulting in significant energy savings. For nanoparticle synthesis, a wide variety of biological resources such as microorganisms (bacteria, yeast, fungi, algae, and viruses) and plants can be used. While microbe-based protocols have been developed as a result of the combined research efforts of several authors, plant-mediated biological synthesis of nanoparticles has only recently gained prominence. Plant extracts, as opposed to microbes, reduce metal ions in a shorter time. Nanoparticles can be synthesized in a matter of minutes or hours, depending on the plant type and concentration of phytochemicals, whereas   microorganis m-based methods take much longer (Herlekar et al., 2014). The main disadvantage of microbe-mediated nanoparticle synthesis is the requirement for aseptic conditions, which necessitates trained personnel and raises the scaling-up cost. All of these factors, combined with the ease with which plants can be found in nature, make plants preferable biological resources to microbes.

The green technique of synthesis of metal oxide (ZnO) nanoparticles is easier and safer to utilize in the development of nanomaterials, and plant-mediated production of nanoparticles using polyphenol as a reducing agent is still a new approach. Biosynthesis often called green synthesis is a technique for making NPs from plant extracts (Yashni et al., 2020). This technology produces biocompatible NPs without the use of harmful chemicals, and it is used in the production of pharmaceuticals. Green synthesis is also a more cost-effective alternative to chemical synthesis, which is quite expensive (Yashni et al., 2020).

Plants that have previously been used to synthesize ZnO NPs include Camellia sinensis (Senthilkumar & Sivakumar, 2016), Cassia fistula (Suresh et al., 2015), Aloe vera (Sangeetha et al., 2011), Solanum nigrum (Ramesh et al., 2014), Agathosma (Thema et al., 2015). In Ethiopia, neem (Azadirachta indica) is a cheap and readily available source; hence a reasercher used neem leaf extract for ZnO NP production.

Due to their large specific surface area and high reactivity, most of the atoms of Metal oxide nanoparticles (ZnO-NPS) occur on the surface of the NPS (hence, they are unstable). Because the surface atoms are not saturated, they can bind with more atoms, resulting in increased chemical activity (Sukri et al., 2021). Metal oxides can be reduced to nanosize to increase surface area, but this increase can also cause instability (Dixit & Hering, 2003). The

nanoparticles with high reactivity will be susceptible to agglomeration during the synthesis process (Khairunnisa et al., 2021). Furthermore, nanoparticles have a high aggregation tendency, which could result in a loss of adsorption efficiency (Homaeigohar, 2020). To avoid these drawbacks, metal oxides are characteristically incorporated into supports or other bulk adsorbents (Dixit & Hering, 2003).

Accordingly, to overcome these all problems in the use of zinc oxide (ZnO) NPs for methylene blue dye removal, eco-friend, and costless surface modification seeks wide investigations. Lignocellulose biomass is valued for its economic and environmental benefits, as well as its availability, renewability, and cost-effectiveness. It can be used in its natural state, as well as carbonized or chemically treated forms, to improve pollutant removal efficiency (N.K.Sankarana rayanan1, 2021). As a result, as a supporting material, it can better address some of the issues with metal oxide nanoparticles. Agricultural waste biomasses can be used to make these products. The high amount of cellulose, lignin, and other polar functional groups of lignin in lignocellulose biomass, such as alcohols, aldehydes, ketones, carboxylic, phenolic, and ether groups, improve the adsorbent binding ability of pollutants via various binding systems (N.K.San karanarayanan1, 2021).

Meanwhile, many findings of recent studies revealed the removal of methylene blue from wastewater by using adsorption techniques with different low-cost materials, such as straw-based adsorbents (Pirbazari & Saberikhah, 2014).

Teff straw, which is readily available as an agricultural waste, requires little processing and can be used as a supporting material with alternative technology (Pirbazari & Saberikhah, 2014). The physicochemical characteristics and removal efficiency of zinc oxide nanoparticles can both be improved by conforming teff straw with ZnO-NPs.

Thus, the main aim of this study was to synthesis and characterize teff straw-assisted ZnO NPs for removal of Methylene blue dye from Textile industry wastewater using the synthesized adsorbent.

1.2. Statement of the problem

Due to fast industrial growth, a diverse range of wastes are generated, which are eventually dumped into water resources, impacting the quality of water. For developing countries, this is a major worry. Because dyes can be mutagenic, carcinogenic, and allergic to people, dye contamination in water poses a risk to aquatic organisms (Tara et al., 2019). One of the most dangerous and long-lasting dyes is methylene blue (Weldegebrieal, 2020)**.** Therefore, there is a general need to remove these dyes before it is released into the water streams (Moawed et al., 2019). To remove dyes from textile industries, the convectional approach is no longer preferred in the production of nanoparticles due to many disadvantages.

Nanoparticles have been revealed to have a high potential in adsorbing organic compounds especially colors from wastewater and sewage tanks due to their high surface-to-volume ratio than other adsorbents. Several investigations on metal oxide nanoparticles for the elimination of MBD using the adsorption approach have been conducted. ZnO is the most common metal oxide nanoparticle and has been found to have a wide range of applications in the process of adsorption (Ahmadi et al., 2020). Although chemical, physical, and biological procedures for producing metal nanoparticles (ZnO-NPS) take less time, they require hazardous chemicals as capping agents to ensure stability, resulting in environmental toxicity (Nithya & Kalyanasundharam, 2019). Most of these nanoparticles lose reactivity towards the adsorbate after the adsorption of Methylene blue dye from textile effluent, posing a danger of toxicity to the environment and agglomeration problematic. Due to their large specific surface area and high reactivity, the majority of the atoms in Metal oxide nanoparticles (ZnO-NPS) occur on the surface of the NPS (hence, they are unstable). The nanoparticles with high reactivity will be susceptible to agglomer ation during the synthesis process (Khairunnisa et al., 2021). Furthermore, nanoparticles have a high aggregation tendency, which could result in a loss of adsorption efficiency (Homaeigohar, 2020). Accordingly, eco-friend surface modification is being investigated to solve all of the challenges associated with the use of zinc oxide (ZnO) NPs for methylene blue dye removal.

Meanwhile, many findings of recent studies revealed to Methylene blue removal from wastewater through utilizing adsorption techniques with a variety of low-cost materials, such as straw-based adsorbents (Pirbazari & Saberikhah, 2014). Thus, it is essential to make the best use of teff straw. Using polyphenol-based green produced teff straw assisted ZnO NPS ; several

problems associated with the usage of metal oxide nanoparticles, such as stability and agglomeration are alleviated.

Therefore, this study was focused on green synthesis, characterization, and application of teff straw-assisted ZnO nanoparticles as adsorbent for removal of Methylene blue dye from Textile industry wastewater.

1.3. Objectives

1.3.1. General objective

The main objective of this study was to synthesize and characterize teff straw-assisted ZnO nanoparticles and study it's applicability for the removal of methylene blue dye from textile industry wastewater.

1.3.2. Specific objectives

➢ To characterize the physicochemical properties of the synthesized teff straw-assisted Zinc Oxide nanoparticles.

➢ To examine the removal efficiency of Methylene blue dye on the surface of teff straw assisted Zinc Oxide nanoparticles.

➢ To study the adsorption parameters (pH, contact time, adsorbent dose, and initial concentration of methylene blue dye) on removal efficiency.

1.4. Significance of the study

The results of this study were believed to provide essential baseline information about the potential of Teff straw as support for ZnO NPs; it was contributed to the green production of ZnO NPs utilizing locally accessible Neem leaf extracts. This study resulted in a technological transfer and was also encourage researchers to investigate Ethiopian native and growing plants for usage in nanoparticle manufacturing.

1.5. The scope and limitation of the study

This study was focused on the Removal of MBD using Teff straw-assisted Zinc oxide Nanoparticles as the adsorbent.

The physicochemical properties of the synthesized ZnO-TSA nanoparticles were characterized by X-ray diffraction (XRD) and Fourier transforms infrared spectroscopy (FTIR). In addition, the effect of selected operating parameters such as pH, adsorbent dose, contact time, and initial concentration of methylene blue dye was also investigated. The challenge encountered during the experimental work of this study was the unavailability of testing materials for instance the missing of scanning electron microscopy retards the study of morphology.

<div align="center">

2. LITERATURE REVIEW

</div>

2.1. Industrialization and effluent water sources

The environment is under severe threat due to the massive amounts of industrial effluents released as as aresult of rapid industrialization (Myneni, 2020). Environmental pollution from industrial and home emissions is becoming a major issue, particularly in developing countries. (Ehssan Nassef, 2020). The textile, chemical, mining, and metallurgical industries produce the majority of the waste materials that pollute the water (Narjes Babadi, 2018). Dyes are one of the most significant toxins that pollute water systems (Ehssan Nassef, 2020). Dyes in effluents are a major source of worry because of their harmful impact on a variety of living things. The environmental discharge of dyes is a source of concern for both toxicological and aesthetic reasons (Rafatullah et al., 2010). Textile, leather, paper, plastics, and other industries employ dyes to color their goods while also consuming large amounts of water. As a result, they produce a large quantity of colored effluent (Rafatullah et al., 2010). So, it is desirable to remove colors from wastewater before it is discharged (Dong et al., 2011).

2.1.1. Dyes in the textile industry

Water is an vital component for living environment. Water contamination by various toxic pollutants has become one of the most important serious problems worldwide (Senthil Kumar et al., 2019). In today's world, environmental contamination caused by the textile industry has become a big concern (Chockalingam et al., 2019). The presence of hazardous and toxic contaminants in industrial wastewaters is one of the most significant environmental issues (Kyzas & Kostoglou, 2014). The textile industry may be found in almost every country, and their numbers are growing. The usage of synthetic complex organic dyes as a coloring source has increased dramatically in these industries. Untreated synthetic dye effluents emitted from businesses have been identified as one of the effects of society's rising water scarcity issue (Miao, 1992).

Food colouring, cosmetics, paper and textiles industries that release from effluent are impure by dyes. Allergic as eczema, skin irritation, cancer and mutation are the example of adverse result kind dye (Daud et al., 2019). This dyes found within the discharges could be a major concern caused by their adverse effects to several varieties of life as an example the marine life.

With the increased demand for textile products, the textile industry and its wastewaters have been increasing proportionally, making it one of the main bases of severe contamination problems worldwide. In particular, the discharge of coloured effluents into the environment is undesirable, not only because of their colour, but also because many dyes from wastewater and their breakdown products are toxic and/or mutagenic to life (dos Santos et al., 2007).

Water contamination as a result of anthropogenic pollution discharge is a serious problem that must be addressed to maintain water quality and a healthy ecosystem. Dyes, often known as coloring agents, are organic chemicals that adhere to the surface of a fabric to impart color (Khatoona & Prakash, 2016). Different conventional methods of color removal from wastewater have been used. These include biological and physical–chemical process (Nasuha et al., 2010).

Some biological and physical or chemical methods for removing dyes from industrial effluents have been used, such as flocculation, coagulation, precipitation, adsorption on activated carbon, membrane filtration, biosorption, electrochemical methods, oxidation/ozonation, and anaerobic/a erobic treatments. The advantages and disadvantages of various dye removal techniques from wastewaters are listed below. Among the many physicochemical methods tested, the adsorption method was the only one deemed best and superior. Some of the advantages of this method over others are as follows: low cost, readily available, simple design, biodegradability, ease of operation, high efficiency, and the ability to treat dyes in more concentrated forms (Sharifi & Shoja, 2018). The principle of adsorption treatment is dye entrapment by a solid compound. Nanoparticles have a high surface area to volume ratio, providing a greater number of active sites for pollutant species interaction and increased adsorption capacity (Nalwa et al., 2017). There are numerous advantages to using materials such as zinc oxide and magnesium oxide nanoparticles as a powerful sorbent on the surface of other adsorbents (for example, AC) (Sharifi & Shoja, 2018). This process can increase the number of sorption active sites on the adsorbent.

Textile industry wastewater contains a variety of colors and their combinations (Munjal, 2015). MB is a model cationic dye used by industries such as the textile industry for a variety of applications (Kyzas & Kostoglou, 2014). Methylene Blue has the molecular formula $C1_6H_{18}N_3Cl$ and is a heterocyclic aromatic chemical molecule. It dissociates into a cation and a chloride anion in an aqueous solution (Raizada et al., 2014).
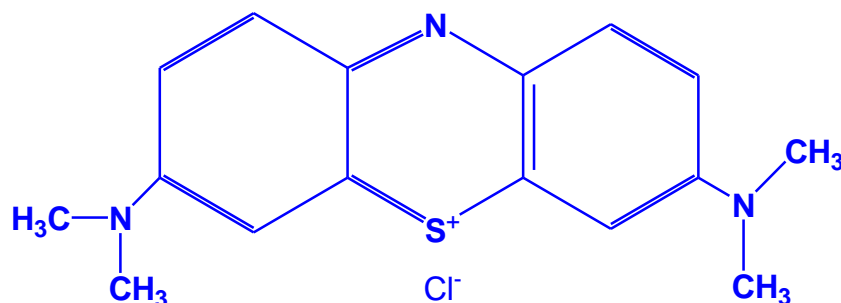
Figure 2.1: Methylene blue's chemical structure (Fatiha & Belkacem, 2016).

Table 2.1: MB dye's physical properties.

Scientific name	Methylene blue
IUPAC name	3,7-bis (dimethylamino)-phenothiazin-5-ium chloride
Molecular formula	$C_{16}H_{18}ClN_3S$
Molecular weight	319.85 g/mol
Maximum adsorption wavelength	663 nm
Color	Blue
Color type	Cationic
Abbreviation	MB

 Source: (Jabbari & Ghasemi, 2021).

Although MB is employed in some medicinal treatments and textile dyeing, it can cause eye damage, nausea, vomiting, excessive perspiration, diarrhea, gastritis, mental confusion, and other side effects. As a result, one of the key environmental problems is the removal of MB from industrial effluents (Kyzas & Kostoglou, 2014).

According to the study conducted by Dargo et al. (2015), the possibility of removing Methylene Blue pollutants with low-cost activated carbon made from rice husk. The amount of dye adsorption rose as the starting concentration, adsorbent dosage, contact time, and temperature were reduced in the experiments. For the given dosage, over 99 percent removal efficiency was achieved.

As stated by Zhong et al. (2010) the effectiveness of treated and untreated activated carbon in removing methylene blue was examined. The impacts of different experimental parameters such

as contact time, solution pH, and adsorbent dosage were investigated. The amount of methylene blue removed rose as the contact time, solution pH, and amount of adsorbent employed increased. The data gathered best matched the Lang model. The adsorption of methylene blue onto dehydrated wheat bran (DWB) was studied at different temperatures (25–45°C), starting methylene blue (MB) concentrations (100–500mgL/1), and adsorbent dosage during different contact times to see if the dye could be removed. The data was analyzed using the pseudo-first-order and pseudo-second-order kinetic models, with the latter proving to be the most accurate (Özer & Dursun, 2007).

According to Dakhil (2013), the adsorption studies were carried out at a constant temperature of 30 oC under various parameters of initial dye concentration (50-500 mg/l), STL dose (0.05-1) g, pH solution (2-11), and contact time (10-180) min. The best conditions were 0.43 g adsorbent per 100 ml dye solution, pH=7, according to the results. The equilibrium isotherms were investigated using the Langmuir method.

As studied by Ahmadi et al. (2020), the process of removing methylene blue (MB) from an aqueous solution with zinc oxide nanoparticles (ZnO-NPs) was explored, as well as the application of nonlinear and linear adsorption isotherms and kinetic models. The impacts of several operational parameters such as pH (3–11), ZnO-NPs dosage (0.1–0.4 g/L), contact period (30–120 min), and initial MB concentration (20–80 mg/L) were investigated.

As studied by Moawed et al. (2019), through a sorption procedure, the efficacy of ZnO nanoparticles for the removal of methylene blue dye from wastewater was investigated. As a result, the effects of many parameters such as solution pH, initial dye concentration, contact time, and temperature were investigated. In addition, assuming a chemisorption process, sorption kinetics followed Pseudo second order and sorption isotherms followed Freundlich.

As reported by Shadmehri & Namvar (2020) textile dyeing wastewaters are typically treated to reduce traditional pollution loads like BOD, COD, SS, and so on. Specific contaminants like dyes, heavy metals, and electrolytes, on the other hand, are difficult to eliminate using traditional waste treatment procedures.
The evaluation included an updated description and analysis of physical, chemical, and biological strategies for removing and degrading contaminants (Ghani et al., 2021).

Table 2.2: Discharge of dye effluent into the environment is required by law (Jadhav & Jadhav2021).

Factors	The standard requirement of effluent allowed
pH	Between 6 and 9
COD	< 50 mg/L
BOD	< 30 mg/L
Suspended solids	< 20 mg/L
Temperature	< 42 °C
Color	< 1ppm
Harmful pollutants	Strictly prohibited

2.1.2. Toxicity of Methylene blue dye

The high amount of dye production and consumption around the world results in colored wastewaters, which are a source of environmental concern. In reality, the environmental release of such effluents is concerning for both toxicological and aesthetic reasons (Métivier-Pignon et al., 2003). MB can induce eye burn, which can cause irreversible damage to both human's and aquatic species' eyes. If consumed by humans, it can cause symptoms such as rapid heartbeat, vomiting, diarrhea, gastrointestinal discomfort with nausea, shock, and mental confusion. When it comes into contact with the skin, it irritates it (Mulushewa & Dinbore, 2021). Cationic dyes, such as MB, have a higher toxicity level than anionic dyes in general. As a result, removing MB from industrial effluents has become one of the most concern environmental issues (Mahmoud et al., 2010).

2.2. Dye removal techniques

Dye removal from wastewater is a major challenge due to its ability to persist in the absence of depletion or degradation. To remove these dyes, it is suggested that you look for ways that can be utilized for the aforementioned goals. Dye removal is accomplished using a variety of

techniques, including physical, chemical, and biological approaches. The following are some of the methods that are discussed:

2.2.1. Coagulation-flocculation

It is one of the earliest forms of conventional treatment. Coagulation and flocculation are two methods for treating drinking water and wastewater, respectively. In the main stage, coagulation and flocculation are frequently followed by sedimentation, filtration, and disinfection, and then chlorination (Muruganandam et al., 2017). Coagulation is a vital technique that involves the addition of coagulants to destabilize and neutralize suspended particles (S. Rathilal, 2021), this results in enormous flocs or aggregates. The flocs are subsequently drawn to the dangling substance. Inorganic coagulants (such as aluminum sulfate and poly aluminum chloride) are employed in wastewater treatment, as are synthetic organic polymers (such as polyacrylamide derivatives and polyethyleneimine) and naturally occurring coagulants (such as chitosan and microbial coagulants). When it comes to the sorts of coagulants used in wastewater treatment, some are toxic to humans and are extremely expensive (Iwuozor, 2019).

Polyelectrolytes are utilized to improve the settling qualities of aluminum or iron coagulant-produced floc (Iwuozor, 2019). As stated by Warade et al. (2016) Polyelectrolytes are commonly utilized as cationic, anionic, and non-anionic coagulant aids. Polyelectrolyte sludge is often compact and easy to dewater for future treatment and disposal. It entails the addition of ferrous sulfate and ferric chloride, which results in efficient dye removal from wastewaters. The appropriate coagulant concentration is determined by the dye's static charge in the solute and the difficulty in removing the sludge generated during the coagulation process (Warade et al., 2016).

2.2.2. Membrane filtration

Membrane technology has evolved rapidly in recent decades as a result of the advantages it provides in water and wastewater treatment (Rathilal et al, 2020). Membrane technology has long been acknowledged as a crucial technique for separating toxins from contaminated sources in water and wastewater treatment (Zirehpour & Rahimpour, 2016). Membranes are selective barriers that separate two phases, allowing certain components to flow while others are retained (Zirehpour & Rahimpour, 2016). It has some unique characteristics that are unmatched by other technologies, such as temperature resilience, chemical toxicity, and microbial attack. The concentrated residue remaining after separation causes disposal issues, as well as significant

capital costs, the risk of clogging, and membrane maintenance. If a textile dye plant uses this kind of filtering, it is appropriate for water recycling (Warade et al., 2016).

The key advantages of these procedures are their low energy consumption, reduced number of processing steps, improved separation efficiency, and increased final product quality (Zirehpour & Rahimpour, 2016). The membranes' weak chemical, mechanical, and thermal resistance, on the other hand, limits their applicability (Zirehpour & Rahimpour, 2016).

2.2.3. Electrochemical treatments

As stated by D'Antoni et al. (2017) it works by passing a direct current through metal electrodes immersed in the effluent, such as aluminum and iron, causing the metal plates to dissolve into the wastewater. Electrochemical techniques have traditionally been utilized for compound synthesis or metal recovery treatments. However, a variety of new applications have lately been proposed. Some of them are presented as solutions to various textile industry technical issues (Sala & Gutiérrez-Bouzán, 2012). Although electrochemical technologies are significant in the above-mentioned textile processes, their broadest range of applications is in color removal in wastewater treatment (Sala & Gutiérrez-Bouzán, 2012), especially in the decomposition of non-biodegradable dyes (such as reactive dyes). As stated by Warade et al. (2016) Electrochemical technologies have been used to purify a variety of industrial wastewaters as well as landfill leachate with great effectiveness. The metabolites that are broken down are generally non-hazardous, making it safe to release treated wastewaters back into waterways. It demonstrates efficient and cost-effective dye removal, as well as high color removal and degradation efficiency for stubborn pollutants (Warade et al., 2016). The cost of electricity utilized is comparable to the cost of chemicals, and relatively high flow rates cause a direct drop-in dye removal.

2.2.4. Ozonation

The use of ozone was pioneered in 1970s, and it is an excellent oxidizing agent due to its high instability (oxidation potential of 2.07) when compared to chlorine (1.36), another oxidizing agent, and H_2O_2 (1.78). Chlorinated hydrocarbons, phenols, insecticides, and aromatic hydrocarbons can all be degraded by ozone oxidation. The amount of dye added to the dye-containing effluent is determined by the total color and residual COD that must be removed

without leaving behind any residue or sludge, as well as no harmful metabolites (Warade et al., 2016).

Ozonation renders the effluent colorless and low in COD, making it safe for release into natural rivers. This approach favors dye molecules that are double-bonded. One major benfit is that ozone can be applied in its gaseous state and therefore does not increase the volume of wastewater and sludge (Robinson et al., 2001; Antoni et al., 2017). The main drawback of ozonation is its short half-life period; this can be again reduced if dyestuffs are present. Acidic condition is more favorable for ozonation, so that careful adjustment of the textile effluent pH is required (Gosavi & Sharma, 2013).

2.2.5. Ion-exchange

Ion exchange is a reversible process where an ion from the solution is exchanged for a likewise charged ion attached to the solid resin (Senthil Kumar et al., 2019). Ion exchange hasn't been frequently employed to treat dye-containing effluents, owing to the belief that ion exchangers can't handle a wide spectrum of dyes. The wastewater is pumped through the ion exchange resin until all of the accessible exchange sites are filled. This method can remove both cation and anion dyes from dye-containing wastewater. This approach has several advantages, including no adsorbent loss during regeneration, solvent reclamation after use, and the removal of soluble dyes. The cost of this approach is a significant disadvantage. Organic solvents are costly, and the ion exchange method for dispersing colors is ineffective (Warade et al., 2016)**.** The review paper of Slama et al. (2021) also addressed that cationic dyes were removed from water throughout the ion-exchange method. This method is great for the elimination of toxic and soluble pollutants from effluent water; but, its use has been restricted because of its high cost.

2.2.6. Electrodialysis

Electrodialysis (ED) is an electrochemical process in which ions migrate over ion-selective membranes due to their attraction due to two electrically charged electrodes (Voutetaki Alexia et al., 2020). The electrodialysis method is a membrane separation technology that is extensively used for wastewater treatment. Electric potential is used as a driving force in ED, and an ion exchange membrane is used to connect the anode and cathode. Negative and positive ions are transported towards the corresponding electrodes based on their polarity when an electric current is applied. Cations pass through the compartment holding a membrane with a negative charge,

and anions pass through the compartment carrying a membrane with a positive charge. The compartments are alternately diluted and concentrated. Current density, pH, flow rate, electrodialysis cell structure, feed water ionic concentration, and ion-exchange membrane properties all affect the performance of an electrodialysis process. Membrane fouling is a significant component that increases energy expenditure while decreasing membrane flow. Membrane selectivity is negatively impacted. Deposition of biomass, colloid, and organic compounds causes fouling. Accumulation can occur on either the inside or outside surface of the membrane (Akhter & Habib, 2018). The ED process has many benefits when compared to high pressure-driven membrane filtration processes as it requires neither high pressure nor chemicals for operation and membrane protection, which translates into lower operating and maintenance costs (Yuzer & Selcuk, 2021).

2.2.7. Phytoremediation

Phytoremediation is the use of live plants to remove colored pollutants from water or soil sources. Phytoremediation is capable of treating dye waste contaminants produced from a variety of sources (Bharathiraja et al., 2018). Tecomastans var, Scirpus, water hyacinth Eichhornia crassipes, and aquatic plant Spirodela polyrrhiza have all been identified as having the ability to degrade dyes. Plants can be used to remove toxins from their environments in a variety of ways. Plants can remove pollutants from the soil, sediment, and/or water by serving as filters or traps. The root system of plants typically uptakes toxins found on-site and protects the environment from their toxicity (Bharathiraja et al., 2018). As a result, pollutants from a variety of sources must be ready to be absorbed by roots, and this phenomenon enables color removal and bioavailability possible. As stated by Farraji et al. (2016) any disability, failure, or unknown response may divert as a factor to plant species, as well as increase the disadvantages of phytoremediation. The disadvantages of phytoremediation could be classified as follows.

1) Physical characteristics and limitations of plant species 2) incorrect treatment application and planning 3) low efficiency 4) low concentration of necessary macro/micronutrients in polluted media 5) The interaction of multiple contaminants 6) Climate conditions and plant species adaptation in polluted areas (Farraji et al., 2016).

2.2.8. Adsorption

Adsorption is a high-quality treatment method for removing dissolved organic pollutants such as dyes from industrial wastewater. The concentration of materials on the surface of solid bodies is defined as adsorption. Adsorption is a surface phenomenon that primarily involves the use of surface forces. When an absorbable solute solution, also known as adsorbate, comes into contact with a solid with a highly porous surface structure, liquid-solid intermolecular forces of attraction cause the solute to be concentrated at the solid surface. Adsorption is one of the unit operations in chemical engineering processes used to separate pollutants from industrial wastewater (Kandisa & Saibaba, 2016). Adsorption is one of the most commonly used tertiary treatment methods in the textile industry (Robinson et al., 2001). The adsorbent's adsorption ability determines the separation efficiency of an adsorption process.

In other words, the surface area exposed and the number of active sites of the adsorbent are critical for contaminant adsorption. As a result of their high surface area and effective active sites, nanomaterials appear to be an excellent adsorbent (Saleem & Zaidi, 2020).

Although activated carbon is an effective dye adsorbent for a wide range of dyes, its high cost and regeneration complexity limits its use in decolorization (D'Antoni et al., 2017). Adsorbents are primarily made from zeolites, charcoal, clays, ores, and other waste resources. Coconut shell, rice husk, petroleum wastes, tannin-rich materials, sawdust, fertilizer wastes, fly ash, sugar industry wastes, blast furnace slag, chitosan and seafood processing wastes, seaweed and algae, peat moss, scrap tires, fruit wastes, and other wastes are used to make adsorbents (Kandisa & Saibaba, 2016).

2.3. Mechanisms of dye adsorption

Adsorption is an exothermic surface-based process in which molecules of a compound in gas or liquid form accumulate at an adsorbent surface (Kecili & Hussain, 2018). Adsorbate is the compound that is adsorbed to the adsorbent. Desorption, on the other hand, is the release of adsorbed molecules from the adsorbent's surface, and it is the inverse of adsorption. Adsorption of molecules to the adsorbent surface can take place in two ways: "physical adsorption," also known as "physisorption," and "chemical sorption," also known as "chemisorption." This is determined by the interactions of the molecules with the surface. In physical adsorption, weak forces such as electrostatic interactions and Van der Waals forces are involved. Chemical adsorption results in the formation of strong chemical bonds, such as covalent bonds, between

the surface and the adsorbed molecules. Chemical adsorption is slower than physical adsorption and usually results in the formation of a monomolecular layer (monolayer) on the adsorbent surface, whereas physical adsorption usually results in the formation of a thick multilayer on the surface (Kecili & Hussain, 2018).

Various adsorption mechanisms are used to achieve dye adsorption from contaminated water on the surface of an adsorbent. It should be noted that electrostatic attraction, p–p interactions, van der Waals forces, hydrogen bonding, acid-base reactions, and hydrophobic interaction all play a role in the adsorption of water pollutants on adsorbents. Furthermore, the ion exchange mechanism entails ion exchange between a liquid (dye solution) and a solid phase (adsorbent).

2.4. Factors affecting the adsorption process

Contact time, adsorbent dosage, pH, and initial dye concentration can all influence dye adsorption.

2.4.1. Effect of contact time

The effect of contact time on adsorption of dye can be done by preparing adsorbent-adsorbate solution with fixed adsorbent dose and initial dye concentration for different time intervals and shaken until equilibrium. To a certain extent, the dye removal rate increases with increasing contact time. Any further increase in contact time will not increase uptake due to dye deposition on the available adsorption site on the adsorbent material. The amount of dye desorbing from the adsorbent is now in dynamic equilibrium with the amount of dye adsorbed onto the adsorbent. The time required to achieve this state of equilibrium is referred to as the equilibrium time, and the amount of dye adsorbed at the equilibrium time represents the adsorbent's maximum adsorption capacity under those operating conditions (Adamu, 2008). Singh et al. (2017) reported that, the percentage dye removal increased from 66% at 10 min to around 84% in 90 min on removal of methylene blue dye using activated carbon prepared from biowaste precursor. It was also clear from the figure that adsorption was rapid initially, which gradually slowed down and appeared to be at equilibrium later on. This can be attributed to the fact that initially a large number of vacant sites were available at the surface of the adsorbent which gradually decreased with time.

2.4.2. Effect of adsorbent dose

Adsorbent dosage is an important parameter in determining the adsorbent's capacity for a given amount of adsorbate under operating conditions. In general, increasing the adsorbent dose leads to an increase in dye removal because the amount of sorption site at the adsorbent increases dye removal percentage. To investigate the effect of adsorbent dose on the adsorption process, prepare an adsorbent-adsorbate solution with varying amounts of adsorbents added to a fixed initial dye concentration and shake until the equilibrium time is reached. The effect of the amount of adsorbent material offerings an idea for the adsorption process, which is economically viable (Soltani et al., 2021). As studied by Tsade Kara et al. (2021), the effect of adsorbent dose on adsorption ability and degree of color removal of MB at the optimum temperature of 25°C, MB initial concentration of 30 mg·L−1, the contact time of 60 min., and solution pH of 8 using Periodiated Modified Nanocellulose . Different doses of $NaIO_4$-NC adsorbent ranged from 0.4 to 2 g were used in the experiments and the results exhibited that the increase of the adsorbent dosage from 0.4 to 1 g increases the % R from 35.51% to 78.50 %. Maximum adsorption efficiency was detected at the optimum adsorbent dose of 1 g.

After this optimum value, the color removal remains constant due to the quantity of ions bond to the adsorbent and the number of mobile ions in the wastewater becomes fixed even with an extra addition of the adsorbents dose. On the contrary, the increased % R efficiency were reported by Tan et al. (2018) for MB dye removal using cellulose-based nanomaterials as an adsorbent from synthetic wastewater. Relatively low efficiency and percent removal were observed in this study due to the computation of other contaminants to the surface of the adsorbent since the study was focused on the removal of cationic dye from real textile industrial wastewater.

2.4.3. Effect of pH

In the adsorption process, the pH factor is critical for dye adsorption. The magnitude of electrostatic charges imparted by ionized dye molecules is controlled by the pH of the medium, and as a result, the adsorption rate varies with the pH of the medium used.

In general, the dye removal percentage for cationic dyes decreases at low pH, while the dye removal percentage for ionic dyes increases. In contrast, cationic dye adsorption is preferred for high pH solutions, whereas anionic dye adsorption is less efficient. As the surface charge density decreases with increasing pH, the electrostatic repulsion between the positively charged dye and the adsorbent surface decreases increase to the adsorption extent (Mohammad Razi et al., 2017).

2.4.4. Effect of initial concentration

It must be noted that an increase in dye concentration shows positive effects up to a certain limit. Further, the increasing tendency of adsorption for high levels of dye contaminants is directly related to the available active sites on the surface of the adsorbent. The enhanced adsorption capacity is initially accelerated due to the presence of unsaturated active sites in the adsorbent. As the surface of the adsorbent becomes saturated, a considerable reduction in the adsorption of dye occurs (Dutta et al., 2021).

According to the study reported by Tan et al. (2012) , the effect of MB initial concentration on cationic dye removal using Fe_3O_4-activated maize poweder Nps was carried out at fixed adsorbent dosage, 0.4g/100 mL, room temperature ($\pm 27^{o}C$), pH 6.0, 200 rpm shaking speed and at different initial concentrations of dye (100, 150, 200, 250 mg/L) for time intervals from 5 minutes to 45 minutes. It showed that, percentage for dye concentration removal decreased from 99.90 % to 94.58 % with increasing initial dye concentration from 100 to 250 mg/L. But, the actual amount of dyes adsorbed per unit mass of adsorbent increased with initial dye concentration. At equilibrium, unit adsorption increased from 31.99 mg/g to 70.29 mg/g as the concentration increased from 100 mg/L to 250 mg/L respectively. This is because the mass transfer driving force would become larger as the initial concentration increased. Hence, it results in higher MB adsorption.

Table 2.3: Summary of drawbacks of dye removal techniques.

Dye removal techniques	Drawbacks	References
Coagulation-flocculation	Large amounts of sludge are produced, resulting in high disposal costs.	(Warade et al., 2016)
Membrane filtration	Because of disposal issues, high capital costs, and the possibility of clogging, the membranes' limited resistance in terms of chemical, mechanical, and thermal resistance limits their application.	(Warade et al., 2016, Zirehpour & Rahimpour, 2016)
Ion exchange	The cost of this method is a significant disadvantage. Organic solvents are expensive, and the ion exchange method for dispersing dyes is ineffective.	(Warade et al., 2016)
Electrochemical treatments	High flow rates result in a direct reduction in dye removal, and the cost of electricity used is comparable to the cost of chemicals.	(Warade et al., 2016)
Ozonation	One disadvantage of Ozonation is its short half-life, which is typically 20 minutes. This time can be reduced further if dyes are present, with salts, pH, and temperature all influencing stability.	(Warade et al., 2016)
Electrodialysis	The deposition of biomass, colloid and organic substances causes fouling. Accumulation can occur on either the inside or outside surface of the membrane.	(Akhter & Habib, 2018)
Phytoremediation	Physiological properties and limitations of plant species, incorrect treatment application, and planning, low efficiency, low concentration of necessary macro/micronutrients in polluted media, the interaction of multiple contaminations 6) Climate conditions and plant species adaptation in	(Farraji et al., 2016)

polluted areas

Adsorption	Adsorbent capacity consistently decreases as the number of cycles increases, as does its high cost and regeneration complexity.	(D'Antoni et al., 2017)
Photocatalyst	The major difficulty is it takes s a long time and limited applications for the treatment of wastewater; the activity of photocatalyst is greatly dependent on its ability to generate an electron-hole (e-h) pair.	(Viswanathan, 2017,Bora et al., 2017)

2.5. Nanotechnology

Nanotechnology is the use of individual atoms and molecules to create materials, electronics, and systems (Sulekha, 2016). In nanotechnology, a nanoparticle is defined as a small object that beh aves as a whole unit in terms of its transport and properties. Nanoscience and nanotechnology are now widely used in a variety of sectors,most notably sensor, electrical, antimicrobial, water puri fication, cosmetic, medi cinal, pharmacutcal, environmental, catalytic, and material applications (Mondal & Maity, 2018)**.**

With the rapid advancement of nanoscale science and engineering, significant potential for developing more cost-effective and ecologically acceptable cleanup techniques has arisen. Water can be cleaned using nanotechnology in a variety of ways, including nanofiltration membranes to improve water quality, nanoscale biosensors to detect pollution in water, the development of environmentally friendly methods for cleaning groundwater, and the improvement of the efficiency of chemical and photocatalytic processes. Many nanoparticles have unique features that can enable revolutionary technologies for pollution removal, microbial control, sensing and monitoring, and resource recovery. Some of the most promising strategies presented by nanotechnology for wastewater treatment are photocatalysis, nanofiltration, and nano-adsorbents (Sulekha, 2016).

2.5.1. Photocatalysis

Photocatalysis (PC) is a green AOP that uses nanostructured oxide materials and light to break down organic impurities in water and immobilize microbiological contaminants. When exciton pairs produced on photocatalyst surfaces are excited by the light above bandgap energy, they interact with their surroundings to produce highly reactive species that can oxidize or decrease pollutants in their vicinity. Commonly used photocatalytic materials, such as titanium dioxide (TiO_2) and zinc oxide (ZnO), are intrinsically wide band-gap semiconductors that absorb the UV portion of the spectrum (4 percent), limiting their efficiency and uses (Bora et al., 2017). The Photocatalysis method can be utilized to reduce environmental contaminants. Photocatalysis is a type of oxidation. This chemical reaction modification is caused by photon adsorption, which has more energy than the energy required to overcome the interstitial of two-electron shells of semiconductor material. When a photon illuminates the catalytic surface, one electron (a negatively charged particle) is transported from the valentine shell to the empty conduction shell, leaving a positive charge "hole" behind it. This "e-h" pair ("electron-hole") produces extremely reactive radicals that bind to pollution molecules and break them down (Zekić et al., 2018).

The majority of the reported photocatalytic dye degradation studies used Titanium dioxide as a photocatalyst. The main disadvantage of TiO_2 is that it absorbs only in the UV region due to its bandgap of around 3.2 Ev (Viswanathan, 2017; Bora et al., 2017). The fundamental issue is that wastewater treatment takes a long time and has restricted applications. In other words, photocatalyst activity is heavily dependent on its ability to create an electron-hole (e-h) pair (Bora et al., 2017).

2.5.2. Nanoadsorbents

Nanoparticle materials have recently been investigated for their potential as adsorbents (Anjum et al., 2016). Nanoparticles have two crucial properties that make them excellent adsorbents. These are nanomaterials' enormous specific surface area and surface multifunctionality, or the capacity to chemically react with and bind to different neighboring atoms and molecules. These qualities make nanoparticles not only excellent adsorbents for diverse pollutants in wastewater, but also allow for long-term stability, as adsorbent degradation (with the addition of catalytic activities of nanoparticles) results in adsorbent degradation and improves adsorption effectiveness (Zekić et al., 2018). Because of their appealing features and significant adsorption capabilities

for diverse organic molecules, nanomaterial based adsorbents have gained growing attention in water and wastewater treatment applications (Awad et al., 2020). Nanoadsorbents are often defined as having at least one dimension between 1 and 100 nm. Based on their source, adsorbents are categorized into four types: agricultural residue, inorganic, polymeric, and composite (Zare et al., 2018). To treat dye containing wastewater, several adsorbents such as bio sorbents, carbon based nano adsorbents, transition metal based oxides, MOFs, and polymer base d adsorbents are currently employed (Dutta et al., 2021).

Metallic nanoparticles (Ag and Au), metal oxide nanoparticles (ZnO and TiO_2), and magnetic nanoparticles (MNPs) (e.g., Fe_3O_4) are excellent candidates as efficient nano adsorbents due to their unique properties such as high reactivity, small size, and high surface-area-to-volume ratio, which provides high adsorption capacities toward the target compound (Kecili & Hussain, 2018). ZnO NPs are environmentally friendly because they are compatible with organisms, making them suitable for wastewater treatment (Abdelbasir & Shalan, 2019). Furthermore, zinc oxide nanoparticles could be employed to heal water bodies (Saleem & Zaidi, 2020). Nanoparticles of organic or inorganic origin have been widely researched for adsorption-based color removal. Their high porosity, tiny size, and vast surface area maximize their interaction with dye molecules via their numerous pollutant binding sites, and therefore their adsorption efficiency (Homaeigohar, 2020).

Metal oxide nanoparticles such as TiO_2, SiO_2, MnO, ZnO, and Fe_2O_3, carbon nanotubes (CNTs), graphene (G), graphene oxide (GO), zeolites, and hydroxyapatite are the most often utilized adsorbents for the removal of heavy metal ions/dyes from wastewater/aqueous solutions (Zare et al., 2018). Aside from TiO_2 NPs, several researchers have shown that ZnO NPs have emerged as another efficient candidate in wastewater treatment due to their unique qualities, particularly variable bandgap in the region of near-UV spectra, strong oxidation capability, and excellent photocatalytic capabilities.

2.5.3. Zinc oxide nano-adsorbents

Metal oxide-based nano-adsorbents have been widely used in wastewater treatment in recent years due to their unique properties such as large surface area, nano-size, high reactivity, ability to blend, and robust solution mobility (Dutta et al., 2021). Metal oxide nanoparticles with large surface areas, such as zinc oxide (ZnO) nanoparticles, have chemical and thermal stability, as

well as antibacterial capabilities. As a result, ZnO nanoparticles are also used as effective nano adsorbents (Kecili & Hussain, 2018). Metal oxide nanoparticles, such as zinc oxide (ZnO) nanoparticles, have a huge surface area and demonstrate chemical and thermal stability, as well as antibacterial capabilities. As a result, ZnO nanoparticles are used as effective nano adsorbents (Muruganandham et al., 2015). ZnO NPs are safe for the environment because they are compatible with organisms (Abdelbasir & Shalan, 2019), this qualifies them for water and wastewater treatment. Zinc oxide nanoparticle (ZnO NP) has received a lot of attention for water treatment due to its nontoxicity, long-term stability, low cost, biocompatibility, and potent antibacterial activities against pathogens commonly present in water (Gu et al., 2020).

As stated by Yashni et al. (2020), When compared to TiO_2, ZnO was found to be more efficient in the degradation of dyes and to be a more cost-effective option in the long term.

2.5.4. Synthesis of metal oxide nanoparticle

There are numerous ways available for the synthesis of nanomaterials, which can create nanomaterials in the form of colloids, clusters, powders, tubes, rods, wires, thin films, and so on. One approach is summed up as "top-down" technology, which refers to the manufacture of very small structures out of material building blocks via grinding, etching, or other mechanical processes (Kannan & Sivakumar, 2016).

Metal oxide nanoparticles have been synthesized utilizing a variety of methods, including chemical, physical, and green/biological processes (Dave & Chopda, 2014). Physical approaches for manufacturing metal oxide nanoparticles fall into several categories. It comprises metal/metal oxide nanoparticle synthesis technologies such as aerosol, electron beam lithography, laser-induced pyrolysis, gas-phase deposition, pulsed laser ablation, and powder ball milling. Through chemical reaction processes, the chemical synthesis procedures utilized to produce metal oxide nanoparticles can be employed to produce more ordered and sophisticated nanomaterials. These are commonly acknowledged processes for producing metal oxide nanoparticles, such as zinc oxide nanoparticles, which are useful in a variety of technological applications. Coprecipitation, microemulsion, hydrothermal, electrochemical disposition, sonochemical, and thermal decompos ition are the major chemical synthesis techniques of metal oxide nanoparticles. There are self-assembly and positional assembly techniques in chemical manufacturing methods. Self-assembly refers to a procedure in which atoms are re-arranged into ordered nanoscale structures between materials, whereas positional assembly refers to a method in which atoms or molecules are

purposefully manipulated and positioned during the process (Saif et al., 2016). Metal and metal oxide nanoparticles are produced using a variety of chemical and physical methods. Though traditional techniques are appropriate for the synthesis of large amounts of nanoparticle materials in a shorter time, with defined shapes and sizes, these defined methods have the disadvantages of being inefficient, costly, intricate, and prone to aggregate formation, which results in loss of reactivity. These synthesis methods also necessitate very toxic reductants, high radiation levels, and stabilizing agents, all of which can be harmful to live organisms, including marine life and humans.

The reducing chemicals utilized in these approaches are highly toxic and reactive reducing agents such as hydrazine hydrate and sodium borohydride, which can have unfavorable effects on the environment, animal life, and vegetation. Furthermore, they increase the danger of toxicity and environmental contamination by releasing toxic by-products that are potentially harmful to the environment (Singh et al., 2018). Furthermore, the operating conditions used in traditional methods of metal/metal oxide nanoparticle synthesis are high temperatures, inert atmospheres, or vacuum settings, which make the manufacture of nanoparticle materials for their specialized applications problematic (Marimón-Bolívar & González, 2018).

2.6. Green synthesis of metal oxide nanoparticle

Currently, green chemistry principles are considered the fundaments to contribute to sustainable development, and comprise instructions to implement new chemical products, new synthesis, and new processes. Concisely, the green chemistry principles are based on 1) atom economy, to improve reaction efficiency, 2) energy efficiency, avoiding high energy consumption process, 3) safer chemicals, to minimize the toxicity of processes and products, 4) prevention, to minimize waste in every stage of the process, 5) renewable feedstocks, using chemicals made of renewable sources, 6) design for degradation, design biodegradable and non-toxic products, 7) less hazardous chemical synthesis, to design safer synthesis routes, 8) reduce derivatives, avoid the use of derivatives such as protectors or stabilizers, 9) pollution prevention, prevent the release of hazardous substances, 10) safer solvents and auxiliaries, to use the least possible hazardous solvent or chemical, 11) catalysis, use catalysis to improve processes like energy consumption or efficiency and 12) accident prevention, to minimize the risks of accident (Bandeira et al., 2020).

The green synthesis of nanoparticles technique is based on green chemistry principles, which include the research and design of nanoparticles utilizing nontoxic chemicals, renewable

materials, environmentally benign solvents, and finally degradable waste products. The use of a nontoxic solvent medium, a nontoxic reducing agent, and environmentally friendly stabilizing agents are three crucial phases in the synthesis of nanoparticles from a green chemistry perspective. Another important issue is the capping compound used to passivate the nanoparticle surface. The capping agent also has an impact on the size ranges, morphologies, and targeted applications. Plant parts such as fruits, leaves, flowers, roots, and seeds are examples of green synthesis. Microorganisms such as fungi, bacteria, algae, and viruses can also be used to replace harmful chemicals in the creation of nanoparticles. Microorganism-based techniques of nanoparticle synthesis necessitate a qualified/skilled individual, a higher cost, and a longer time frame, which are considered to be the key limitations of microorganism-mediated synthesis. However, as compared o microorganism-assisted synthesis of metal oxide nanoparticles, the use of plant extract for the manufacture of metal oxide nanoparticles is the most cost-effective, reproducible, simple, and straightforward process. They create more stable metal/metal oxide nanoparticles and have proven to be the most suitable method for large-scale production. Plant-based synthesis is quick and does not take long, demonstrating the potential of plant extract to reduce metal ions in a short minutes or hours. Previous research shown physiologically decrease metallic ions in the creation of nanoparticles and are more ecologically friendly ways (Annu et al., 2018). Green synthesis methods based on biological precursors are affected by reaction parameters such as solvent, temperature, pressure, and pH (acidic, basic, or neutral).

 Plant biodiversity has been widely considered for the synthesis of metal/metal oxide nanoparticles due to the availability of effective phytochemicals in various plant extracts, particularly leaves, such as ketones, aldehydes, flavones, amides, terpenoids, carboxylic acids, phenols, and ascorbic acids can convert metal salts into metal nanoparticles (Singh et al., 2018). Many reaction factors include pressure, solution pH, temperature, and solvent, influence green synthesis approaches (Herlekar et al., 2014). In general, high pressure, temperature, and additional energy inputs are not required in green synthesis.

The production of nanoparticle nanomaterials from reducing metal salts using plant extract is a room-temperature technique that involves mixing metal salt solutions with plant extract. The immediate reduction of the salt solution begins in this process, resulting in the synthesis of nanoparticles, and lastly, the change in the color of the reaction mixture indicates the development of the nanoparticles. Nanoparticles aggregate to create a variety of morphologies as

they expand, including spheres, pentagons, triangles, cubes, hexagons, and rods. The size, quality, and morphology of the synthesized nanoparticle can be influenced by reaction time, pH, metal salt concentration, temperature, and plant extract concentration. Plant-based materials have received special attention and are widely recognized as the best material due to its biodegradability, simplicity of use, and abundance. Plant extracts are mostly composed of biomolecules and carbohydrates, which can be employed as reducing agents to promote the synthesis of metallic/metal oxide nanoparticles of nanomaterials. It was also shown that proteins with amino ($-NH_2$) functional groups found in plant extracts can actively participate in the reduction of metal ions for the creation of nanoparticles. Other functional groups that can help with the synthesis of metallic nanoparticles are given below as well. Functional groups found in phytochemicals such as anthracenes, alkaloids, flavones, and phenols ($-C=O-$, $-C-O-$, $-C-O-$, $-C-O-C-$, and $-C=C-$) can lead to the formation of metallic/metal oxide nanoparticles (Singh et al., 2018).

Despite the numerous advantages of green synthesis, this approach of producing nanoparticles is still not widely adopted. This is owing to a lack of understanding of the nanoparticles' reactivity, physicochemical properties, and agglomeration.

In general, researchers utilized a strong base (reducing agent), such as sodium borohydride or sodium hydroxide, in metal ion reduction from salt solutions, followed by the addition of a capping agent or a stabilizer to synthesize MNPs and MONPs (stabilizing agent) (Shafey, 2020). To dissolve the stabilizers, they used solvents and reagents that act as reducing agents, which are toxic substances with counteractive and harmful effects if the rest of these materials are left in the back part of the nano-system, as the bottom-up path to synthesize the nanoparticles frequently requires offensive chemical reduction agents such as sodium borohydride and hydrazine, as well as Cappi. Although these processes may effectively generate pure products, the manufacturing cost is extremely high, both in terms of material and environmental impact. This may provide a new stand-by synthesis and direct them to examine the safety uses of MNPs and MPs. The green synthesis of MNPs and MONPs is one of the approaches that use biological systems and is based on green chemistry concepts (Shafey, 2020).

Green Chemistry is described as the design of chemical products and processes to limit or eliminate the usage and manufacture of hazardous compounds, and it was founded in principles to guide chemists in their quest for greenness. Thus, it is the practice of chemical research and

manufacturing in a way that is sustainable, safe, and non-polluting, consuming the least number of resources and energy and producing little or no waste. It starts with recognizing the manufacturing, processing, use, and final disposal of chemical products that can cause harm if done incorrectly. Green Chemistry and green chemical engineering may modify or completely redesign chemical goods and processes to meet their goals of decreasing waste and the use or manufacture of, particularly hazardous materials. It does it in an economically feasible and cost-effective manner. It has been discovered that it is the most effective and least expensive method of practicing chemistry. As a result, all expenses associated with the practice of chemistry, including dangers and potential environmental harm are considered. This strategy focuses on the employment of environmentally safe, cost-effective, natural, and biocompatible reducing agents for the production of NPs, such as ZnO Nps (S. Prathap et al., 2006). The biosynthesis of the main principle of green chemistry is the production of metal or metal oxide nanoparticles using environmentally friendly methods and without the use of harsh, toxic reducing agents (e.g., hydrazine hydrate, sodium borohydride, dimethylformamide, ethylene glycol, and so on) and expensive chemicals. Green chemistry is the design, development, and implementation of chemical products and processes that decrease or eliminate the use and production of hazardous compounds to human health and the environment. There are three areas of opportunity for green chemistry in the creation of metal oxide NPs by reduction of the respective metal ions: (i) Choice of solvent (ii) the reducing agent employed, and (iii) the capping agent used as cited in (Gopalakrishnan et al., 2012).
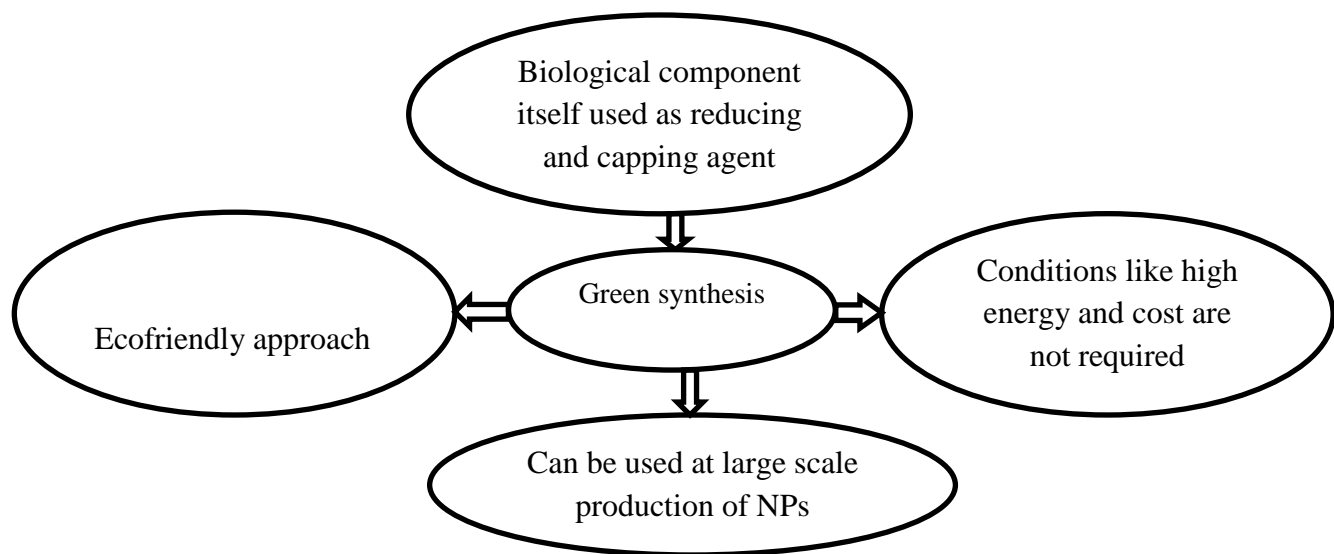
Figure 2.2: Main benefits of green synthesis method (Singh et al., 2018).

2.6.1. Synthesis methods of ZnO nanoparticles

Nanoparticles can be created by lowering the size of the material from a micro or larger scale to a nanoscale, which is known as the top-down technique, or by forming atoms or molecules into nanoparticles, which is known as the bottom-up strategy (Khairunnisa et al., 2021). In general, there are two techniques to NP synthesis: top-down and bottom-up (Khalil et al., 2013). NPS are created via top-down ways by size reduction from a suitable starting material. Various physical and chemical treatments are used to reduce size. Top-down manufacturing methods introduce defects in the product's surface structure, and other physical attributes of NPs are largely dependent on the surface structure. Bottom-up synthesis creates NPs from smaller entities, such as combining atoms, molecules, and smaller particles. The nanostructured building blocks of NPs are generated first, and then the finished particles are assembled. Bottom-up synthesis is mostly based on chemical and physical manufacturing processes (Mittal et al., 2013). ZnO is synthesized using several synthetic processes. These approaches are roughly classified into three types: chemical, biological, and physical procedures (Sundaramurthy & Parthiban, 2015).

2.6.1.1. Physical and chemical synthesis methods

Nanoparticles have been synthesized using arrays of traditional methods. They are primarily classified as physical and chemical approaches. Radiolysis, microwave, ultrasonication, laser

ablation, and electrochemical processes are some of the physical methods used to create nanoparticles (Das et al., 2017). Physical procedures include pulsed laser ablation, vacuum vapor deposition, and mechanical milling. In comparison to chemical techniques, the advantages of physical approaches include the absence of solvent contamination in the created thin films and the uniformity of NPs distribution. However, the material's quality is not as great as that of chemically manufactured materials. It consumes a lot of energy while raising the temperature around the source material, and it takes a long time to establish thermal stability. The physio-chemical approaches for the production of metal nanostructures are expensive; they necessitate a substantial amount of labor and time. Furthermore, considerable amounts of secondary waste are produced as a result of the use of chemical agents for precipitation and reduction in operations (Sundaraselvan & Darlin Quine, 2017). Pure, well-defined nanoparticles can be produced using chemical and physical processes. However, these approaches are more expensive, require more energy, and may be harmful to the environment (Okafor et al., 2013).

2.6.1.2. Green chemistry (biological) methods

Green chemistry is the development of goods and procedures that decrease or eliminate the usage of hazardous compounds and, ultimately, their disposal in the environment. Green chemistry, which was enacted as a Pollution Prevention Act in 1990, is a novel approach to pollution control that focuses on preventing environmental problems before they occur. Synthesis of NPs utilizing plants and microorganisms such as bacteria, viruses, fungi, and yeast has recently been found to be an environmentally benign alternative technique of synthesizing a wide range of NPS. The synthesis of NPs using plant parts and plant extracts is the most cost-effective and straightforward of these biological entities because it does not require multi-step methods including sophisticated culturing and isolation techniques. Plants' ability to hyper-accumulate and physiologically decrease metal ions has been known since the early 1900s and has been utilized to recover valuable metals from areas that would otherwise be unsuitable for mining. However, the use of whole plants in the synthesis of NPS has several drawbacks, such as the heterogeneity of the size and shape of the NPS produced, which makes them difficult to employ. For example, in clinical applications, cell size and shape are essential parameters influencing cell uptake, pace, and site-specific medication administration from the system. Plant extracts have been considered as a simpler alternative for generating NPs in this regard. Plant extracts

containing functional groups such as C=C (alkenyl), C=N (amide), -O-H (phenolic and alcohol), N-H (amine), C-H, and COO- (carboxylic group) are primarily responsible for the reduction and stability of metallic ions into metal oxide NPs. The plant portion is boiled during the extraction process. The extract obtained contains the reducing and capping agents required to decrease metallic ions (Nethavhanani, 2017).

2.7. Limitation of conventional methods

Chemical procedures have the disadvantage of contaminating the environment with harmful solvents and producing hazardous byproducts. The disadvantage of the physical technique is that the resulting NPs have defective surface formation, a low production rate, a high manufacturing cost, and a large energy requirement, it raises the environmental temperature around the source material, and it takes a long time to achieve thermal stability (Naseem & Durrani, 2021). Almost all of the viable chemical processes use toxic chemicals and energy-intensive ways, making these options environmentally dangerous and precluding their use in biology, medicine, and clinical applications. Where flammable or corrosive reducing agents such as titanium tetrachloride and hydrazine have been employed, they are not safe. Strong and weak chemical reducing agents, as well as capping agents such as sodium borohydride, sodium citrate, and alcohols, are also required for this technique. These agents are typically highly poisonous, combustible, and difficult to dispose of. Some wet chemical procedures require a hazardous organic reactant like ethylene glycol, while others need an extra reducing agent like salt. They also involve the use of hazardous compounds and their byproducts, concentrated reduction agents, high levels of radiation, and contamination from precursor chemicals. As a result, it is a fact that reproducibility and stability of NPs with controlled size are extremely difficult to achieve using popular chemical reduction methods, which involve expensive reagents, hazardous reaction conditions, and a time-consuming and labor-intensive process to isolate NPs, posing an alarming threat to flora, fauna, and human health. Biological technologies based on microorganis ms are safe, nonhazardous, environmentally beneficial, and energy-efficient. These are carried out at ambient temperatures and decrease metal ions at a faster pace. Microorganisms can live in harsh environments, such as high metal concentrations, by using survival mechanisms such as the efflux system, extracellular combination and precipitation, and chemical detoxification (Devi & Singh, 2014).

2.8. Plant mediated green synthesis of ZnO nanoparticles

Plants and plant extracts as machinery for metal NPs synthesis are intriguing because they eliminate the need for hazardous materials as well as the time-consuming culturing and downstream processing. Plant extracts, on the other hand, are more appealing because the methodology is much simpler and less expensive. Plant extracts are used in in vitro approaches to bio reduce a specific zinc salt (zinc nitrate, sulfate, chloride, and many others) and provide control over the size and shape of the nanoparticles Plants contain a variety of primary and secondary metabolites, such as tannins, terpenoids, saponins, starches, polypeptides, flavonoids, and phenolic acids, which act as excellent reducing and capping agents. Mild solvents such as water, ethanol, or methanol are used to extract plant metabolites, which are then allowed to react with zinc salt solution under various conditions to maximize yield (Okafor et al., 2013). Plant parts like leaf, root, latex, seed and stem are widely being used for metal- and metal oxide-based NP synthesis. Plant extracts are bioactive polyphenols, proteins, phenolic acids, alkaloids, sugars, terpenoids, etc., which are primarily composed to play a major role in relegating the metallic ions and then alleviating them. The discrepancy in concentration and conformation of these active biomolecules among different plants and their consequential association with aqueous metal ions are assumed to be the main supporting factor in the various sizes and shapes of fabricated nanoparticle (Sajjad et al., 2018).

The bio variations of plants give plentiful biochemical properties and introduce a particular source to synthesize nanoparticles. The extract from the plant leaf is relatively easy to obtain and contains several metabolites that act as reducing agents in the synthesis of nanoparticles. The quality, stabilization, quantity generated, and production rate of nanoparticles are all affected by elements such as pH, temperature, contact time, metal salt concentration, and phytochemical profile of plant leaf particles (Singh et al., 2018). It is critical to pay close attention to the phenomenon of agglomeration development during nanoparticle biogenesis. The bioactive chemicals are thought to operate as capping agents, preventing agglomeration (Sajjad et al., 2018; Khairunnisa et al., 2021).

2.8.1. The Neem (Azadirachta Indica) plant

Neem (Azadirachta Indica A. Juss) is a Meliaceae plant native to the Indian subcontinent. It was then imported into numerous tropical American and African countries. Neem is a fast-growing tree that can grow to a height of 15–20 m and, in rare cases, 35–40 m. It is evergreen, but in times of severe drought, it may lose most or all of its leaves. Azadirachta Indica is also known as the Sacred Tree. The drought resistance of the Neem tree is well known (Pankaj et al., 2011).

The A. Indica is a very helpful traditional medicinal plant in the African subcontinent, and every component of the tree has medicinal properties. Neem trees (leaf, stem, bark, and seed) have antibacterial and antifungal properties against several pathogenic microbes, as well as antiviral properties against Vaccinia, Chikungunya, and measles (Alzohairy, 2016). Neem also contains physiologically active components separated from various portions of the plant, such as azadirachtin, Meliacin, gun, Salinan, Nimbin, Valassis, and numerous additional derivatives of these principles (Khaing et al., 2018). Antimicrobial activities are due to the secondary metabolites synthesized by the plants such as phenolic compounds. Leaf is one of the highest accumulated plant part of such compounds neem leaf extract is used in the synthesis of various nanoparticles like gold, zinc oxide, silver etc. The phytochemicals present in Neem are namely terpenoids and flavanones, which act as reducing as well as capping agent and helping in stabilizing the nanoparticles (Geetha, 2017).

Table 2.4: Classification of Neem

Kingdom	Plantae
Division	Magnoliophyta
Order	Sapindales
Family	Meliaceae
Genius	Azadirachta
Specius	Indica

2.8.2. Studies Related to Phytochemical Constituents of Neem leaf

Secondary metabolites found in medicinal plants include alkaloids, flavonoids, saponins, and other active metabolites that have a high therapeutic value and have been widely exploited in the

medicine and pharmaceutical industries. Many biological and therapeutic effects have been identified for these secondary metabolites. A variety of research on the Phytochemistry of medicinal plants, particularly the vegetative components such as leaves and stems have recently been published. Alkaloids, flavonoids, and glycosides have been shown to have a variety of biological effects, including anti-inflammatory, anti-allergic, antioxidant, anti-diabetic, anti-viral, anti-cancer, anti-leprosy, and antimicrobial activity. The phytochemical ingredients are widely known for their medicinal effect against a variety of human ailments including ulcers, swelling liver, malaria, dysentery, diarrhea, and so on. A wide range of herbs and herbal extracts contain phytochemicals with biological action that can have a beneficial therapeutic impact. Phytochemicals, which are non-nutrient molecules, have been linked to much of the protective impact of herbal plants (Ravva & Korn, 2015).

Azadirachtin, Nimbin, and nimbidin are the most common active compounds found in neem. Alkaloids, tannins, flavonoids, and phenolic compounds are the most important plant bioactive constituents. The most active chemical compounds are slightly hydrophilic; however, they are freely lipophilic and more soluble in organic solvents such as water, alcohol, ketones, and esters, and could be used as reducing, stabilizing, chelating, and capping agents to react with zinc ions, as well as scaffolds to direct the formation of ZnO NPs in solution (Alzohairy, 2016).

2.8.3. Mechanism of Zinc oxide nanoparticles formation

Plant ingredients such as terpenoids, polyphenols, alkaloids, and phenolic acids are involved in the production of zinc oxide nanoparticles. Flavonoids are polyphenolic chemicals that contain a variety of functional groups capable of donating electrons for the reduction of Zn^{2+} ions to the creation of ZnO NPs. The active element responsible for Zn^{2+} ion reduction differs based on the plant extract or bioactive compounds employed. Zinc oxide nanoparticles were created in this study by combining extracted neem leaf with zinc nitrate solution in a green synthesis process. The neem leaves include biomolecules such as phenolic acids, flavonoids, proteins, terpenoids, and alkaloids that could be employed as reducing, stabilizing, chelating, and capping agents when reacting with zinc ions, as well as scaffolds to drive the synthesis of ZnO NPs in solution. Although the precise method for the production of nanoparticles utilizing extracts has yet to be determined, it has been proposed that distinct polyol components are involved in the synthesis of the nanoparticles. The presence of plant extracts resulted in the synthesis of ZnO NPs is

confirmed by the FT-IR spectra. The peaks in the spectrum indicate the secretion of some water-soluble organic components (phytochemicals) from plants, which could have contributed to the creation of ZnO NPs by a similar mechanism. This provides compelling evidence for the role of polyphenols in fast production as well as the stability of metallic oxide nanoparticles in aqueous media. This demonstrates that flavonoids, polyphenols, and other phytochemicals contained in plant extracts are responsible for the creation of nanoparticles such as ZnO NPs by first donating electrons to the metallic cation and then stabilizing them the newly created nanoparticles. Since neem leaves include phytochemicals such as phenolic acids, flavonoids, and alkaloids, it was anticipated that they might aid in the synthesis of ZnO NPs by donating electrons to the zinc (II) cation of the zinc nitrate solution (Banala & Karnati, 2015). Overall, the findings demonstrated the presence of phenolic chemicals, terpenoids, or proteins linked to the surface of ZnO nanoparticles. The interaction of free amino and carboxylic groups with the zinc surface may explain the stability of ZnO nanoparticles.

Functional group bonds such as –CO–C–, –C–O–, and –C=C– were formed from heterocyclic compounds, and amide bands derived from proteins were present in the leaf extract and served as the nanoparticles capping ligands. Furthermore, the proteins in the medium inhibited agglomeration and aided instability by producing a coat that covered the metallic nanoparticles. Furthermore, the proteins in the medium inhibited agglomeration and aided instability by producing a coat that covered the metallic nanoparticles. In the green synthesis of ZnO NPs, biomolecules found in Neem leaf extract induce the reduction of Zn^{2+} ions from Zn $(NO_3)_2.6H_2O$ to ZnO NPs, or in another synthesis, the plant extract of neem acts as a ligation, and the aromatic hydroxyl group present in Polyphenolic ellagic acid ligates with zinc ions to form the zinc-delegate complex. This combination is calcined at 400 °C for 2 hours in the static air, resulting in the production of ZnO NPs (Kahraman et al., 2018).

$$Zn\ (NO_3)_2 \longrightarrow Zn^{2+} + 2NO_3^-$$
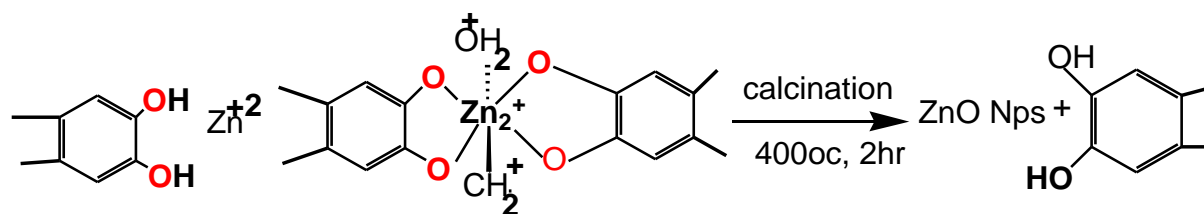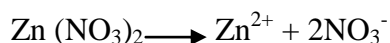
Figure 2.3: Mechanisms of ZnO NP production via plant leaf extracts (Kahraman et al., 2018).

2.9. Agricultural wastes as supportive porous materials

Research is ongoing to attempt and utilize agricultural as well as industrial waste as low cost adsorbents (Manyangadze et al., 2020). There is a growing interest in adopting low-cost adsorbents for adsorption uses. Adsorption will be a promising strategy if an adsorbent is affordable and ready to use (Hina, Khatoona & Jai Prakash, 2016). Agricultural waste be presumed to be cost-effective adsorbents since they are present in large amounts in nature, cheap, need slight proceeding, and are productive resources as well as it can can be converted into less expensive and more valuable bio-adsorbents. So that, it may have the potential as absorptive due to their economic and physio-chemical characteristic. The key elements of agricultural waste include water, hemicelluloses, proteins, lignin, simple sugars, hydrocarbons, starches, and lipids, encompassing several forms of functional groups. These functional groups lead to an increase of active sites and greater adsorption of impurities (Verma, R. K et al., 2021; Ali & Hassaan, 2017). Furthermore, agricultural wastes feature loose and porous structures, as well as more critical functional groups such as hydroxyl and carboxyl groups, which allow for adsorption and hence can be employed as a supporting material for nanoparticle materials (Hina, Khatoona & Jai Prakash, 2016).

Various studies have investigated the removal of hazardous dyes from wastewater utilizing various agricultural biomasses such as straw, fiber, husk, stalk, and so on (Hina, Khatoona & Jai Prakash, 2016). Teff straw has no commercial value except for its use as animal feed, open-burning fuel, and mud-composite for rural house building. Every year, around two million tons of teff straw are discarded as waste (Bageru & Srivastava, 2018).

As an agricultural waste, locally available teff straw, low cost, require little processing, and cost-effective technology can be used as bio-adsorbents in dye removal (Hina, Khatoona & Jai Prakash, 2016). Teff straw, as a type of abundant agriculture waste, is rich in various natural polymers. The hydroxyl functional groups found in Teff straw play a vital role in combining nanoparticles with the straw which then enables in modifying the properties of nanoparticles. Straws can stabilize nanoparticle nanomaterials. It also has a biodegradable properties so that it can be easily degraded in the natural environment without producing secondary pollution to the environment (Hina, Khatoona & Jai Prakash, 2016).

In general, straw-based adsorbents have been already paid more attention to wastewater purification, and they are believed to be a kind of low-cost, non-toxic, and environment-friendly materials. Additionally, using materials with a special functional group or loose porous structure materials as supports of nanoparticles recover reactivity and stability. They can be applied in the removal of dyes, heavy metal ions, and other hazardous substances contained in industrial sewage (Pirbazari A, 2015).

2.10. Comparision between Zinic oxide and Teff straw assisted Zinic oxide nanoparticles

Natural resources, as well as waste materials (or products) from industrial and agricultural activities, can be used to make more affordable and effective adsorbents. The majority of agricultural waste is made up of lignocellulosic material (containing 35-36 % cellulose, 25-35 % hemicelluloses, 20-30 % lignin and other components). These feature a porous structure, a large free-surface volume, and plant-derived lignocellulosic resources. As a result, agricultural waste exhibits sorption properties for a wide range of solutes (Guncha Munjal, 2015). Lignocellulose biomass is valued for its economic and environmental benefits, as well as its availability, renewability, and cost-effectiveness. It can be used in its natural state, carbonized, or chemically treated state to improve pollution removal efficiency, as stated by Danish et al. (2018). The high amount of cellulose, lignin, and other polar functional groups of lignin in lignocellulose biomass, such as alcohols, aldehydes, ketones, carboxylic, phenolic, and ether groups, improves the adsorbent binding ability of pollutants via various binding systems (Danish et al., 2018). Surfaces of adsorbents must have a large specific surface area, sorption capacity, and active sites (Mahmoud et al., 2010). The highly specific surface area could increase the adsorption ability of the materials due to more adsorption sites. Commonly, nanoadsorbent materials have some intrinsic limitations and most of the nanoadsorbent materials have less sorption ability. The facts propose that NPs are not as effective when used in their pure forms. In this regard, functionalization or surface modification of nanoadsorbents is one of the be st methods to increase the sorption ability as well as the stability of the materials, even in harsh conditions (Chauhan et al., 2021).

There are numerous advantages to using materials like zinc oxide nanoparticles as a potent sorbent on the surface of other adsorbents. This process can result in an increase in the number of sorption active sites on the adsorbent (Sharifi & Shoja, 2018).

In the same scenario, surface modification of nanoparticles has been shown as a tool to significantly improve their applicability in terms of adsorption capacity, adsorption efficiency, dispensability, and stability and/or inertness in harsh environments. Surface modification has also been shown to prevent the problem of particle aggregation (Manyangadze et al., 2020) . So, pure zinc oxide nanoparticles have a lower removal percentage efficiency than Teff straw assisted Zinc oxide nanoparticles.The reason for this is that, the powdered teff straw has a smaller particle size, which increases the surface area of the adsorbent (zinc oxide nps), which inturn increases active sites and improves removal effectiveness since the nanoparticles become surface modified or functionalized.

<div align="center">

3. MATERIALS AND METHODS

</div>

3.1. Materials

3.1.1 Chemicals and reagents

In this thesis, fresh leaves of neem for phenol extraction were collected from Jimma, around Jimma Institute of Technology (JIT) Campus, and Teff straws which used as porous materials were collected from the agricultural farm field of Wolkite, Gubre, Gurage zone using plastic bags and used as raw materials. The Materials**,** chemicals, and reagents required for the experimentation were: Methylene blue ($C_{16}H_{18}N_3CLS$, AR 85% Merck, Bangalore, India), and analytical grade zinc nitrate (99 %) (Merck, India) used for stock solution preparation, potassium bromide or KBr (to form pellet paste), Distilled water, sodium chloride (99.5 %) (LOBA Chemie, India) for the analysis of point of zero charges, hydrochloric acid (HCl, 99%, Sigma-Aldrich, Bangalore, India) and sodium hydroxide (99.8%) (ATDM, Turkey) for pH adjustment, deionized and distilled water for solutions preparations,Potassium dichromate (K_2CrO_3) and Silv er nitrate ($AgNO_3$) for chloride testing, Potassium dichromate, standard sulfuric acid (St. H_2SO_4) and ferrous ammonium solution for COD testing, Ferroin indicator as an indicator for the color c hange.

The apparatus used were Ceramic crucible, Burrete, conical flasks, measuring cylinders, funnel, test tubes, spatula, filter paper, hot plate, furnace (oven), magnetic stirrer, refrigerator, knife, mor tal and pastel (grinder), pipettes, PH meter, centrifuge and beaker, Hach COD apparatus, Incubati on bottles, and water bath electronic beam balance. The Equipments such as XRD (DW-XRD-Y7000,China), UV-Vis Spectrophotometer (UV- 1800, Germany), and FTIR (Perkin Elmer spectrum Two, China) were used to characterize synthesized ZnO-TSA nanoparticles.

3.2. Methods

3.2.1. Methodological Design
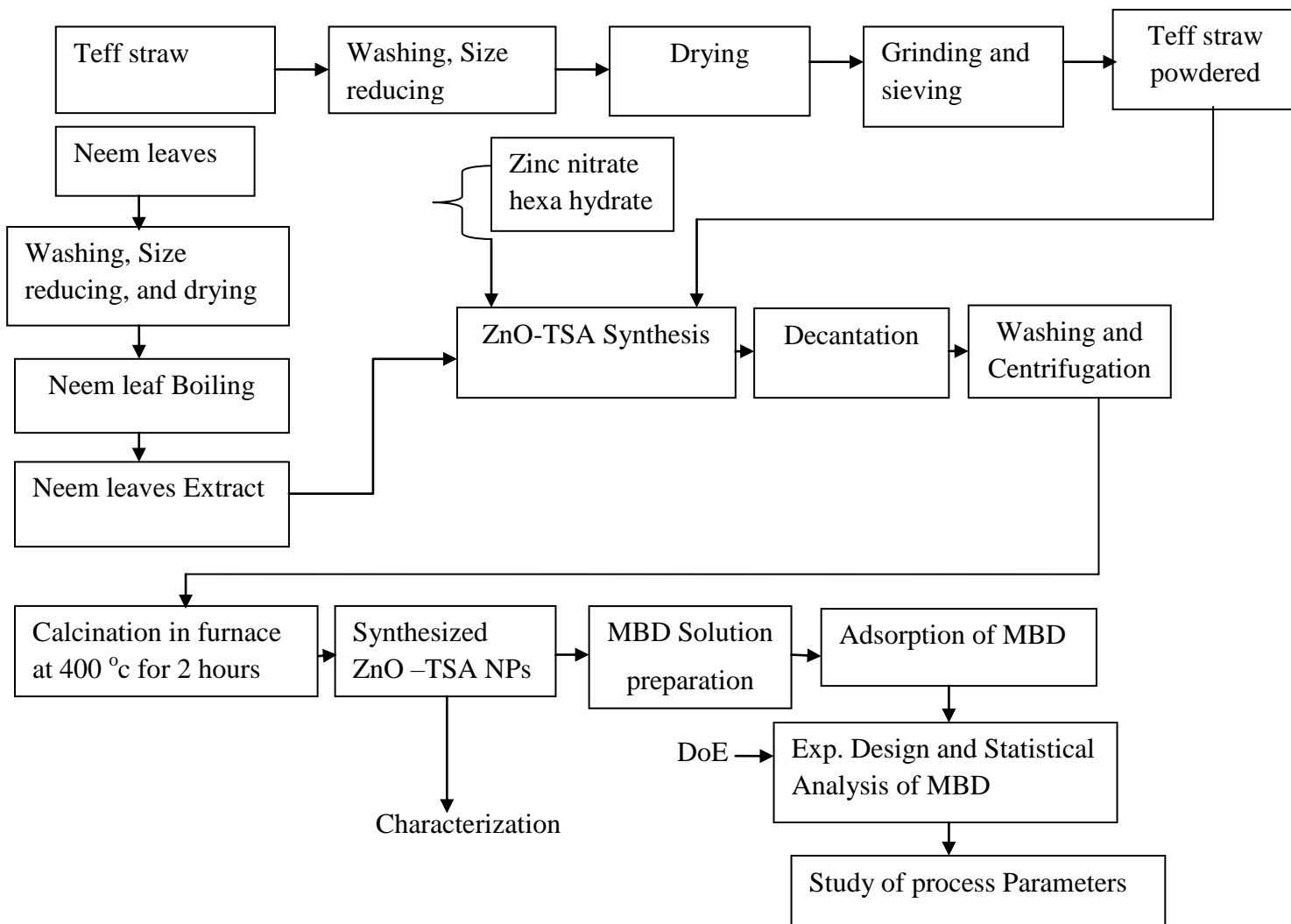
Figure 3.1: Scheme showing the synthesis of ZnO-TSA Nps and removal of MBD

3.3. Experimental Procedures

3.3.1. Collection and Preparation of Teff straw porous material sample

After collection, the straw samples were air-dried , cut into smaller pieces to reduce the size and then washed five times with distilled water to remove dust particles and other soluble impurities. The samples were ground in an electric mill after drying and allowed to pass through a 0.25 mm. The powdered samples were dried for 24 hours in a 105°C oven until the bulk of the powdered sample was constant (Razali et al., 2020).

3.3.2. Collection and Preparation of Neem (Azadirachta Indica) leaf extract

According to Senthilkumar et al. (2017) with slight modification, the collected neem leaves were washed thoroughly 2-3 times with distilled water before use. The leaves were allowed to dry at room temperature (25 ^{0}C), and 10g were taken for synthesis. 10g of leaves were boiled in 100 mL of distilled water for 20 min at 60 degrees Celsius. During the boiling process, a light-yellow solution was formed that was cool at room temperature. The yellow-colored extract was then filtered with filter paper (Whatman No.1) and refrigerated. The resulting extract was used in the synthesis of zinc oxide and Teff straw-assisted zinc oxide nanoparticles as neem extract solutions.

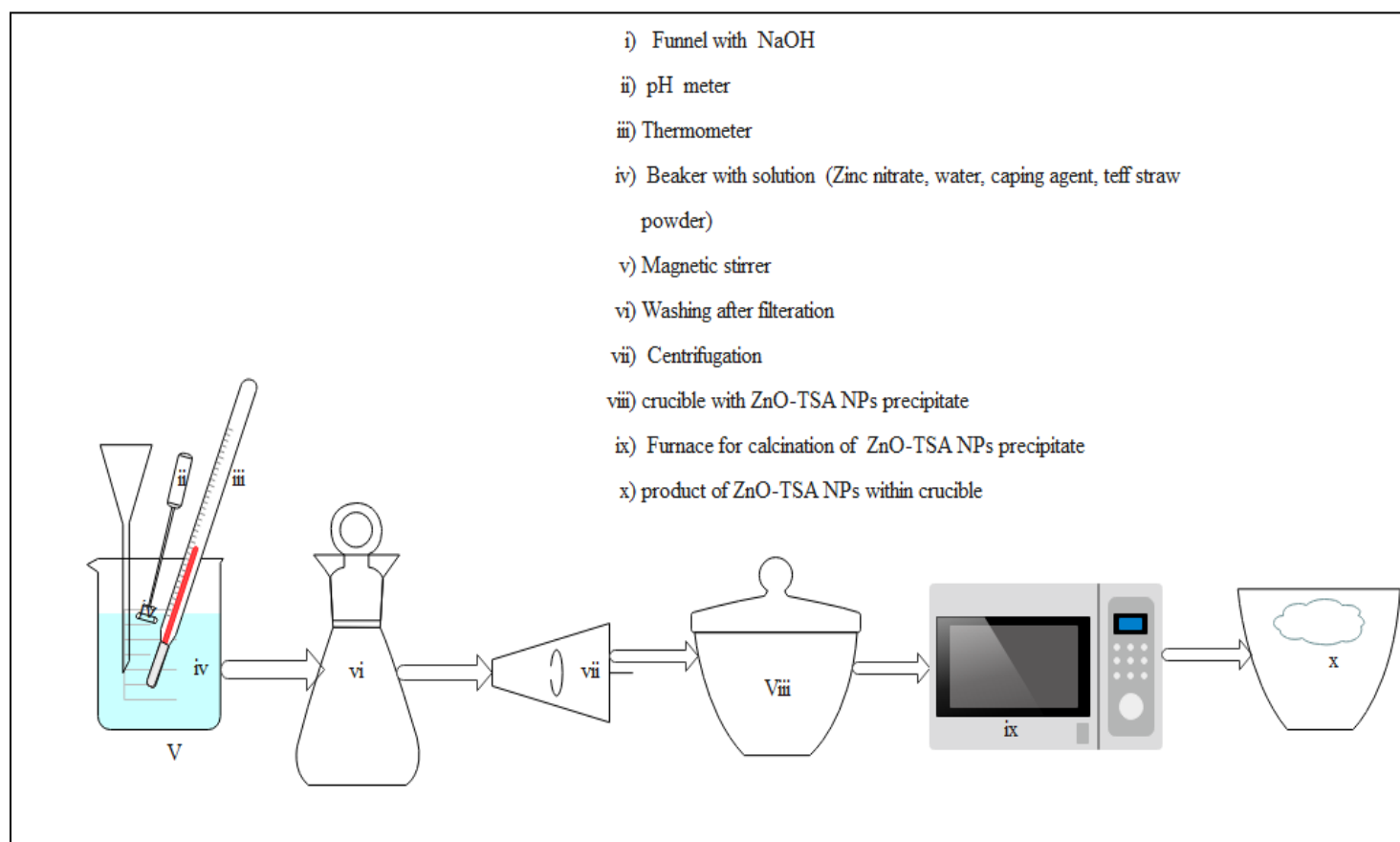#### 3.3.3. Green synthesis of ZnO nanoparticles

A typical procedure was used to synthesize zinc oxide nanoparticles. 10 mL of neem leaf aqueous extract was taken from the stock solution (stored in the refrigerator). Later, 2g of zinc nitrate hexahydrate crystal was dissolved in the neem leaf extract solution while using a magnetic stirrer to maintain constant stirring. After the mixture was completely dissolved, the solution was boiled at 60 °C with a magnetic stirrer until a deep yellow colored paste formed. The paste was transferred to a ceramic crucible cup and placed in a 400 ^{o}C furnace for 2 hours (Senthilkumar et al ., 2017). Finally, the resultant light yellow powder is used for further characterization teff straw assisted zinc oxide of nanoparticles.

3.3.4. Teff straw assisted ZnO nanoparticles

Two grams of Zn $(NO_3)_2.6H_2O$ were dissolved in 100 mL deionized water and added to a 250 mL beaker with 10 mL of neem leaf extract and 0.5 g of ground teff straw powder, then heated

for two hours at 60 ^{0}C under mild string using a magnetic stirrer. Then 4ml of 2 M (8g) NaOH was added dropwise until the pH of the solution reached 10 and the solution changed to a deep yellow color, indicating the formation of Teff straw assisted ZnO nanoparticles. The solution was left undisturbed, and the deep yellow precipitates accumulated at the flask's bottom. The solution was left alone, and the yellow precipitates accumulated at the bottom of the flask. After decanting the solution, the precipitates were isolated and washed twice with deionized water. Following that, the solution was centrifuged at 250 rpm for 20 minutes. The centrifugation and washing procedures were carried out three times each. The precipitates were then carefully transferred to a ceramic crucible and dried in a furnace at 400 °C for 2 hours.

Finally, the Product was kept in appropriate place for characterization and applicability for Removal of Methylene Blue Dye from Textile industry wastewater (adsorption purposes) (Pirbazari & Saberikhah, 2014; Razali et al., 2020).

i)   Funnel with NaOH

ii) pH meter

iii) Thermometer

iv) Beaker with solution (Zinc nitrate, water, caping agent, teff straw powder)

v) Magnetic stirrer

vi) Washing after filteration

vii) Centrifugation

viii) crucible with ZnO-TSA NPs precipitate

ix) Furnace for calcination of ZnO-TSA NPs precipitate

x) product of ZnO-TSA NPs within crucible

Figure 3.2: Experimental setup for the synthesis of ZnO-TSA nanoparticles

3.3.5. Characterization techniques of the synthesized ZnO Nps

The synthesized ZnO NPs characterized by UV–Visible absorption spectroscopy, X-ray diffractometer spectroscopy, and Fourier Transform Infrared spectroscopy analyses.

3.3.5.1. UV-visible spectrophotometer analysis

The UV-visible spectral analysis confirmed the synthesis of ZnO-TSA NPS. For the analysis, a small aliquot of the supernatant of the synthesized ZnO or ZnO-TSA nanoparticles was used. As a result, the characteristic absorption peak for the synthesized ZnO-TSA nanoparticles was recorded and analyzed in a spectrophotometer with a resolution of 1 nm using UV–visible absorption spectroscopy in the wavelength range of 200 to 800 nm.

3.3.5.2. X-ray diffraction (XRD) analysis

X-ray diffraction (DW-XRD-Y7000) was used to study the crystallite size and crystallinity of green synthesized ZnO-TSA NPS. Characterization was performed on the well-dried and powdered samples. It was used with CuK radiation (=0.154021 nm) at 30 kV and 25 mA. The scanning was done from 10 to 80o in $0.03°s^{-1}$ steps to collect 2θ data. Match! Software version 3.10.2.173 and were used to analyze the phase and pattern of the XRD data. Scherer's Equation was used to calculate the average crystalline size of ZnO-TSA NPS.

$$D = \frac{k\lambda}{\beta \cos\theta}$$
(3.1)

Where D is the mean crystalline size, κ is the Scherer's constant (shape factor) with the value of 0.9, λ is the X-ray wavelength (0.154021 nm), β is the full width at half maximum (FWHM) in radians, and θ is the Bragg angle.

3.3.5.3. Fourier Transform Infrared (FT-IR) spectrum analysis

The surface functionalization of the synthesized ZnO-TSA NPS was characterized using Fourier transform infrared (FT-IR) spectroscopy (Perkins Elmer L1600300). The synthesized adsorbent was dried, ground, and mixed in appropriate ratios with KBr powder to form a pellet for FT-IR spectroscopy analysis. The pelletized sample was then analyzed using FT-IR spectra before the adsorption experiments. These measurements were carried out, and spectra in the 500-4000 cm^{-1} range were collected.

3.4. Preparation of Methylene blue adsorbate

In this study, MB powder was used as the adsorbate molecule in adsorption experiments. Preparation of stock solution of MB was carried out by dissolving 1 g of MB in 1000 mL distilled water to get 1000 mg/L. The intermediate solution of 100 mg/L of MB was prepared from the stock solution of 1000 mg/L by using dilution law. Additional, 10, 30, 50, 70, and 90 mg/L of working standard solutions of MB were prepared from the intermediate dye solution by dilution. The working standard solution was prepared by adding real sample solution (Mulushewa et al., 2021).

3.4.1. Adsorption Experiments

With a slight modification as stated by Ahmadi et al. (2020), at room temperature, all adsorption experiments were performed. A stock solution of MB at a concentration of 1000 mg/L was prepared for the experiments. The various MB concentrations were prepared by dilution in deionized water (using the $C_1V_1=C_2V_2$ relationship). On MB removal, the effects of ZnO-TSA NPS dosage (0.2, 0.3, and 0.4g/L), contact time (40, 60, and 80 min), pH (5, 8, and 11), and initial MB concentration (30, 50, and 70 mg/L) will be investigated. 0.1M HCl or 0.1M NaOH solutions will be used to adjust the pH of the solution. Each experiment's solution volume was 100 ml. A mixer at 180 rpm was used to mix the mixture for different contact times. Following the specified contact time, each sample was filtered through Whatman filter paper and analyzed for MBD residuals. The absorbance of MBD residuals was measured using a UV-Visible spectrophotometer at 664 nm, and the concentration of MBD residues was calculated using the calibration curve. The following equation was used to calculate the adsorption capacity of the NPs (qe) (3.2).

$$qe = \frac{(Co - Ce)V}{M}$$

(3.2)

Also, the removal efficiency (%R) was calculated based on Eq. (3.3)

$$\% R = \frac{(Co - Cf)}{Co} * 100$$

(3.3)

Where C0 (mg/L) is the initial concentration of MB and Ce (mg/L) is the equilibrium liquid phase concentration of MB, Cf (mg/L) is the final concentration, V is the volume of the solution (L) and M is the amount of ZnO-TSA NPs used (g).

| Stock solution of (1000 mg/L) MBD prepared | → | Various MBD concentrations were prepared using dilution law | → | Different amount of MBD concentrations (30, 50,and 70 mg/L) taken from stock solution | → | The PH of the MBD solution adjusted to (5,8,and 11) | → | The adsorbent dosage adjusted to (0.2, 0.3,and 0.4 g/L) |

| Mixing the solution properly with contact time 40,60,and 80 min) and mixing speed of 180 rpm | → | The samples was filtered at different time interval using what-man filter paper and stored | → | The filtered and stored supernatant analysis of MBD ion in asolution was performed using Uv | → | Concentration of MBD residues was calculated using the calibration curve |

Figure 3.3: Experimental procedures of batch adsorption studies for determination of optimum pH, initial concentration, adsorbent dosage, and contact time.

3.5. Characterization of Textile Wastewater

The textile wastewater was obtained (collected through polyethylene bottle) from the Arbaminch textile factory. It is necessary to identify the concentration of Physico-chemical parameters before conducting treatment experiments. Thus, an initial experiment is carried out to determine the character of wastewater in terms of parameters namely COD, TSS, TDS, TS, turbidity, and pH. These experiments are conducted in the Environmental engineering laboratory Of Jimma institute of technology based on procedures that are provided under standard methods for the examination of water and wastewater.

3.5.1. UV- analysis of methylene blue in the textile wastewater

To decide the concentration of MB in the textile wastewater, five series of standard MB solutions of (10, 30, 50, 70, and 90 mg/L) were prepared by diluting the intermediate solution of MB with distilled water.

Blank solution and working standards were run in UV Spectrophotometer at a maximum wavelength of 664 nm and five point calibration curves were established.

Then, textile wastewater sample solutions were taken to the UV spectrophotometer and direct readings of the sample absorbance were recorded and the concentration of the sample was calculated from the standard calibrated equation (Mulushewa et al., 2021; Getasew et al., 2019).

$$y= mx+b \qquad\qquad\qquad (3.4)$$

Where, y is absorbance,m is slope,x is final or equilibrium concentration,and b is interecept.

1.   Chemical oxygen demand (COD) determination

COD testing was performed in accordance with (ASTM D1252, 1989). Hatch photometer (model DR 1451) used to measure the COD Value. 2-3 drops of standardized COD reagent ($K_2Cr_2O_6$) was pipetted into culture tubes containing 2.5 ml of sample water,then inverting each vial up and down several times, the reagent was mixed with the sample and inserted into COD reactor. Ablank were prepared based on my COD range by mixing equal amount of distilled water (2.5 ml) with respective reagent (2-3) drop. Meanwhile,the COD reactor (HANNA reactor) was warmed up until it reaches up to 150 ^{0}c with strong oxidizing agent, K_2CrO_6 digestion solution,which oxidizes organic matter chemically.Then the sample and the blank was feed into the reactor and stayed there for two hours at the same temperature. After two hours, the reactor was off and waiting for some time,until the system cools down to areasonable temperature,the sample and the blank was taken out and put into arack until it cools down to room temperature. Finally Hatch photometer (model DR 1451) as calibrated using the blank,the sample was inserted in the photometer for reading.

```
┌────────────────────┐   ┌────────────────────┐   ┌────────────────────┐   ┌────────────────────┐
│ Mix 3-drops of     │   │ Blank was prepared │   │ Feed sample and    │   │                    │
│ COD reagent        │──▶│ (3-drops of COD    │──▶│ blank into COD     │──▶│ Off Reactor after  │
│ (K₂CrO₃) with      │   │ reagent + 2.5ml    │   │ reactor for 2 hrs  │   │ 2 hrs              │
│ 2.5ml water        │   │ water sample)      │   │ @ 105 ⁰c           │   │                    │
│ sample in tube     │   │                    │   │                    │   │                    │
└────────────────────┘   └────────────────────┘   └────────────────────┘   └────────────────────┘

┌────────────────────┐   ┌────────────────────┐
│ Take and put into  │   │ Insert into Hatch  │
│ rack until         │──▶│ photometer         │
│ sample and blank   │   │ for reading        │
│ cools down         │   │                    │
└────────────────────┘   └────────────────────┘
```
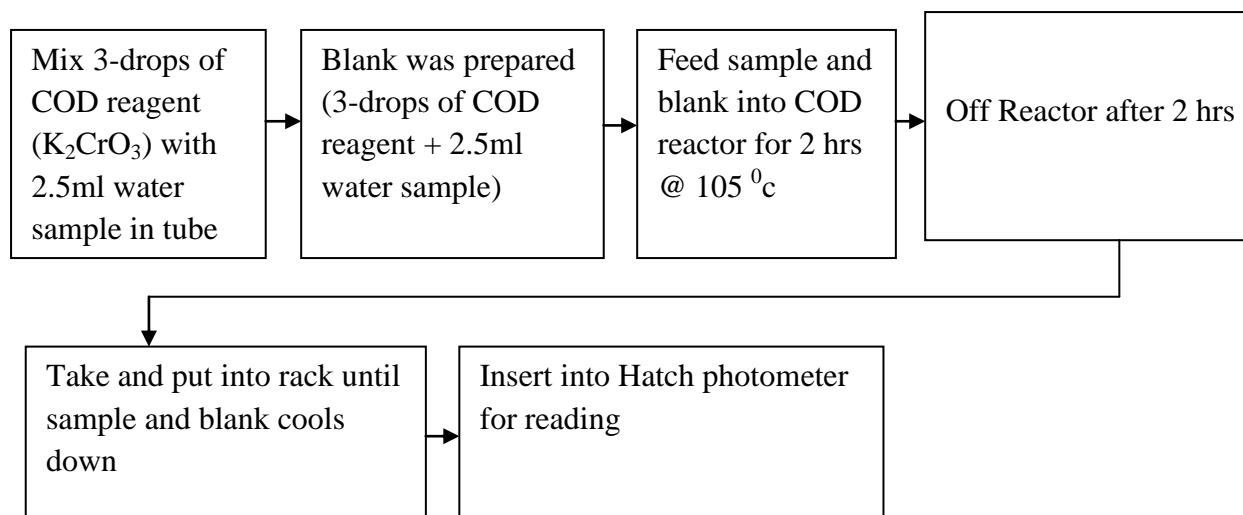
Figure 3.4: Experimental procedures for Chemical oxygen demand (COD) determination

2. pH and Turbidity determination

pH rand turbidity were directly measured with pH meter (3505 PH meter, model and HI 93703 PH meter) respectively.The digital pH meter was calibrated using several buffer solutions before inserting the electrode into the sample and recording the measurement (ASTM D3838- 05, 2017).

3.Total dissolved solid (TDS), Total solid (TS), and Total suspended solid (TSS) determination

TDS determination**:** The total dissolved solids of the wastewater sample were determined using a conductivity/TDS meter.The test for TDS was performed in accordance with (ASTM D1252, 1989), in which the sample of wastewater was filtered by vacuum filter and the residue retained on filter was collected in ceramic crucible and dried in an oven at (103-105) ^{0}c then ,weighed. Finally TDS was calculated as:

$$TDS = \frac{Amount\ of\ dried\ sample\ (mg)}{Volume\ of\ sample\ water(L)}$$

(3.5)

TSS=TS-TDS   (3.6)

TS are obtained by evaporating the water at 180 ^{0}c and the remaining solid residue was weighed.

4. Chloride determination

In chloride determination of wastewater, testing of textile wastewater chloride before treatment and after treatment was carried out. This can be performed using volume of silver nitrate consumed by sample and volume of silver nitrate consumed by blank. This can be calculated using equation (3.7).

$$Cl^-(mg/L) = \frac{(A-B) * 0.0282 \, N * 35.5 * 100}{20}$$

(3.7)

Where, A= Volume of silver nitrate ($AgNO_3$) consumed by sample (mg/L),B= Volume of silver nitrate ($AgNO_3$) consumed by blank (mg/L) and N=Normality of ferious ammonium solution.

3.6. Adsorption Isotherms

Adsorption isotherms are very useful for defining the adsorption capabilities of different adsorbents. The adsorption isotherm is the relationship between the amount of adsorbate adsorbed on the adsorbent and the equilibrium concentrations of adsorbate at constant temperatures. The adsorption isotherm indicates how the adsorption molecules distribute between the liquid phase and the solid phase when the adsorption process reaches an equilibrium state.

The study of equilibrium adsorption data, by fitting them to different isotherm models, is an important step to find the suitable model that can be used for design purpose . Adsorption isotherm study was carried out on two well-known isotherms, Langmuir and Freundlich. The applicability of the isotherm equation was compared by judging the correlation coefficients, R^2.

3.6.1. Langmuir Adsorption Isotherm

According to the Langmuir model, the adsorbent surface has numerous active interaction sites for the adsorption process. It is concerned with the relationship between adsorbed material and its equilibrium concentration. The linear form of the Langmuir adsorption isotherm model is described, allowing for the processes of adsorption and desorption of molecules on the surface (Khoshhesab et al., 2010).

$$\frac{C_e}{q_e} = \frac{1}{bq_{max}} + \frac{C_e}{q_{max}}$$

(3.8)

Where qe denotes the mass of adsorbate adsorbed over adsorbent (mg/g); Ce denotes the equilibrium concentration of adsorbate acquired in liquid phase after adsorption (mg/L); qmax denotes the maximum adsorbate that can be adsorbed (monolayer capacity) (mg/g), and b denotes the Langmuir isotherm constant (L/mg). In another manner, using the equation given by, the separation factor (dimensionless), also known as the RL factor or the equilibrium parameter, was also be determined using the equation given by (Zaidi et al., 2021; Sharifi & Shoja, 2018).

$$R_L = \frac{1}{1 + bC_o}$$

(3.9)

The value of RL indicates the adsorbent's suitability for adsorption, i.e., the affinity between adsorbate and adsorbent. If 0<RL<1.0 represents favorable adsorption, RL > 1.0 represents unfavorable adsorption, and RL = 0 represents irreversible adsorption (Dar et al., 2013).

3.6.2. Freundlich adsorption isotherm

It is a relationship between the amount of an adsorbate absorbed per unit weight of adsorbent and the adsorbate equilibrium concentration (Ce) in the fluid.

The Freundlich model, unlike the Langmuir model, is based on multilayer adsorption and may be expressed as an equation (Khoshhesab et al., 2010).

$$\frac{X}{M} = KC_e^{1/n}$$

(3.10)

Where, K and n are the Freundlich coefficients, X is the weight of adsorbate adsorbed on M unit weight of adsorbent, and Ce is the adsorbate equilibrium concentration. However, it is possible to express the equilibrium condition as an equation.

$$\log(q_e) = \log(k_f) + \frac{1}{n \log(C_e)}$$

(3.11)

Where, qe is the mass of adsorbate adsorbed over adsorbent (mg/g); K_f, is the Freundlich capacity factor (units determined by qe); C_e is the equilibrium concentration of adsorbate in liquid phase after adsorption (mg/L); n is Freundlich intensity parameter. The intercept and slope of a plot of log (q_e) versus log (C_e) can be used to determine the value of coefficients k_f and n.

3.6.3. Determination of point of zero charge

The pH$_{pzc}$ (point of zero charges) is pH when the charge on the surface is zero. The procedure of the pH drift method could be described as follows: to a series of nine 250 mL conical flasks, 50 mL of 0.01 M NaCl was added. Then, the initial solution pH values (initial pH) were adjusted as 2,3,4,5,6,7,8,9, and 10 using 0.01 M HCl solutions and 0.01 M NaOH. After constant value of initial pH had been reached, 0.10 g of ZnO-TSA Nps sample was added into each conical flask and caped them immediately. This mixture was kept undisturbed for 12 h till reaching equilibrium. After 12 h, the pH of the solution was measured carefully by using a pH meter and noted as pH final. The pH$_{pzc}$ of the ZnO-TSA Nps sample is the point when pH initial = pH final. The plot of the initial pH versus difference in final pH was constructed and the pH of point of zero charges (pH$_{pzc}$) was obtained as the intercept on an x-axis of the plot. Similar reports was stated by Bageru & Srivastava (2018) ; Swamy et al. (2017).

3.7. Experimental Design and Statistical Analysis

Data analysis was using Design-Expert version 11.1.2.0 software tool by RSM using Central Composite Design to evaluate the effects of the process variables. CCD is a common and efficient design in RSM; it was selected as a designing tool to investigate the interactive effect of process variables and in building mathematical models to describe the overall Methylene blue dye adsorption process. To study the process parameters, four major factors: ZnO-TSA NPS dosage (0.1- 0.5 g/L), initial Methylene blue dye concentration (10-90 mg/L), solution pH (2-14), and contact time (20-100 minutes) were selected.

Ranges of factors were selected by considering the earlier related works (Ahmadi et al., 2020). The response variable was removal percentage. The design of the experiment helps to optimize and set of combination of process parameters. The significance of the result was set from the analysis of variance (ANOVA) (Ahmadi et al., 2020; Afolabi et al., 2021).

Table 3.1: Experimental levels of selected variables using Response surface methodology with the central composite design.

Name	Units	Low	High	-alpha	+alpha
ZnO-NPs dosage	g/L	0.2	0.4	0.1	0.5
Contact time	Min	40	80	20	100
Intial Concentration of methylene blue dye	mg/L	30	70	10	90
pH		5	11	2	14

The total number of the experiments (N) was estimated using equation 3.12. The experiments were conducted using four independent process variables consisting of 16 factorial points, 8 axial points, and 6 center points (Afolabi et al., 2021;Ahmadi et al., 2020).

$$N=2^n+2n+n_c \qquad (3.12)$$

$$2^4+2*4+6 = 16+8+6 = 30$$

The optimum conditions obtained using the CCD model were validated by conducting laboratory experiments. Statistically, the optimum conditions were obtained by the following model equation:

$$Y = \beta_O + \sum_{i=1}^{k} \beta_i x_i + \sum_{i=1}^{k} \beta_{ii} x_i^2 + \sum_{i=1}^{k}\sum_{j=i+1}^{k} \beta_{ij} x_i x_j + \varepsilon \qquad (3.13)$$

Where Y is a response of the process, i stands for linear coefficient and j represents quadratic coefficients, x_i and x_j are the independent variables, β_0 is standing for regression coefficient, k is the number of factors in the design, and ε represents an error (Afolabi et al., 2021; Ahmadi et al., 2020).

4. RESULTS AND DISCUSSION

4.1. Characterization of synthesized ZnO-TSA nanoparticles

4.1.1. UV-Visible spectrophotometer analysis

The UV-Visible spectrum of the synthesized ZnO Nps and ZnO-TSA nanoparticles are shown in Figure 4.1. A UV-visible spectrophotometer was used to investigate the optical characteristics of teff straw-assisted zinc oxide nanoparticles. Because of the surface plasmon resonance (SPR) effect, conducting electrons begin to oscillate at a specific wavelength range. The production of green synthesized ZnO-TSA was confirmed when the absorption peak (lambda max) was detected near 321 nm (Set al., 2020). The typical surface plasmon resonance absorption peak at 321 nm by UV-Visible spectroscopy revealed the formation of ZnO-TSA nanoparticles. This confirms the synthesize of ZnO-TSA nanoparticles by the reduction of zinc nitrate hexahydrate solution using neem leaf extract containing polyphenol as a reducing and capping agent. A corr esponding study of UV-Vis spectra of neem leaf extract has been shown to confirm the formation of Zinc oxide nanoparticles. In the same manner, surface plasmon resonance absorption peak of the synthesized ZnO Nps was at 312 nm.
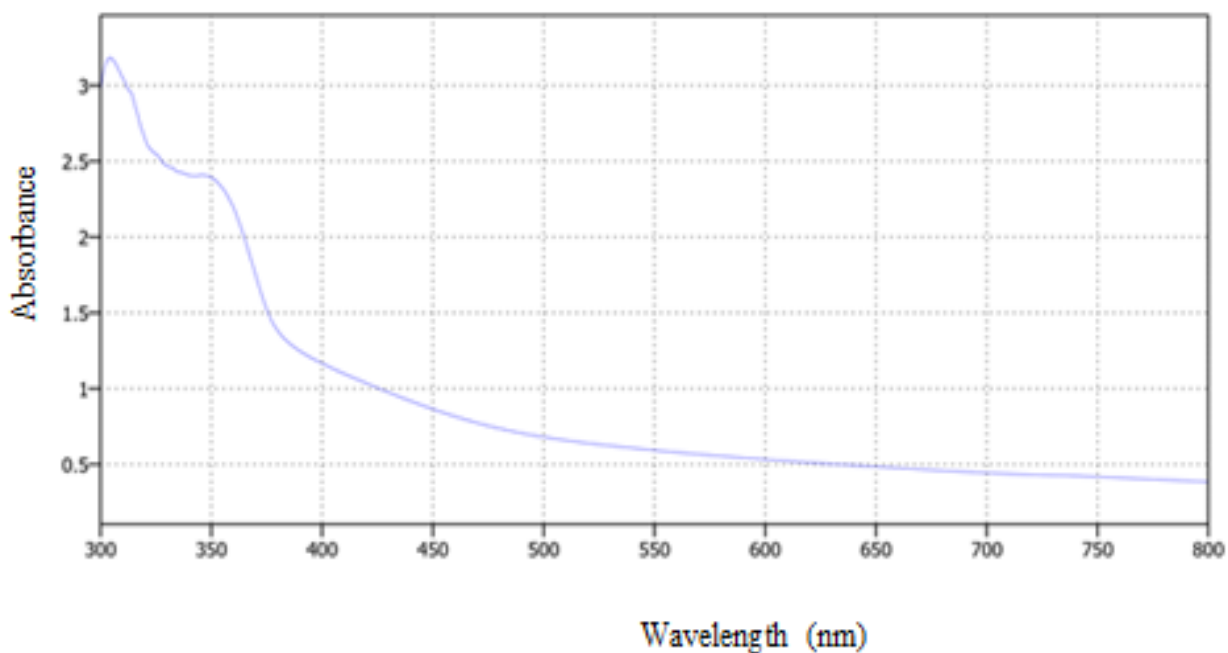
(a)
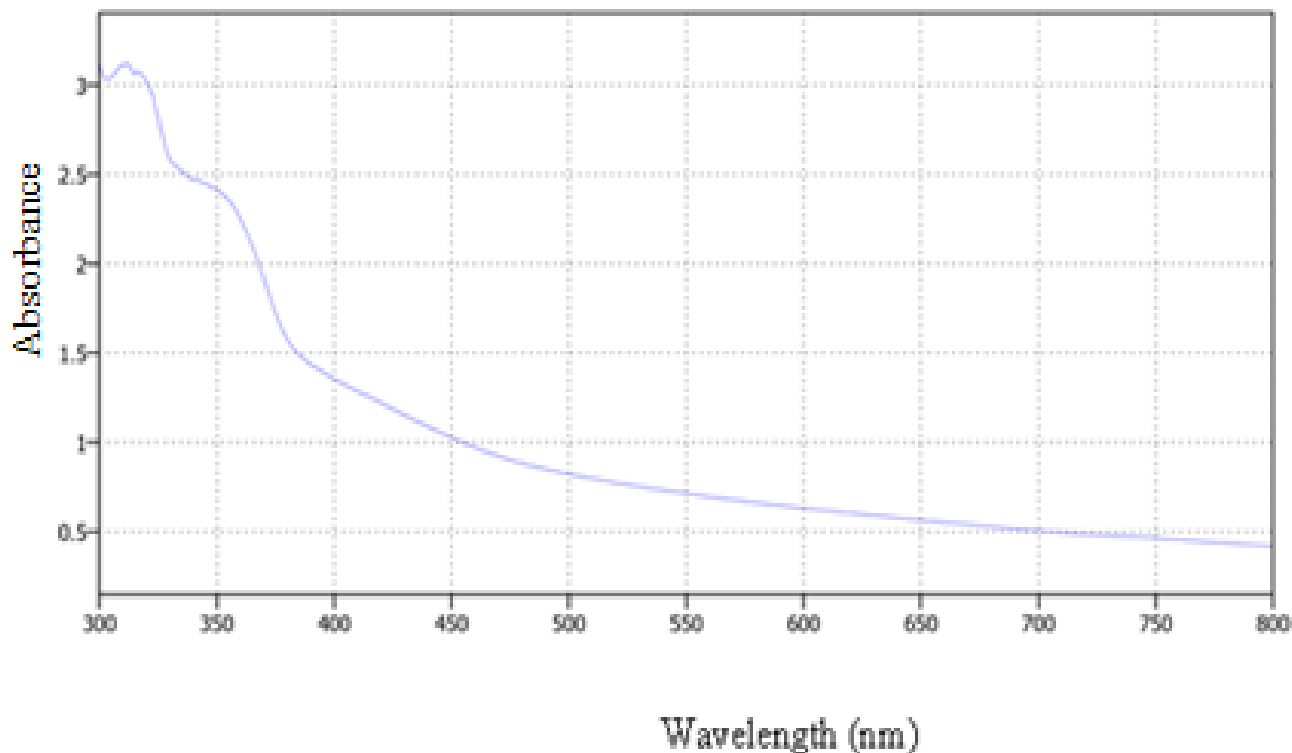
(b)

Figure 4.1: UV−Visible absorption spectra of the synthesized ZnO-NPs (a) and ZnO-TSA NPs (b)

4.1.2. Fourier Transform Infrared (FT-IR) spectrum analysis

Fourier transform infrared spectroscopy was used to characterize functional groups and surface functionalization. The FT-IR spectrum revealed that distinct functional groups were present on the surface of the produced ZnO-TSA nanoparticles.

The FTIR spectroscopy approach notices the different groups present in adsorbent that are possible locations for dye ion binding on the adsorbent surface. The spectra of ZnO-TSA nanoparticles before MB adsorption were examined in the range of 500-4000 cm-1 (Figure 4.2), which was attributed to aliphatic C-H asymmetric stretching found in biomass structure (cellulose, hemicellulose, and lignin). The peak at 1639 cm^{-1} corresponds to amide group C=O stretching vibration. The bands in the range 1591 cm^{-1} are assigned by the C=C aromatic stretching of lignin. C-O and C-C bending vibrations are represented by the bands at 1095 cm^{-1} and 1089 cm^{-1}, respectively. The band at 559 cm^{-1} and 613 cm^{-1} can be caused by the bending

vibration of C-H. These findings revealed that the ZnO-TSA nanoparticles include various functional groups that are responsible for MBD adsorption, including O-H, C=O, and C-O (Sharifi & Shoja, 2018). Similar results have been reported by Oyewo et al. (2020); Pirbazari & Saberikhah (2014); Razali et al. (2020).

The intensity of the peaks of O-H and C=O decreased after MB adsorption, showing that an interaction occurred between MB and these groups. After adsorption, some new peaks were detected on the ZnO-TSA nanoparticles spectrum at 1380 and 1591 cm^{-1} for aromatic stretching of lignin, which was attributed to the presence of MB molecules on the adsorbent surface (Sharifi & Shoja, 2018).
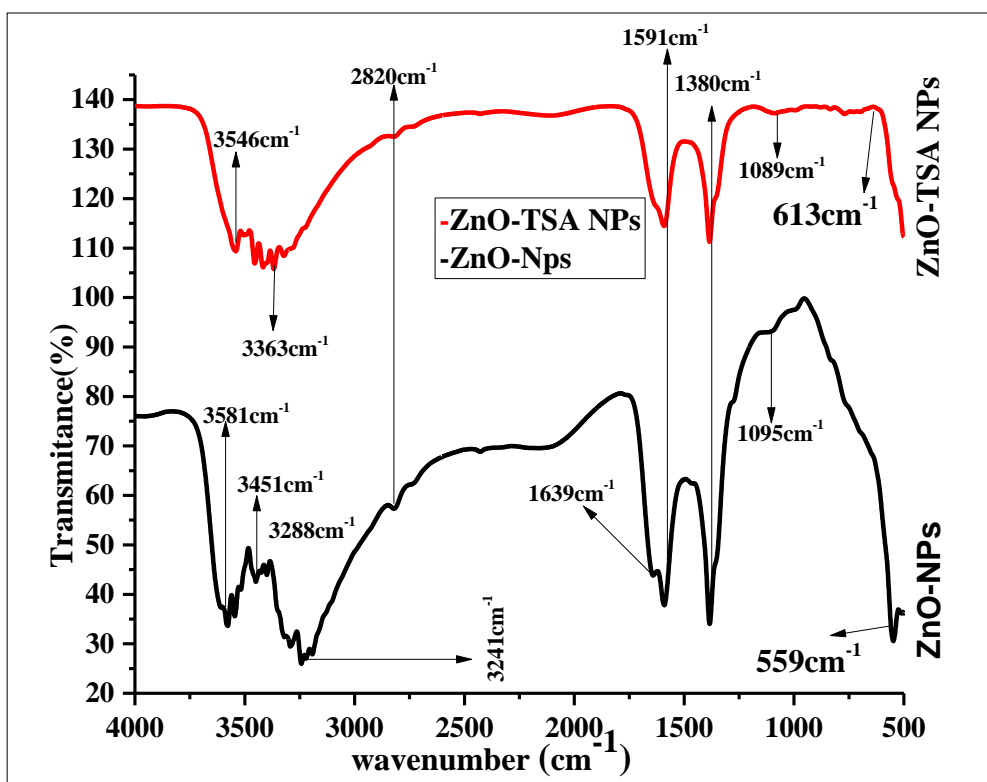
Figure 4.2: FT-IR spectra of synthesized ZnO-TSA NPs and ZnO NPs before MBD removal

4.1.3. X-ray diffraction (XRD) analysis
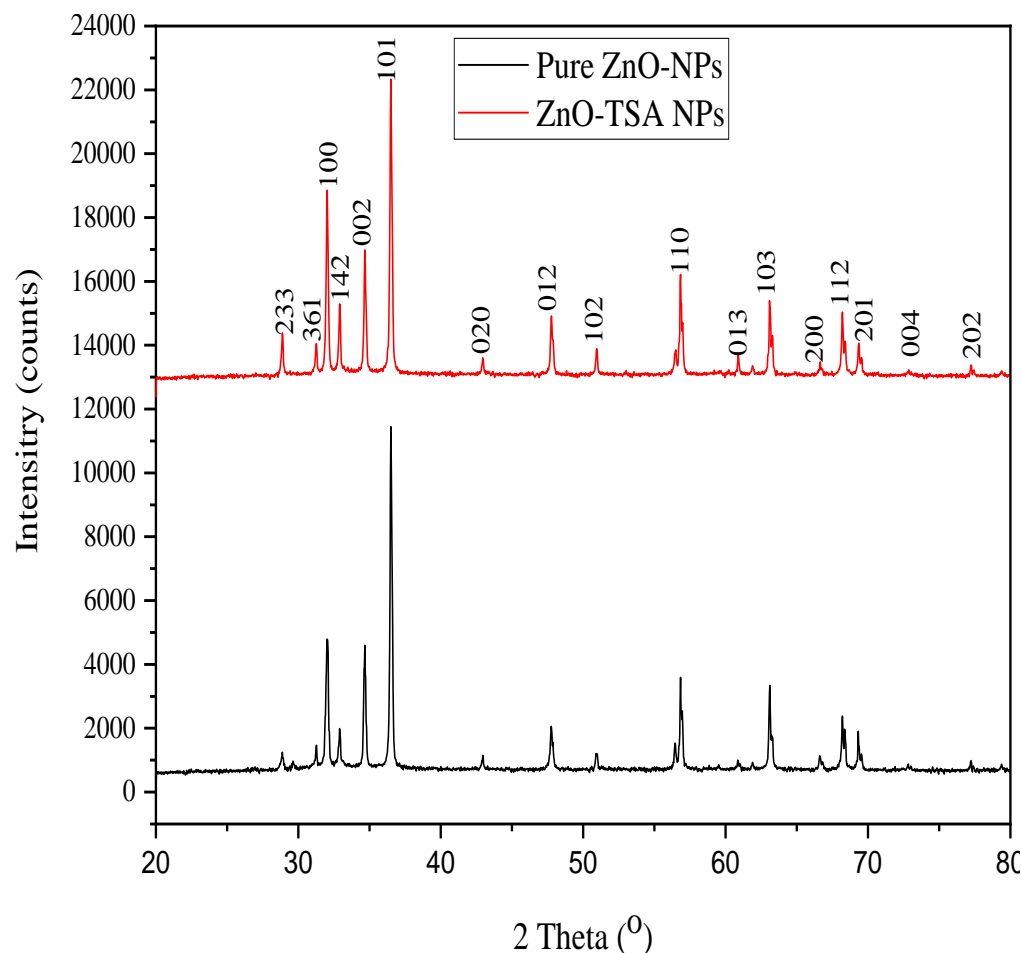
Figure 4.3: XRD patterns of the unassisted (top) and the teff straw assisted (bottom) zinc oxide nanoparticles

The analysis of XRD confirmed the green synthesis of ZnO NPs. Powder X-ray diffraction is used to radian tell the crystalline size and structural properties of ZnO nanoparticles. The XRD is performed using Cu Ka radiation (k = 0.1540 nm) and 2θ values ranging from 20 to 80 degrees. The diffraction peaks are sharp and narrow, representing that the product is crystalline (S et al., 2020).

Entirely the diffraction peaks at angles (2θ) of 28.87°,31.25°,32.03°, 32.90°,34.68°, 36.507°, 42.95°, 47.79°, 50.93°, 56.86°,61.07°,63.14°,66.66°,68.24°,69.38°,72.82°,and77.23° corresponds to the reflection from (233), (361), (100), (142),(002), (101), (020),(012), (102), (110),(013), (103), (200), (112), (201), (004), and (202) crystal planes of ZnO nanoparticles.

The sharp and intense peaks are representing that the ZnO-TSA nanoparticles were highly crystalline. The diffraction peaks corresponding to the slight impurity were found in the XRD patterns, confirming the somewhat purity of the synthesized products (Set al., 2020). These peaks validate and provide information about ZnO-TSA NPs. This spectrum demonstrates a very strong peak and the nature of zinc oxide nanoparticles.

As a result, the XRD result is analogous to (Raj & Lawerence, 2018). The average crystalline size of the synthesized ZnO-TSA nanoparticles was calculated using Debye-formula Scherer's (Equation 3.1) from the FWHM reflection planes of the XRD data and was found to be 27.196 nm. In similar manner, the calculated average Crystalline srieze aof normal, pure synthesized ZnO NPs in XRD was 24.619 nm.

4.1.4. Determination of point of zero charge

An adsorbent's point of zero charges is a key characteristic parameter that defines the net surface charge of an ion in a given solution**.** It determines the adsorbent's electrical neutrality at a specified pH value, and thus the charge on the surface of a specific adsorbent becomes zero. The pH of the point of zero charges (pHpzc) of ZnO-TSA nanoparticles was shown in Figure 4.4. As a result, the pHpzc of the ZnO-TSA nano-adsorbent was determined to be around 4.35 to understand the change in the surface character of the synthesized adsorbent under changing pH values. This demonstrates that the surface of ZnO-TSA nanoparticles is positively charged when the solution pH is less than pHpzc (4.35), but negatively charged when the solution pH exceeds pHpzc (4.35). As a result, when the pH of the solution exceeds pHpzc, MBD adsorption is enhanced. The pHpzc findings of trials with the ZnO-TSA adsorbent where the pH ranged from 2 to 10. Below the pHPZC value, the surface of the ZnO-TSA nanoparticles is positively charged due to protonation, encouraging anion adsorption because MB is a basic dye (Cationic dye). The surface of the ZnO-TSA nanoparticles contains a negative charge above the pHPZC, which inhibits anion species adsorption (Swamy et al., 2017). Besides, the dye's removal efficiency in the pH range examined shows the good removal efficiency of teff straw assisted Zinc oxide nanoparticles under simple conditions. Furthermore, as the pH increased from 2 to 8.0, the removal efficiency of MB improved somewhat better. As MB$^+$, MB is soluble with a positive charge. As the pH rises, more (OH) can be deposited on the surface of ZnO, resulting in greater chemical precipitation (Chemingui et al., 2021).
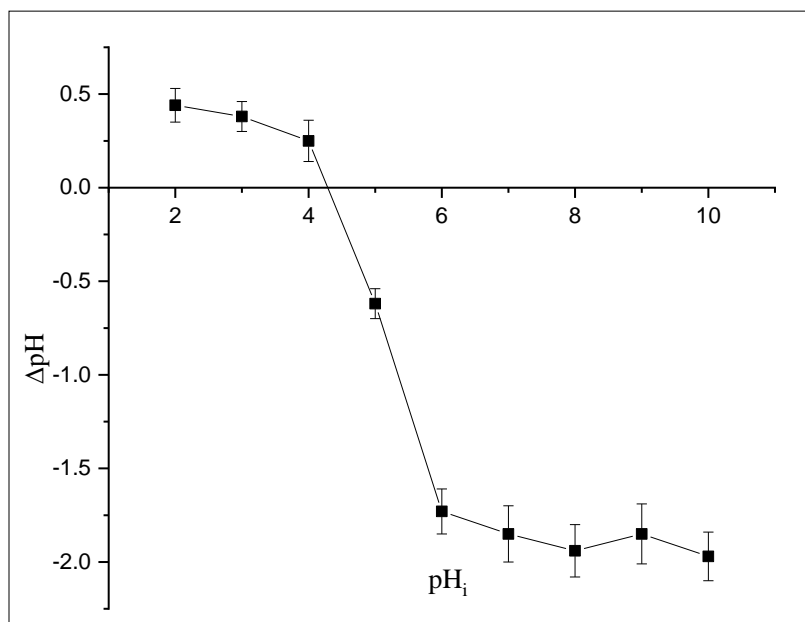
Figure 4.4: Point of zero charge

4.2. MBD Removal studies

4.2.1. Effect of the pH solution on MBD removal

The pH solutions' influence on MBD removal was tested at room temperature using a 100 mL of 40 mg/L starting MBD solution in the pH range of 5-11, an adsorbent dose of 0.4 g, a shaking speed of 180 rpm, and a contact period of 40 minutes. As demonstrated in Figure 4.5, the removal of MBD on ZnO-TSA nanoparticles is mostly affected by solution pH, with the lowest and highest adsorption capacities occurring at pH 14 and 8, respectively. As shown in Figure 4.5, the removal of MBD on ZnO-TSA nanoparticles increases up to the center point and then slightly decreases. The electrostatic repulsion between the positive charges of the ZnO-TSA nano adsorbent and the cationic species of MBD resulted in significant MBD removal effectiven ess at low pH. Hydrogen ions compete with cationic MB species for binding sites on ZnO-TSA nanoparticles.

This takes place because of an excess of H^+ ions in the adsorbate and the negatively charged surface adsorbent, resulting in competition adsorption between MBD and H^+, resulting in a decrease in MBD adsorption (Nasuha et al., 2010).

As the pH of the solution increased, more electronegative charges were formed on the surface of the nano-adsorbents; as a result, there is an electrostatic attraction between the cationic species of

MBD and the adsorbent, and the adsorption capacity of MBD ions decreased, possibly due to the production of MBD ions as OH complexes.According to the study conducted by Ghalehkhondabi et al. (2021; Sharifi & Shoja (2018), increasing the pH from 3 to 11 enhances the dye removal percentage from 45 to 82 percent.
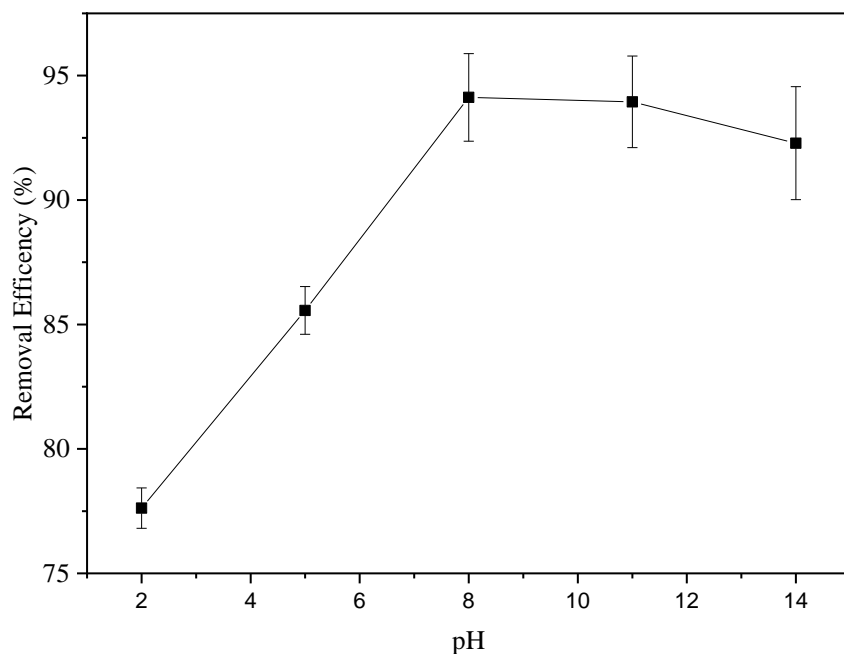
Figure 4.5: Effect of the pH on MBD removal

In similar way, in an aqueous solution, the surface of ZnO-TSA attains a surface charge in the deprotonation or protonation of the Zn-OH surface site which can play a vital role in the MBD removal.

The process of protonation or deprotonation of the Zn-OH surface site depends on the pHpzc of the ZnO-TSA nano-adsorbent and the solution pH. At pH < pHpzc, protonation occurs, thus, methylene blue ions are the dominant species for ZnO-TSA nanoparticles, and as a result, the protonated adsorption sites make the MBD adsorption unfavorable owing to electrostatic repulsion between positively charged sites and positively charged dye ions. However, at pH > pHpzc, Zn-O is dominant, and therefore the deprotonated adsorption sites make the MBD adsorption favorable because of electrostatic attraction for MBD onto the negatively charged sites. These results were in good agreement with previous findings reported by Mohammad Razi et al. (2017).

4.2.2. Effect of the contact time on MBD removal

The effect of contact time on MBD removal was studied at room temperature for 20-100 minutes, with 10-minute intervals, using a 100 mL of 40 mg/L initial MBD solution with an adsorbent dosage of ZnO-TSA = 0.2 g, a shaking speed of 180 rpm, and a pH of 8. Figure 4.6 depicts the experimental result for the effect of contact time. The adsorption capacity of ZnO-TSA nanoparticles rose dramatically with increasing contact time, as shown in Figure 4.6. (20-G80 minutes). It was discovered that around 94.181 percent of MBD was removed during the first 20 minutes of adsorption, indicating that adsorption of MBD onto ZnO-TSA nanoparticles was very fast during the beginning stage of the adsorption processes (Khoshhesab et al., 2010). The presence of a large number of free negatively charged active sites on the adsorbent's surface resulted in the rapid removal of MBD. Adsorption processes were increased by the efficient binding of the surface functional groups of ZnO-TSA nanoparticles with MBD ions (Chauhan et al., 2021). However, it was discovered that extending the contract duration after 80 minutes had no significant influence on MBD adsorption. When the contact time was exceeded beyond 80 minutes, there were a few changes in the % removal of MBD, which could be indicating the absence of unoccupied active sites on the adsorbent surface above the equilibrium. This suggests that at these contact times, the adsorbed MBD on the surface of ZnO-TSA NPS is in equilibrium with the adsorbent's desorbed MBD (Ghalehkhondabi et al., 2021). This was demonstrated because the availability of active sites on the surface adsorbents has a substantial effect on MBD binding with contact time.
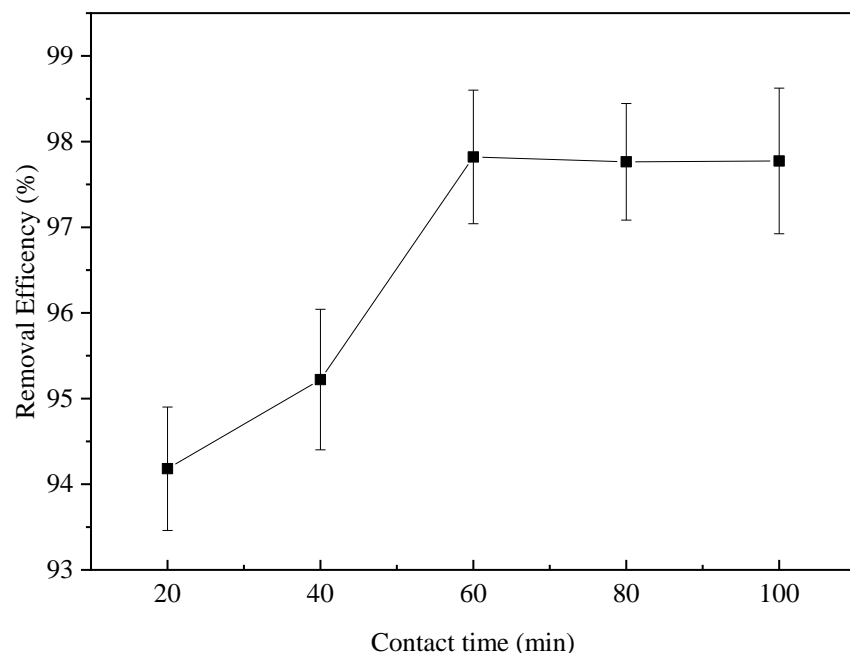
Figure 4.6: Effect of the contact time on MBD removal

4.2.3. Effect of the adsorbent dose on MBD removal

At room temperature, the effect of adsorbent dose on the removal of MBD from aqueous solution was examined by varying the adsorbent dose (0.1, 0.2, 0.3, 0.4, and 0.5 g) with an initial MBD concentration of 40 mg/L. The solutions were shaken for 40 minutes at 180 rpm and had a pH of 8. Finally, the residuals of MBD ions were examined after each sample was filtered with Whatman filter paper. The effect of adsorbent dose was shown to be particularly critical on the removal of MBD as examined, and the results are shown in Figure 4.7. The investigation revealed that as the dose of ZnO-TSA nanoparticles was increased from 0.1 to 0.4 g, the percentage elimination of MBD increased from 93.162 to 97.164 percent. This result primarily suggests that the synthesized adsorbent was practically free of aggregation; thus, increasing the adsorbent dosage resulted in equivalent removal efficiency as the optimum dosage of ZnO-TSA nanoparticles. The percent removal of MB increased is basically due to the number of active sites and available surface area increase with dosage (Nasuha et al., 2010). Aggregated adsorbents have a low surface area, which reduces the removal effectiveness of the adsorbate and has a similar effect on the effect of adsorbent doses. This outcome is in agreement with data reported by different researchers studies (Abate et al., 2020, Simeonidis et al., 2016, Nang An et al., 2020). In general case,the percentage removal increased by increasing the amount of adsorbents

due to the increase in contact surface of adsorbent with MB and the greater availability of the ad
sorbents with increase the number of adsorption sites available for adsorption. Maximum remov
al of MB reduced with aditional increase in adsorbent dose at constant dye concentration and
volume. Particles aggregation saturated adsorption sites and decrease sorption capacity.
Aggregation would lead to a decrease in total surface area of the adsorbent and increase in
diffusional path length(Abate et al., 2020; Pirbazari & Saberikhah, 2014)**.**
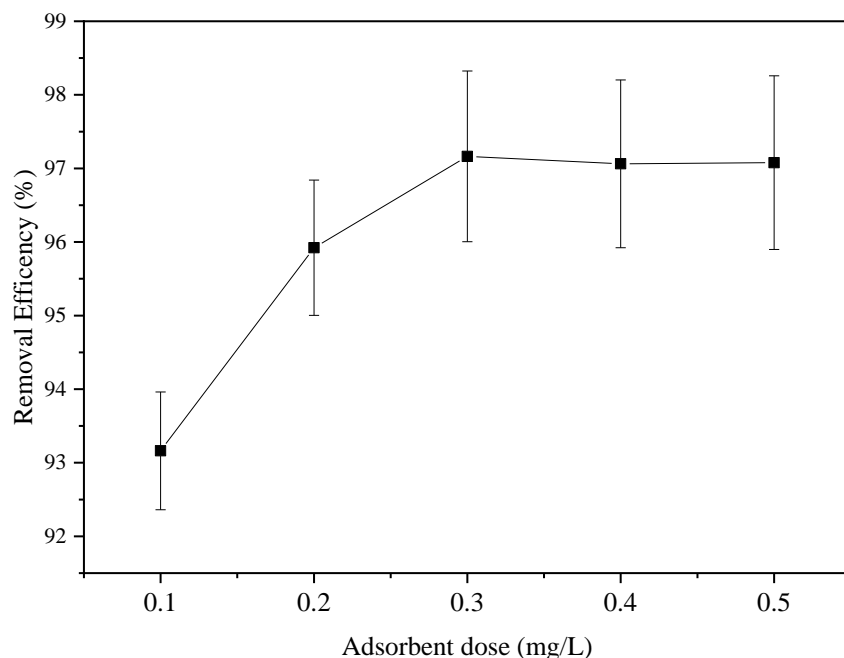
Figure 4.7: Effect of adsorbent dosage on MBD removal

4.2.4. Effect of the initial concentration onto MBD removal

At room temperature, the effect of initial MBD concentration on the percentage removal of MBD
ions from aqueous solution by ZnO-TSA nanoparticles was investigated by changing the initial
concentration (10, 30, 50, 70, and 90 mg/L) while maintaining other parameters such as
adsorbent dose 0.2 g, contact time 40 minutes, and pH of 8. The solutions were shaken for 40
minutes at 180 rpm, and each sample was filtered through Whatman filter paper before being
tested for MBD residuals.

Figure 4.8 describes the results of the influence of initial MBD concentration on MBD
elimination. It was noticed that increasing the initial concentration of MBD resulted in a lower
% elimination of MBD. At starting MBD concentrations of 10 mg/L and 90 mg/L, respectively,

the maximum and lowest percentage removal were 99.62 and 81.79 percent. This is because at a low starting concentration of MBD, the chance of the availability of adsorbent active sites is high, and as a result, the accessible MBD can be captured. However, as the initial concentration increased and/or the adsorbent's adsorption active sites became saturated, the removal percentage decreased (Ghalehkhondabi et al., 2021).
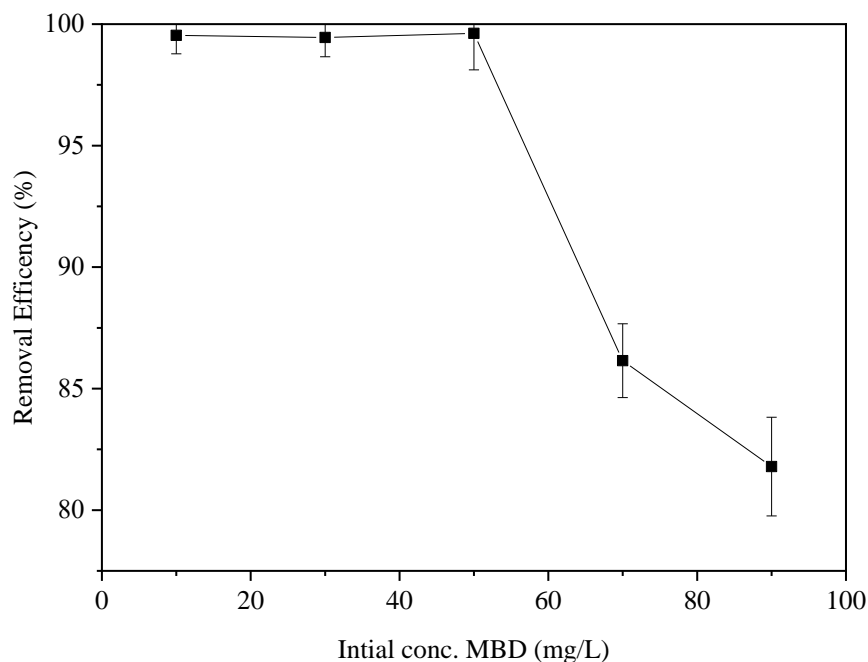
Figure 4.8: Effect of initial concentration on MBD removal

4.3. Experimental design and statistical analysis of the experimental results

The obtained experimental results were calculated after the experimental works were recorded for the corresponding run order of parameters, and analyzed by the software. Consequently, the well-fitted regression model of the adsorption process was determined from statistical analysis of response surface methodology (RSM). Process parameters such as initial dye concentration, pH of the solution, contact of time, and dosage of the adsorbent were optimized by CCD.

4.3.1. Model summary statistics for percentage removal of MBD using ZnO-TSA Nps

To fit the experimental results found from batch adsorption experiments, four key models were used as indicated in Table 4.1. From these, the quadratic model with a correlation coefficient of 0.9967 was selected and is suggested for fitting as well as to indicate the process of the removal of MBD.

Table 4.1: Model summary statistics and suggested design for percentage removal of MBD

Source	Std. Dev.	R²	Adjusted R²	Predicted R²	PRESS	
Linear	7.38	0.1764	0.0447	-0.1967	1975.90	
2FI	8.27	0.2127	-0.2016	-0.2704	2097.55	
Quadratic	**0.6012**	**0.9967**	**0.9937**	**0.9830**	**28.01**	**Suggested**
Cubic	0.3317	0.9995	0.9981	0.9973	4.52	Aliased

4.3.2. Analysis of variance

Analysis of variance (ANOVA) was used to confirm the statistical significance of every factor and their respective interactions in the acquired quadratic model as already shown in Table 4.2. In the present work, the F-value for the empirical model developed for the removal of MBD is 325.22 which is high indicating the developed model has high reliability. There is only a 0.01% probability that an F-value this large could occur due to some noise. Also, the P-value for the model is very low (0.0001) which shows the significance of the model. p-values less than 0.0500 indicate model terms are significant (Afolabi et al., 2021; Sharifi & Shoja, 2018).

Table 4.2: Analysis of variance (ANOVA) for the quadratic model on the adsorption of MBD

Source	Sum of Squares	Df	Mean Square	F-value	p-value	
Model	1645.72	14	117.55	325.22	< 0.0001	Significant
A-ZnO-NPS dosage	42.55	1	42.55	117.73	< 0.0001	
B-Contact time	17.71	1	17.71	49.00	< 0.0001	
C-Initial conc.MBD	2.38	1	2.38	6.58	0.0216	
D-pH	228.69	1	228.69	632.71	< 0.0001	
AB	0.0089	1	0.0089	0.0246	0.8775	
AC	3.44	1	3.44	9.52	0.0075	
AD	0.0047	1	0.0047	0.0131	0.9105	

BC	19.53	1	19.53	54.03	< 0.0001
BD	18.31	1	18.31	50.66	< 0.0001
CD	18.64	1	18.64	51.57	< 0.0001
A²	59.52	1	59.52	164.66	< 0.0001
B²	9.91	1	9.91	27.41	0.0001
C²	0.0122	1	0.0122	0.0336	0.8569
D²	1255.43	1	1255.43	3473.34	< 0.0001
Residual	5.42	15	0.3614		
Lack of Fit	4.68	10	0.4676	3.13	0.1097	not significant
Pure Error	0.7462	5	0.1492		
Cor Total	1651.14	29			

The Model F-value of 325.22 implies the model is significant. There is only a 0.01% chance that an F-value this large could occur due to noise. In this case, A, B, C, D, AC, BC, BD, CD, A², B², D² are significant model terms whereas, AB, AD, and C² are not significant. P-Values greater than 0.0500 indicate the model terms are not significant (Afolabi et al., 2021). The Lack of Fit F-value for the developed empirical model is 3.13. This value implies the Lack of Fit is not significant relative to the pure error. There is a 10.97% probability that a Lack of Fit F-value this large could occur due to some kind of noise. A non-significant lack of fit is good because a non-significant Lack of Fit shows the model is well fitted and is very nearer to the perfect fitness as it was obtained by the model (Afolabi et al., 2021;Ghalehkhondabi et al., 2021).

4.3.3. Model adequacy checking

Model adequacy can be deduced by considering the regression coefficients of R^2. Hence, the regression coefficient (R^2) was used to determine the relationship between the experimental and the predicted responses. As represented in Table 4.3, the response of R^2 was 0.9967 which

recommends that 99.67% of the response variability in adsorption capacity can be described by the analyzed process parameters and it could not describe nearly about 29 of the variation of the response. It was obtained that the value of R^2 is very close to 1, showing the very correlation between the experimental and predicted value, thus showing the adequacy of the model. In another way, the determinant coefficients of R^2 and adjusted R^2 shown in Table 4.3, indicates the close agreement of experimental and predicted values. The Predicted R^2 of 0.9830 is in reasonable agreement with the Adjusted R^2 of 0.9937; i.e the difference is less than 0.2. Adeq Precision measures the signal-to-noise ratio. A ratio greater than 4 is desirable. The ratio of 79.4621 indicates an adequate signal. This model can be used to navigate the design space. The low coefficient of variation 0.6567 was obtained, which is the standard deviation divided by the mean indicating the good precision of the experiments (Afolabi et al., 2021;Ghalehkhondabi et al., 2021).

Table 4.3: Model fit statistics of the design

Std. Dev.	0.6012	R²	0.9967
Mean	91.55	Adjusted R²	0.9937
C.V. %	0.6567	Predicted R²	0.9830
		Adeq Precision	79.4621

The Predicted R² of 0.9830 is in reasonable agreement with the Adjusted R² of 0.9937; i.e. the difference is less than 0.2. The regression coefficient (R^2) quantitatively evaluates the correlation between the experimental data and predicted response. Since the value of R^2 is closely related to 1, the regression line is perfectly fitted to the data of the experiment. From this value, it was suggested that only 99.67% of the total variance was described by the developed regression model. Therefore, the obtained correlation coefficient (R^2) from the quadratic model able to represent in the actual laboratory results over a 95% confident interval suggests a good adjustment to the experimental results (Afolabi et al., 2021). Adeq Precision measures the signal-to-noise ratio. A ratio greater than 4 is desirable and a ratio of 79.4621 indicated an adequate signal (Afolabi et al., 2021;Ghalehkhondabi et al., 2021).

4.3.4. Model equation development

The final model equation obtained was used to determine the relationship between responses and independent parameters. As shown in Table 4.1 the quadratic model was selected, because it

effectively fits the statistics. Thus, the quadratic model that relates the removal efficiency of MBD with independent process parameters was described by the second-order polynomial equation, and the percentage removal of MBD as a function of independent parameters (coded variables) is given in equation 3.14.

Removal= +98.64-1.33*A+0.8590*B+0.314*C-3.09*D +0.4637*AC+1.10*BC +1.07BD+ 1.08 *CD-1.47*A^2-0.6011*B^2 -6.77*D^2 3.14

Where R is the removal efficiency, A is the ZnO-NPS dosage, B is the Contact time, C is the Initial conc.MBD, and D is the pH.

Equation (3.11) indicates the effect of variables on the percentage removal of MBD. In general, the negative coefficients describe that the factors negatively affect the adsorption of MBD whereas the positive coefficient values indicate that the factors positively affect the adsorption of MBD. The effect of D on the percentage removal of MBD was dominant compared to the effect of A, B, and C.

4.3.5. Model diagnostic plot

 A diagnostic plot indicates a graphical representation of the model that can be used to interpret the chance variation of the values. The normal plot of residuals is given in Figure 4.9. As it was observed from the normal probability plot, the residuals are following a normal distribution, thus the residuals were approximated along a straight line confirming that the normality assumption was satisfied. This indicates the selected quadratic polynomial model is satisfactory for the MBD adsorption analysis.
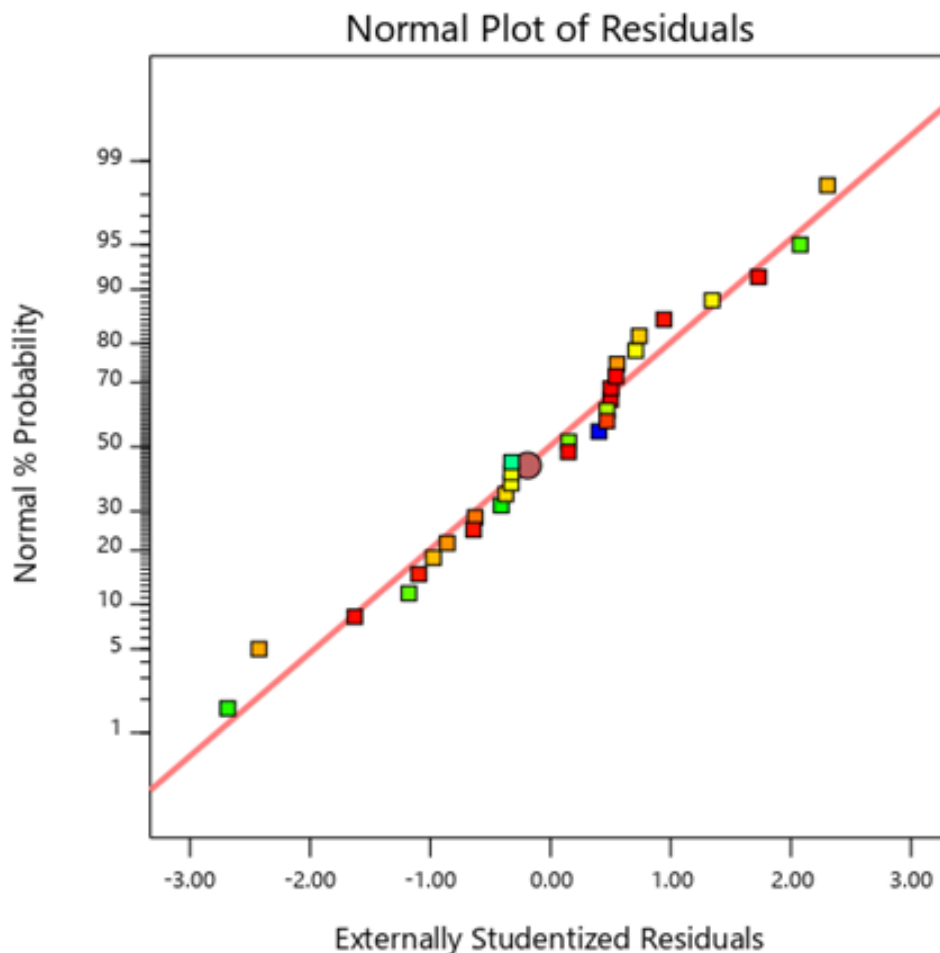
Figure 4.9: Normal % probability versus residuals plot for MBD adsorption

One more very important diagnostic tool for checking the adequacy of the fitted model for predicting the response is a residual versus predicted plot, which shows the random scattering of the residuals. It checks for the assumption of constant variance, thus there are no upward or downward pattern curves observed. Accordingly, Figure 4.10 shows that the residuals of the predicted values were randomly scattered on the plot, representing that the fitted values are structureless; therefore there is no need for modification to reduce the personal error for the model.
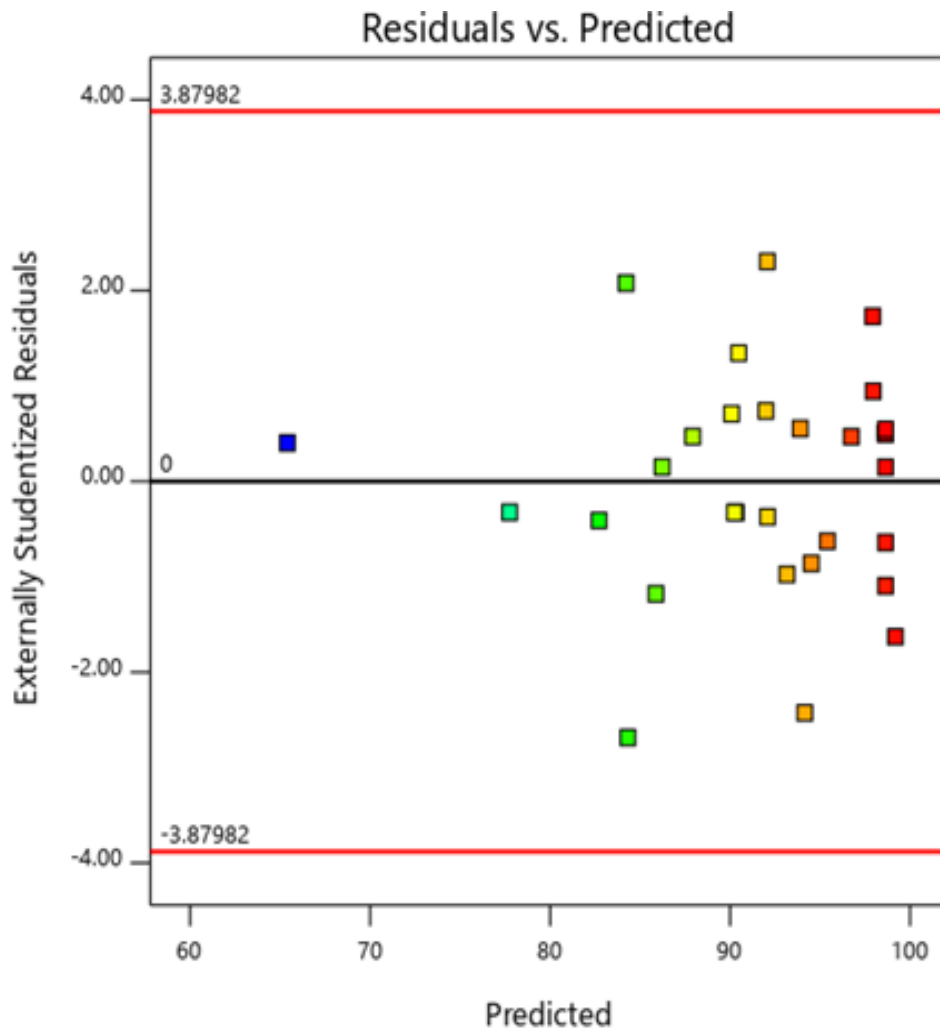
Figure 4.10: Residual versus predicted plot for MBD adsorption

The close agreement between actual and predicted values is shown in Figure 4.11. The predicted values obtained by the model were very close to the experimental values and lies reasonably close to the straight-line. So, the result indicates that the actual values were in good agreement with the predicted values as shown in the plot.
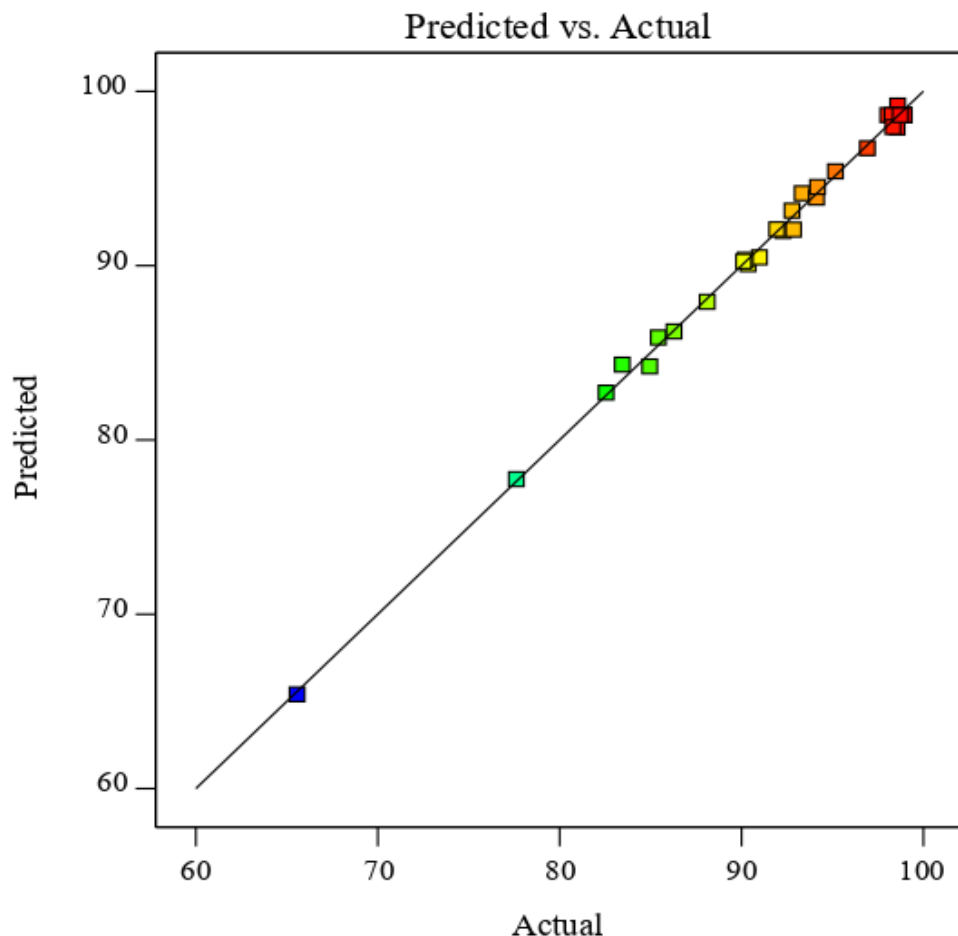
Figure 4.11: Predicted versus actual plot for MBD adsorption

4.3.6. Interaction effect of process parameters on MBD removal

An interaction effect takes place if there is an interaction between the independent parameters that affect the dependent parameter. In this study, it was found that the combined effect between adsorbent dosage and initial concentration, contact time and initial concentration, contact time and pH, initial concentration, and pH has a significant effect on percentage removal of MBD. Therefore, the interaction effects between A and C, B and C have a significant effect on the MBD removal, followed by BD and then CD.

1. Interaction effects of initial concentration of MBD and ZnO-TSA Nps dosage (AC)

In general case, the decrease in initial conc. of MBD and the increase in adsorbent dosage increased by removal percent of MBD. But according to the model in equation (3.14) and Figure (4.12), it have been seen that, the removal efficiency was decreased as the adsorbent dosage was increased above 0.3g, which may be due to the amount of adsorbent is increased, the total surface area available for the adsorption of MB reduces as a result of overlapping or aggregation of adsorption sites. The maximum adsorption was noticed least for higher amount of doses. Nevertheless, the rise concentrations of doses lead to decrease adsorption with increasing adsorbent dose. This decrease may be due to unsaturation of adsorption sites.

Adsorption studies of Zinc oxide nanoparticles of teff straw show that the percentage of dye removal efficiency was higher at a higher concentration of methylene blue. With more increase in dye concentration the interaction between the dye and the adsorbent increased apart from providing necessary driving force to overcome. This shows that the dye uptake increased with increase in concentration till equilibrium was achieved, then there is no more uptake of the dye due to absence of void space for the dye absorption. The maximum removal efficiency was at 90.8% % at 10.7 mg/L of methylene blue solution. The removal efficiency was greater since increased contact of adsorbate with available sites of adsorbent. This can be because the increase of the initial adsorbent concentration is a driving force to resolve the resistance of the dye to mass transfer between the aqueous and solid phases (Ghalehkhondabi et al., 2021; Khosravi & Arabi, 2016;Afolabi et al., 2021).
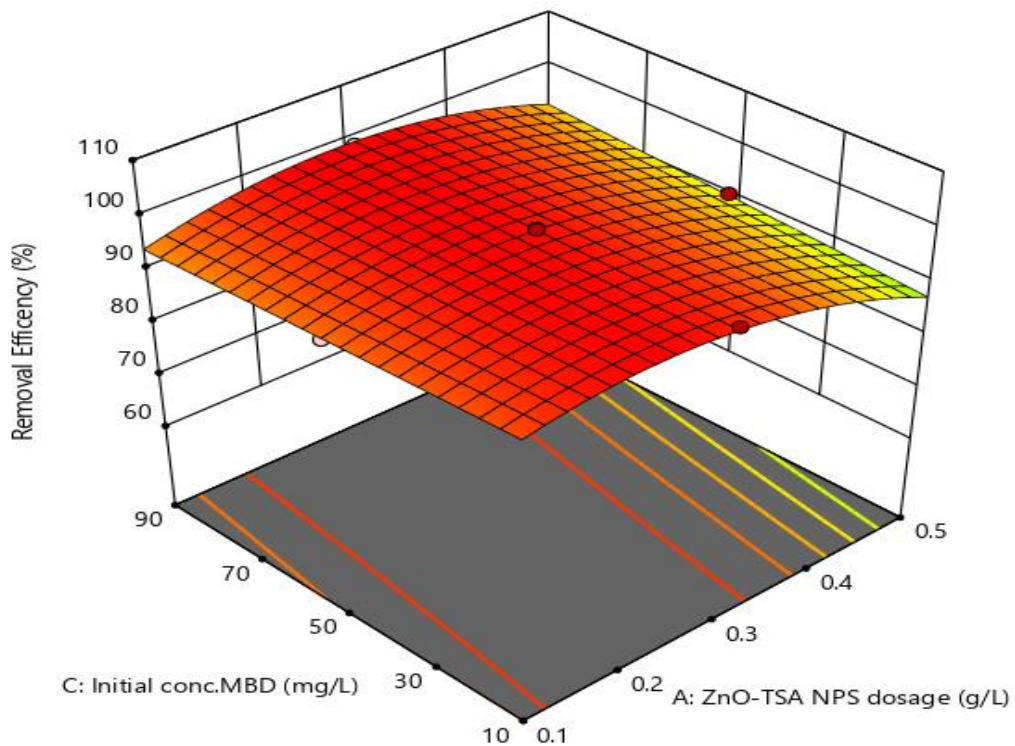
Figure 4.12: 3D plot for the combined effect of adsorbent dosage and initial conc. of MBD on MBD removal
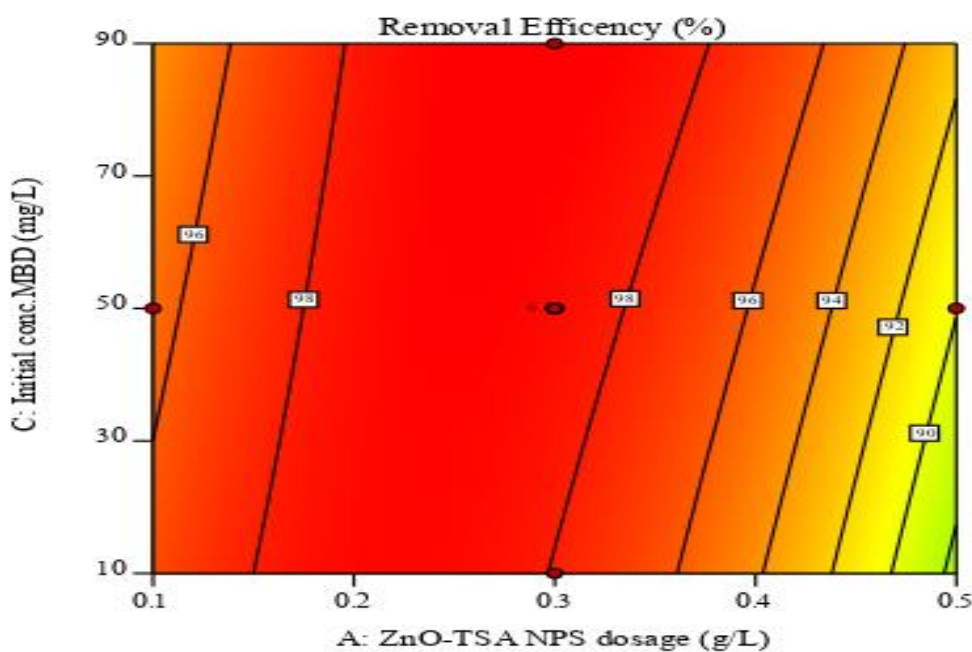
Figure 4.13: Contour plot for the combined effect of pH and adsorbent dosage on MBD removal

2. **Interaction effects of Contact time and initial Concentration of MBD (BC)**

Figure 4.14. Shows the interactive effect of the initial concentration of MBD and contact time on MBD removal. From the diagram, the percent removal of MBD increases as both initial concentration of MBD and contact time increases. The increase in removal efficiency with increasing initial concentration was because the absence of a constant number of adsorption active sites on the adsorbent's surface, which is because at high dye concentrations, the ratio of surface active sites to total molecules is low, and accordingly all molecules in slow stick to the ZnO-TSA Nps dosage surface. But, there are enough spaces for all of the molecules in a dye with a high concentration. A maximum removal percentage of MBD 100% occurred at a contact time of 99.8 min and an initial conc. of MBD of 89.20. In general, the adsorption rate was higher at initial contact time as enough active sites were available for adsorption. However through time, a higher amount of MBD ion got adsorbed on the ZnO-TSA Nps dosage surface and so the surface area reduced. Similar studies were observed by Ghalehkhondabi et al. (2021; Khosrav & Arabi (2016); Afolabi et al. (2021).
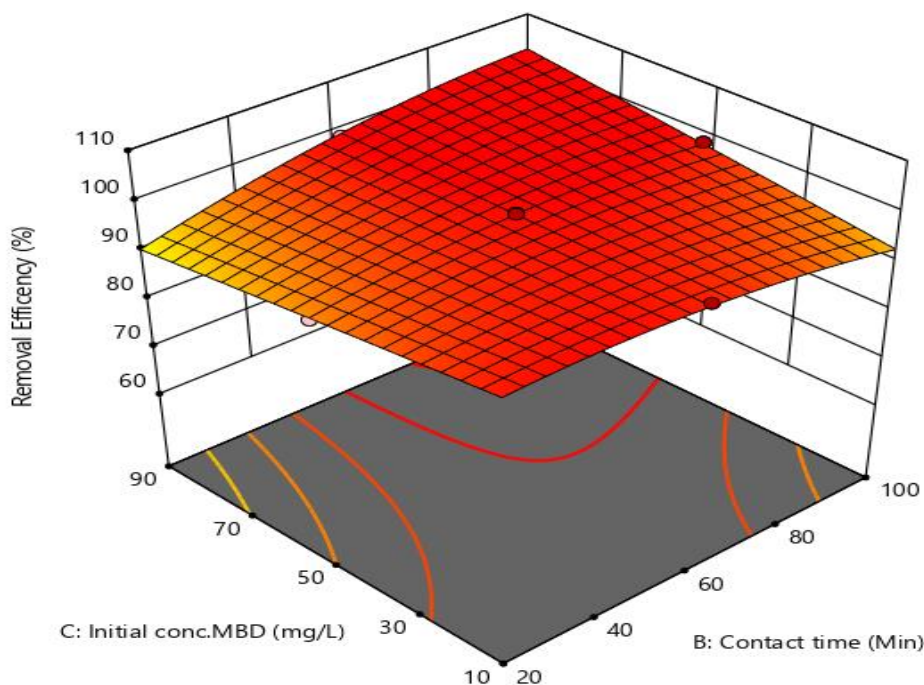
Figure 4.14: 3D plot for the combined effect of contact time and initial conc. of MBD on MBD removal
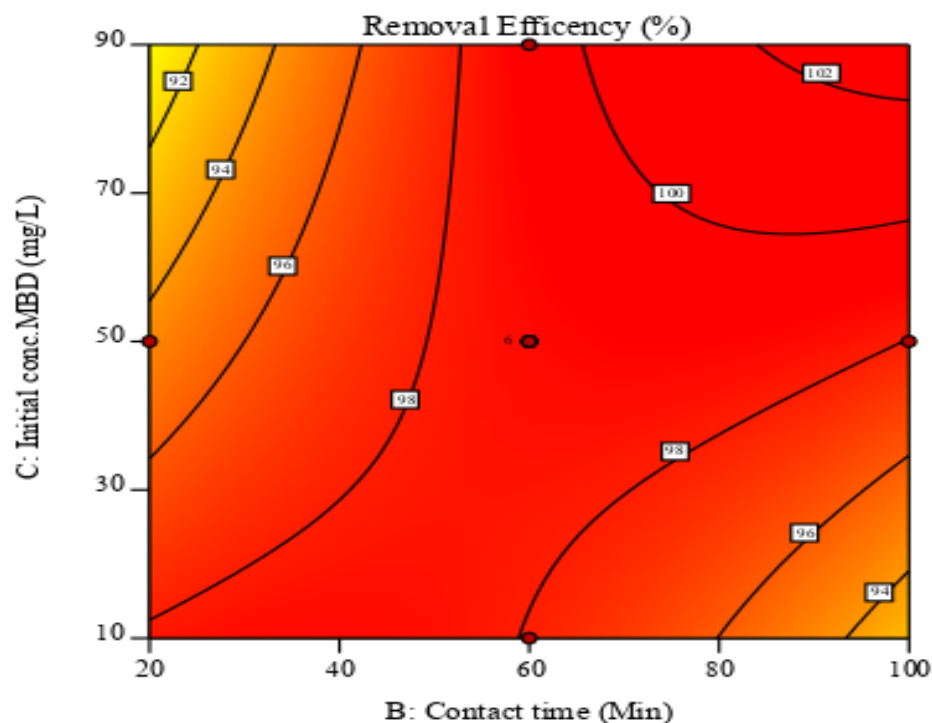
Figure 4.15: Contour plot for combined effect of Contact time and Conc. of MBD on MBD removal

3. Interaction effects of Contact time and pH (BD)

The interaction effect of the Contact time and pH on MBD removal is shown in Figures 4.16. According to the justification based on this the model, the efficiency of MBD removal increases with decreasing solution pH and increasing contact time. The maximum removal efficiency (94.16%) of the ZnO-TSA nps was found at the pH 8 ,contact time 70.92 min ,and the remaining two variables place at their medium level. At higher pH values, the removal efficiency decreases gradually, because MB is cationic dye (Ghalehkhondabi et al., 2021; Khosravi & Arabi, 2016;Afolabi et al., 2021).
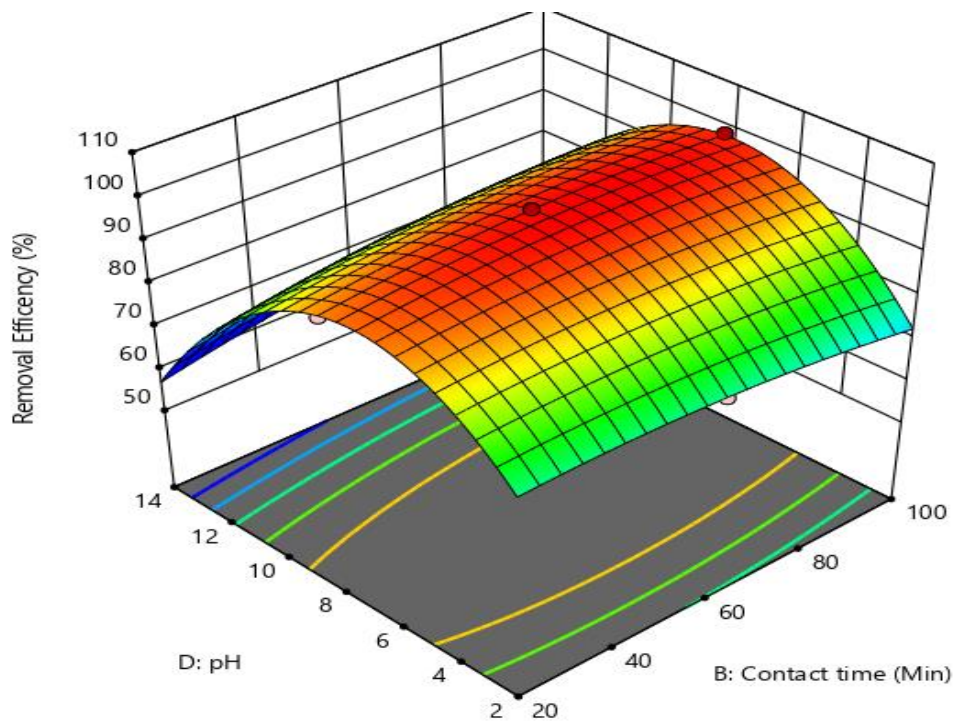
Figure 4.16: The 3D plot for the combined effect of Contact time and pH on MBD removal
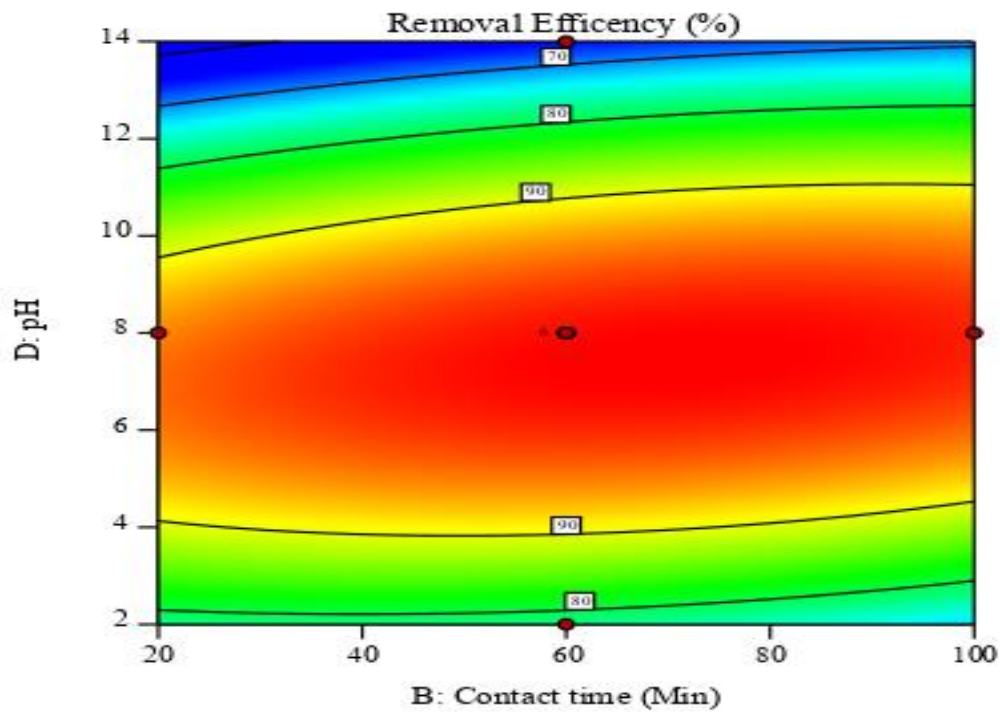
Figure 4.17: Contour plot for the combined effect of Contact time and pH on MBD removal

4. Interaction effects of pH and initial concentration of MBD (CD)

The interaction effect of the initial concentration of MBD and pH on MBD removal is shown in Figure 4.18. The removal efficiency of MBD was decreased at lower initial concentration with increasing pH and was decreased when pH reaches beyond optimal value. The maximum removal efficiency of the ZnO-TSA nps was found at the pH 8 and at higher pH values, the removal efficiency decreases gradually, because MB is Cationic dye. Adsorption studies of Zinc oxide nanoparticles of teff straw show that the percentage of dye removal efficiency was higher at a higher concentration of methylene blue.The removal efficiency maybe due to increased contact of adsorbate with available sites of adsorbent. This can be because the increase of the initial adsorbent concentration is a driving force to resolve the resistance of the dye to mass transfer between the aqueous and solid phases (Afolabi et al., 2021; Ghalehkhondabi et al., 2021).
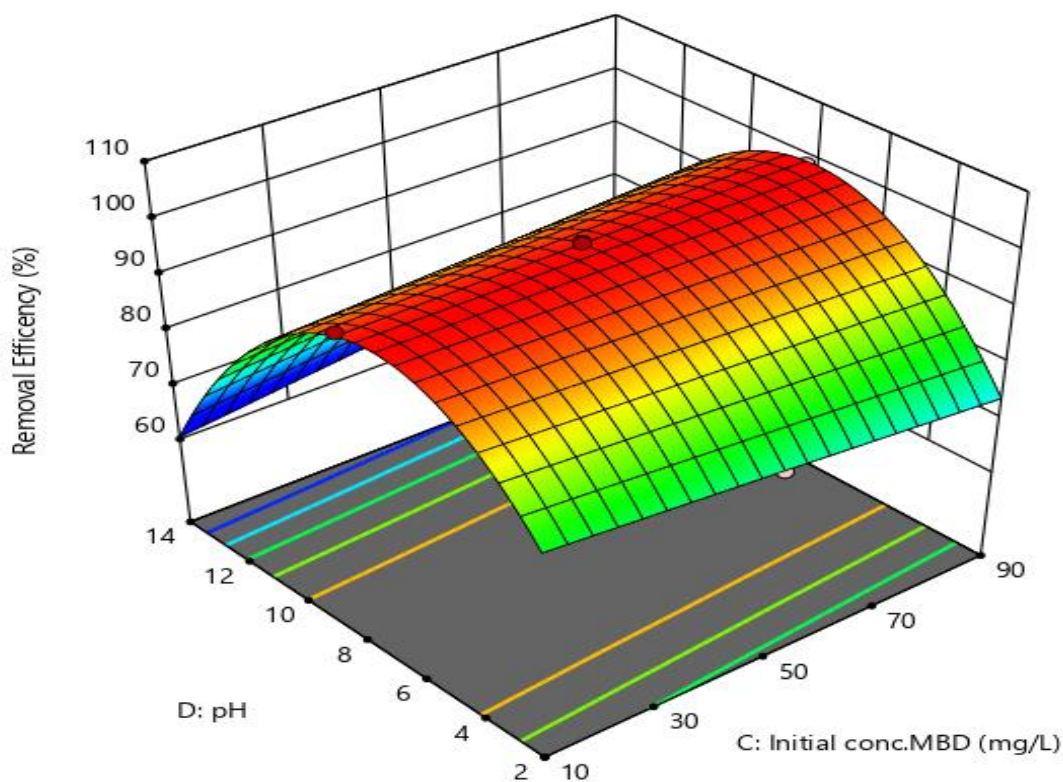
Figure 4.18: 3D plot for the combined effect of Intial conc. of MBD and pH on MBD removal

Figure 4.19: Contour plot for the combined effect of Initial conc. of MBD and pH on MBD removal

4.3.7. Optimization of the adsorption process for MBD removal

The optimization of process parameters such as adsorbent dose, initial dye concentration, pH, and contact time on the performance of percentage removal of MBD was done using CCD. The goals for numerical optimization of each variable were given in Table 4.6. After optimization, the experimental data were validated by performing experiments.

Table 4.4: Process parameters and goals for optimization

Name	Goal	Lower Limit	Upper Limit	Importance
A: ZnO-TSA NPS dosage	is in range	0.2	0.4	3
B:Contact time	is in range	40	80	3
C:Initial conc.MBD	is in range	30	70	3
D:pH	is in range	5	11	3
Removal	Maximize	65.565	98.946	3

So, by considering the desirability function, the numerical optimization gave optimum points for independent variables that could maximize the response. Among the obtained solutions, numerical optimization gave optimum points for the analyzed independent processes parameters as initial MBD concentration of 68.489 mg/L, the adsorbent dosage of 0.265, pH of 6.904, and contact time of 77.873 minutes. At these optimum points of independent parameters, the maximum removal efficiency of MBD ions was found to be 99.769%. The percentage removal of MBD in optimized conditions was compared by different adsorbents used in previous studies. The results shown in Table 4.5 indicate the synthesized nano adsorbent (ZnO-TSA NPS) has a good performance compared to other modified adsorbents presented in previous studies.

Therefore, the present study showed that Teff straw-supported Zinc oxide nanoparticles have potential adsorption ability in MBD removal and the result was in the acceptable range with previous studies (Afolabi et al., 2021).

Table 4.5: Comparison of different adsorbents for MBD removal

Adsorbent	C_o (mg/L)	Adsorption Capacity (mg/g)	%MBD removal	Reference
Acid treated sugarcane bagasse	6	64.9351	98.57	(Nharingo et al., 2013)
Pine Cone Biomass of Pinus radiate	20	109.89	92.62	(Sen et al., 2011)
Banana trunk	25	166.51	96	(Danish et al., 2018)
Lantana camera stem	50	19.84	85	(Amuda et al., 2014)
Rejected tea	50	147	94	(Nasuha et al., 2010)

Table 4.6: Comparison of various adsorbents for percentage removal of MBD

Adsorbent	C_o (mg/L)	Adsorbent dosage (g)	PH	Contact time (min)	%MBD removal	Reference
sawdust/MgO nano biocomposite	50	3.5	11	-	94.05	(Sharifi & Shoja, 2018)
MgO/AC Nps	10.9	69.4	10.2	149.1	99.6	(Ghalehkhondabi et al., 2021)
Fe_3O_4 Nps -extract of centaurea cyanus plant	90	3.6	5	93	83.96	(Davarnejad et al., 2020)
ZnO-TSA NPs	68.489	0.265	6.904	77.873	98.940	This study

Table 4.7: Optimum possible conditions for MBD removal

Number	ZnO-TSA NPS dosage	Contact time	Initial conc.MBD	pH	Removal Efficiency	Desirability	
1	**0.265**	**77.873**	**68.489**	**6.904**	**99.769**	**1.000**	**Selected**

The optimal conditions selected were shown on-ramps in Figures 4.20. Optimal points responsible for optimum removal efficiency were indicated on the ramps that connect the values of the process variables. Thus, optimal removal efficiency indicted on-ramps was obtained at optimal parameters where ZnO-TSA is 0.265g; initial MBD concentration is 68.489mg/mL; solution pH is 6.904, and contact time is 77.873 min.
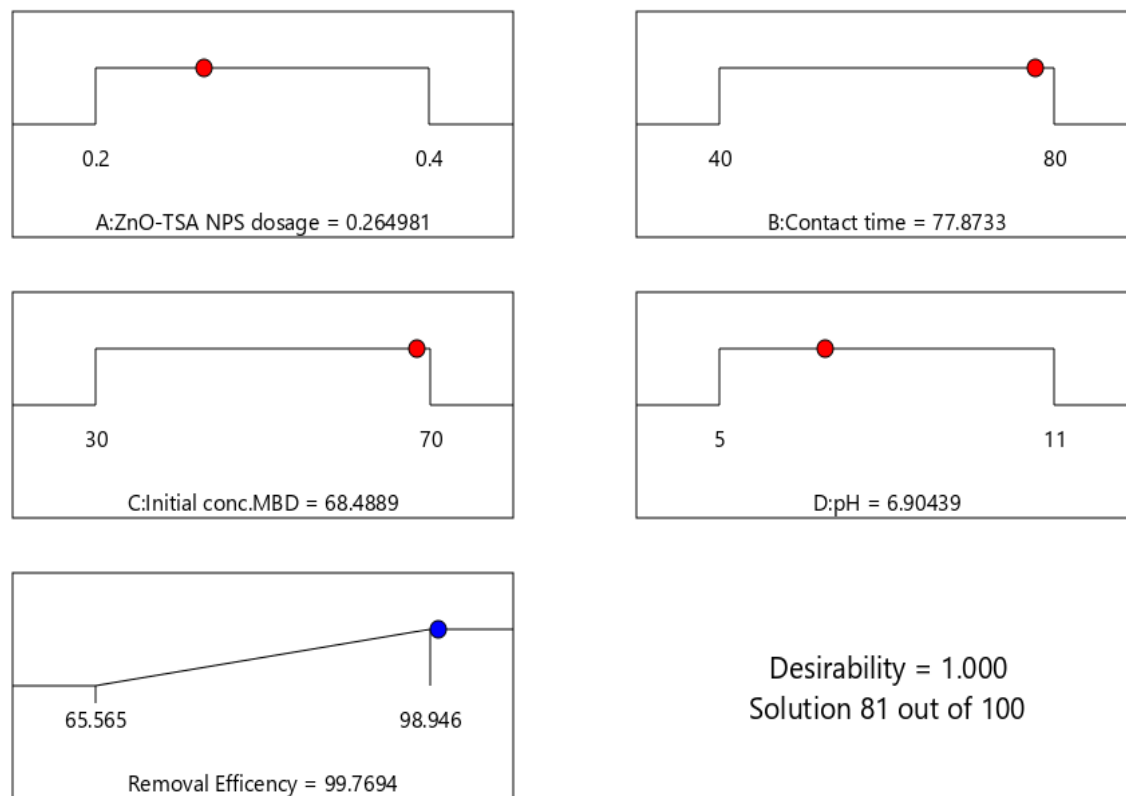
Figure 4.20: Desirability ramp for the optimization of the response and the parameters

4.3.8. Model Validation

Numerous tests were carried out to check the validity of the model at predicted optimum process parameters. As a result, quadruplicate tests were conducted using the predicted optimum process parameters, and the average removal efficiency of MBD was experimentally found to be 98.940% showing the high reliability of the model. It was found that the predicted and experimental values were near to each other. There was only a slight percentage difference (0.83%) between the predicted and experimental values. So, the validity of the model was confirmed because it is less than 3%, showing that the quadratic models adopted could predict the experimental result well. Similarily,the efficiency of normal Zinc oxide nps using the optimized parameters of teff straw assisted zinc oxide nanoparticles was tested experimentally and was reported as 97.878%.Therefore, as compared both the efficiencies of teff straw assisted zinc oxide nanoparticles with normal zinc oxide nps,the teff straw assisted zinc oxide nps was highly efficient one.

4.4. Arbaminch Wastewater characterization and Treatment

The Characteristics of Arbaminch Textile Industry Wastewater before and after adsorption through experiment conducted was obtained at an optimum level.

4.4.1. Dye removal from textile wastewater

Next to determining the optimal conditions for the adsorption of MB dye from aqueous solutions, teff straw supported zinc oxide nanoparticles capability for the removal of MB dye from wastewater of a textile factory, was tested. Two samples (50mL) of effluent, with 0.265g adsorbent were contacted in the optimum conditions. 68mg/L of the dye was manually added to asample, and another sample without adding any dye was studied at Contact time 78 min, and pH=6.904. The results indicated that about 92.5% of the dye were removed. In addition to MB dye, industrial textile contains large amounts of other common dyes. Thus, the results of this study show the high performance of teff straw assisted Zinc oxide nanoparticles for MB dye removal from wastewater (Khoshhesab et al., 2010). The removal efficiency of wastewater after treatment of impurities were 75%.

Table 4.8: Comparison between Raw and Treated Arbaminch Wastewater

Textile wastewater parameter	Impurities before Treatment	Impurities after Treatment	Removal Efficiency (%)
COD (mg/L)	512	128	75
Chloride (mg/L)	53	15	71
TS (mg/L)	1055	940	10.9
TDS (mg/L)	625	563	9.92
Turbidity (Ftu)	96.5	36.2	62
pH	7.8	7.08	-
BOD (mg/L)	269.5	67.36	75
TSS (mg/L)	430	377	-

4.4.2. Adsorption isotherm studies

The studies of adsorption isotherm were performed by differing initial concentrations of MBD from 10-90 mg/L at room temperature using 100 mL of initial methylene blue solutions with an adsorbent dose of 0.265 g, shaking speed of 180 rpm, the contact time of 77.873 min and pH of 6.904.The adsorption behaviour between the ZnO-TSA nanoparticles and MBD ions under different concentrations was interpreted by a Langmuir model and Freundlich isotherms models as shown in Figure 4.21 and 4.22 respectively. The outcomes set in Table 4.8 shows the experim ental data were fitted with both Langmuir and Freundlich adsorption isotherm model. But, Figure 4.22 describes that the result from experimental data fitted very well with the Freundlich isother m model than the Langmuir adsorption isotherm model with a good correlation coefficient (R^2) of 0.999.

Thus, it indicates the adsorption of MBD ions on the surface of ZnO-TSA nanoparticles effectively undergo the monolayer and homogeneous adsorption process of MBD ions than the multilayer adsorption process. The values of separation factor R_L $(0<R_L< 1)$ given in Table 4. 8, designates favorability of adsorption process with maximum adsorption capacity (qmax) of 2.32 mg*g^{-1} (Table 4.8). Furthermore, a value of Langmuir coefficient (b) which is 0.4311 L mg^{-1} implies strong binding sites exist on the surface of the adsorbent, thus the adsorbents can adsorb dyes effectively. In another hand, as represented in Table 4.8, the value of Freundlich constant (n) which is greater than 1 indicates favorable adsorption condition with a correlation coefficient (R^2) of 0.999 representing that heterogeneous condition can exist.

Generally, in this thesis study, the Freundlich isotherm model gives the best fit to the experimental data in contrast to the languimer isotherm model with a maximum correlation coefficient as indicated in Table 4.8 below.
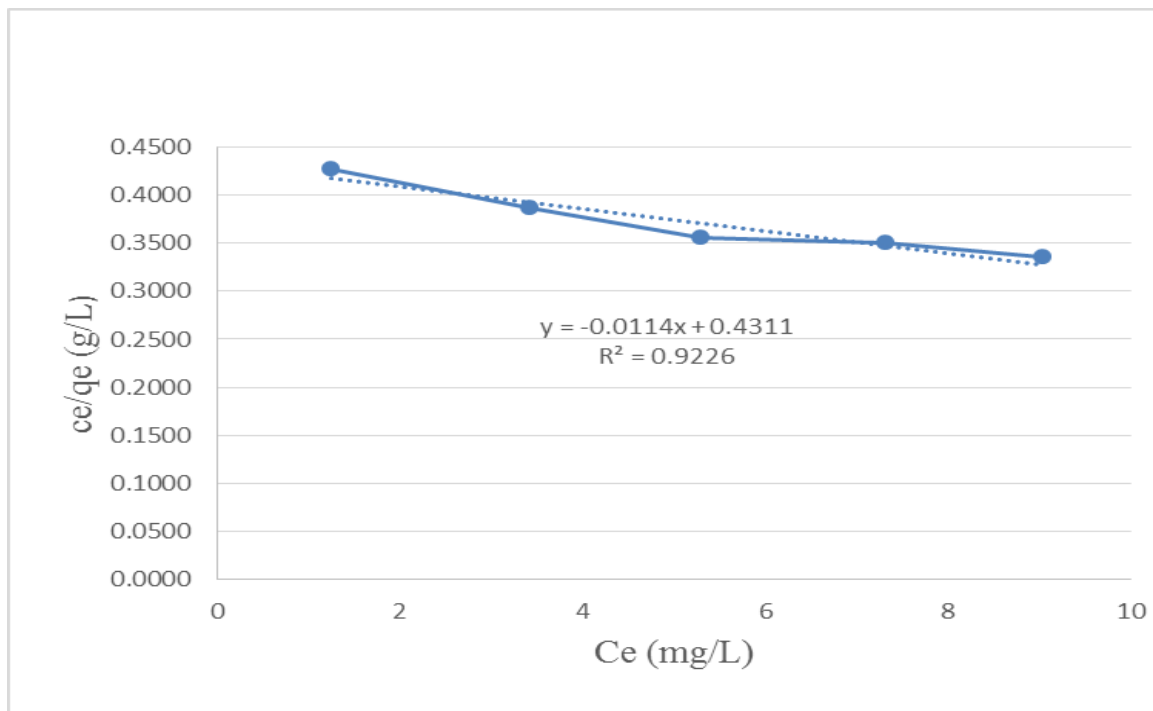
Figure 4.21: Languimuir isotherm model of MBD removal
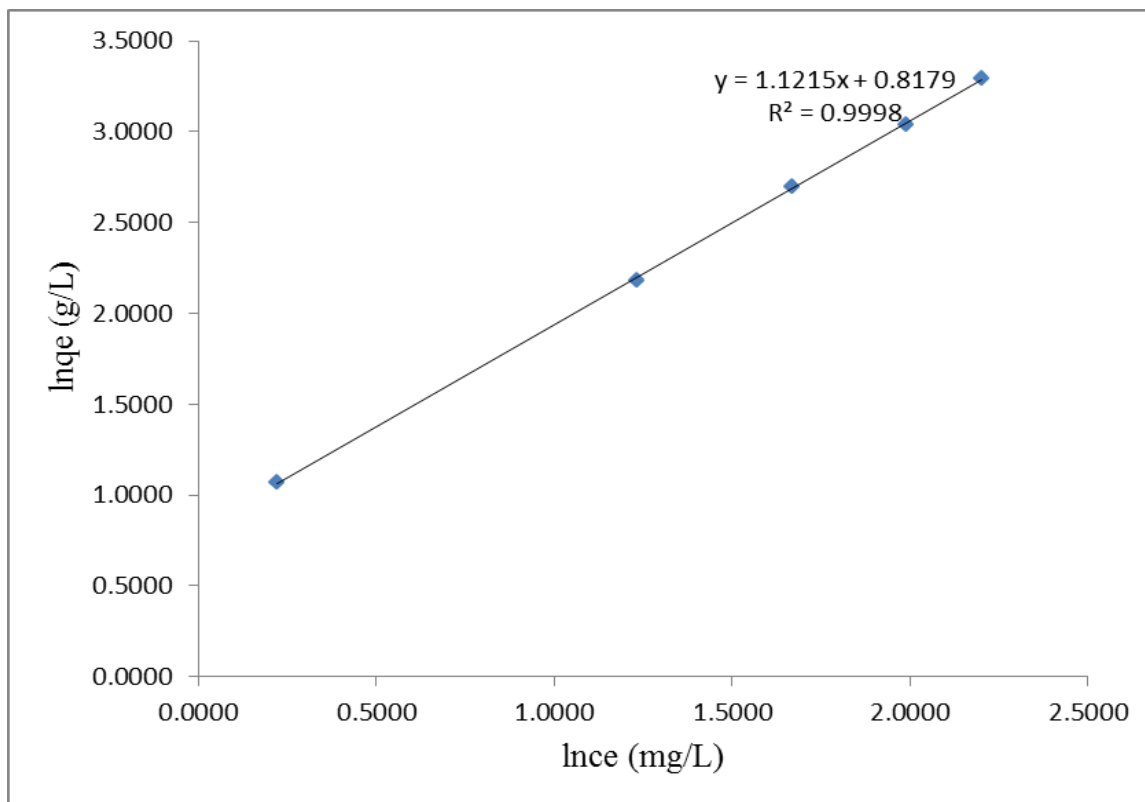
Figure 4.22: Freundlich isotherm model of MBD removal

Table 4.9: Langmuir and Freundlich parameters for the removal of MBD using ZnO-TSA nanoparticles.

Adsorbent	Languimer			Freundlich			
	Qmax (mg/g)	b (l/mg)	R^2	K_f	n	1/n	R^2
ZnO-TSA NPs	2.32	0.4311	0.9226	6.58	0.89	1.1215	0.999

Table 4.10: Langmuir separation factor (RL)

C_O	10	30	50	70	90
R_L	0.20	0.07	0.044	0.032	0.021

5. CONCLUSIONS AND RECOMMENDATION

5.1. Conclusion

In this study, ZnO-TSA nanoparticles were effectively synthesized by the green method and the surface-modified nano-adsorbent was used for MBD removal from Textile wastewater. The physicochemical properties of Teff straw-assisted ZnO nanoparticles were characterized using XRD, and FT-IR analysis techniques. FT-IR spectrum, XRD analysis showed that the ZnO-TSA nanoparticles were synthesized and were efficiently functionalized. The analysis of XRD also revealed that Teff straw-supported ZnO-TSA nanoparticles have average crystalline sizes of 27.196nm. Removal of MBD was investigated using the synthesized ZnO-TSA nanoparticles and was found that different parameters pH, contact time, the dosage of ZnO-TSA nanoparticles, and initial concentration significantly affect the removal of MBD. RSM with CCD was utilized for the optimization of adsorption of MBD from wastewater using ZnO-TSA NPs. Based on the analysis, the optimum adsorption parameters acquired by the quadratic model for maximum removal efficiency of MBD were 6.904, 68.489 mg/L, 0.265 g, and 77.873 min for pH, initial MBD concentration, the dosage of ZnO-TSA NPs, and contact time respectively. On these optimum process parameters, the maximum removal efficiency of MBD was found to be 99.769 %. The result from the model also confirmed that all the independent adsorption parameters significantly affected the adsorption of MBD and most importantly, pH and adsorbent dose were the dominant ones. The experimental removal efficiency (98.940%) agreed with the predicted one (99.7694%) confirming the fitness of the model used and the success of response surface methodology in optimizing of removal of MBD from Textile wastewater. The MBD removal was adequately fitted into the Freundlich isotherm model with correlation coefficients of 0.99.

Also, the water quality parameters in real textile wastewater were determined and compared with synthetic MBD removal. Thus, the maximum removal efficiency of MBD from real textile wastewater was found to be 92.5%. Generally , this study showed that green synthesized Teff straw assisted ZnO-TSA nanoparticles as an efficient nano-adsorbent for the removal of MBD.

5.2. Recommendation

In this thesis study, surface-modified ZnO-TSA nanoparticles were synthesized and utilized for the removal of MBD. The result from the experimental study demonstrated that the synthesized nano-adsorbent has an efficient capacity for the removal of MBD from Textile wastewater. Thus, the effectiveness of ZnO-TSA nanoparticles on MBD removal from real wastewater like paper industry, paint industry, leather industry, and the like needs further study. The study on surface modification of metal oxide nanoparticles using agricultural waste biomass specifically on green-based synthesis, optimization of process variables like plant extract, mass of precursor, temperature that affect plant extraction,controlling the calicination temperature during synthesis znic oxide nps, Physico-chemical parameters such as BET, Surface area, Particle density, Moisture content, ash content, and the like needs further studies.

Additional characterization of ZnO-TSA nanoparticles by TEM, TGA, SEM, DLS, and other characterization techniques is also needed in order to know the nanoparticles morphology, size and the like. Further researches can be also do on adsorption kinetics studies and the use of residue left after adsorption of dye for cycling and regeneration purposes. Also, Competitive adsorption of other dyes and adsorption thermodynamics study needs an investigation by future researchers.The potential of Zinc oxide nanoparticles and agricultural residue in dye removal from wastewater is clearly towards a future dreams, but it requires the mutual efforts of study and industrial persons to become visible, economical, and viable water treatment technology. Through working with mutually, it will be promising to solve water contamination from the textile industry worldwide.

REFERENCES

Abate, G. Y., Alene, A. N., Habte, A. T., & Getahun, D. M. (2020). Adsorptive removal of malachite green dye from aqueous solution onto activated carbon of Catha edulis stem as a low cost bio-adsorbent. *Environmental Systems Research*, *9*(1), 29. https://doi.org/10.1186/s40068-020-00191-4

Abdelbasir, S. M., & Shalan, A. E. (2019). An overview of nanomaterials for industrial wastewater treatment. *Korean Journal of Chemical Engineering*, *36*(8), 1209–1225. https://doi.org/10.1007/s11814-019-0306-y

Adamu, A. (2008). Adsorptive removal of reactive azo dyes using industrial residue, *Msc. thesis, Ethiopia:* Addis Ababa University.

Afolabi, F., Musonge, P., & Bakare, B. (2021). Evaluation of Lead (II) Removal from WastewaterUsing Banana Peels: Optimization Study. *Polish Journal of Environmental Studies*, *30*(2), 1487–1496. https://doi.org/10.15244/pjoes/122449

Ahmadi, S., Engineering, E. H., & Igwegbe, C. A. (2020). Removal of Methylene Blue on Zinc Oxide Nanoparticles: Nonlinear and Linear Adsorption Isotherms and Kinetics Study. *Sigma J Eng & Nat Sci*, *1*(38), 289–303.

Akhter, M., & Habib, G. (2018). Application of electrodialysis in waste water treatment and impact of fouling on process performances. *Journal of Medical Case Reports and Reviews*, *7*, 89–100.

Ali, H. R., & Hassaan, M. A. (2017). *Applications of Bio-waste Materials as Green Synthesis of Nanoparticles and Water Purification*. *April*. https://doi.org/10.11648/j.am.20170605.16

Alzohairy, M. A. (2016). Therapeutics role of Azadirachta indica (Neem) and their active constituents in diseases prevention and treatment. *Evidence-Based Complementary and Alternative Medicine*.

Amuda, O. S., Olayiwola, A. O., Alade, A. O., Farombi, A. G., & Adebisi, S. A. (2014). AAdsorption of Methylene Blue from Aqueous Solution Using Steam-Activated Carbon

Produced from Lantana camara Stem. *Journal of Environmental Protection*, *05*, 1352–1363. https://doi.org/10.4236/jep.2014.513129

Anjum, M., Miandad, R., Waqas, M., Gehany, F., & Barakat, M. A. (2016). Remediation of wastewater using various nano-materials. *Arabian Journal of Chemistry*, 1–23. https://doi.org/10.1016/j.arabjc.2016.10.004

Annu, Ali, A., & Ahmed, S. (2018). Green Synthesis of Metal, Metal Oxide Nanoparticles, and Their Various Applications. In *Handbook of Ecomaterials*. https://doi.org/10.1007/978-3-319-48281-1_115-1

Awad, A. M., Jalab, R., Benamor, A., Nasser, M. S., Ba-Abbad, M. M., El-Naas, M., & Mohammad, A. W. (2020). Adsorption of organic pollutants by nanomaterial-based adsorbents: An overview. *Journal of Molecular Liquids*, *301*, 112335. https://doi.org/10.1016/j.molliq.2019.112335

Bageru, A. B., & Srivastava, V. C. (2018). Biosilica preparation from abundantly available African biomass Teff (Eragrostis tef) straw ash by sol-gel method and its characterization. *Biomass Conversion and Biorefinery*, *8*(4), 971–978. https://doi.org/10.1007/s13399-018-0335-5

Banala, R. R., Nagati, V. B., & Karnati, P. R. (2015). Green synthesis and characterization of Carica papaya leaf extract coated silver nanoparticles through X-ray diffraction, electron microscopy and evaluation of bactericidal properties. *Saudi Journal of Biological Sciences, 22*(5), 637–644.

Bandeira, M., Giovanela, M., Roesch-Ely, M., Devine, D. M., & da Silva Crespo, J. (2020). Green synthesis of zinc oxide nanoparticles: A review of the synthesis methodology and mechanism of formation. *Sustainable Chemistry and Pharmacy*, *15*, 100223. https://doi.org/10.1016/j.scp.2020.100223

Basnet, P., Chanu, T. I., Samanta, D., & Chatterjee, S. (2018). A review on bio-synthesized zinc oxide nanoparticles using plant extracts as reductants and stabilizing agents. *Journal of Photochemistry and Photobiology B: Biology*, *183*, 201-221.

Bharathiraja, B., Jayamuthunagai, J., Praveenkumar, R., & Iyyappan, J. (2018). Phytoremediation Techniques for the Removal of Dye in Wastewater. *Energy, Environment, and Sustainability*, 243–252. https://doi.org/10.1007/978-981-10-7485-1_12.

B. M. D'Antoni, F. Iracà, & Romero, M. (2017). *Abstract review on: Current treatment technologies and practical approaches on textile wastewater Dyes Removal*. https://doi.org/10.13140/RG.2.2.11472.71689

Bora, T., Sathe, P., Laxman, K., Dobretsov, S., & Dutta, J. (2017). Defect engineered visible light active ZnO nanorods for photocatalytic treatment of water. *Catalysis Today*, *284*, 11–18. https://doi.org/10.1016/j.cattod.2016.09.014

Chauhan, D., Talreja, N., & Ashfaq, M. (2021). Nanoadsorbents for wastewater remediation. In *Aquananotechnology* (pp. 273–290). Elsevier. https://doi.org/10.1016/B978-0-12-821141-0.00017-3

Chemingui, H., Rezma, S., Lafi, R., Alhalili, Z., Missaoui, T., Harbi, I., Smiri, M., & Hafiane, A. (2021). Investigation of methylene blue adsorption from aqueous solution onto ZnO nanoparticles: Equilibrium and Box-Behnken optimisation design. *International Journal of Environmental Analytical Chemistry*, 1–26. https://doi.org/10.1080/03067319.2021.1897121

Chockalingam, N., Banerjee, S., & Muruhan, S. (2019). *Characterization of Physicochemical Parameters of Textile Effluents and Its Impacts on Environment*. *17*(2), 41–53. https://doi.org/10.32526/ennrj.17.2.2019.11

Dakhil, I. H. (2013). Adsorption of Methylene Blue Dye from Wastewater By Spent Tea Leaves. *Journal of Kerbala University*, *11*(3), 5–14.

Danish, M., Ahmad, T., Majeed, S., Ahmad, M., Ziyang, L., Pin, Z., & Shakeel Iqubal, S. M. (2018). Use of banana trunk waste as activated carbon in scavenging methylene blue dye: Kinetic, thermodynamic, and isotherm studies. *Bioresource Technology Reports*, *3*, 127–137. https://doi.org/10.1016/j.biteb.2018.07.007

D'Antoni, B. M., Iracà, F., & Romero, M. (2017). Abstract review on: Current treatment technologies and practical approaches on textile wastewater dyes removal. *Panta Rei Srl-Water Solutions*, 1–10. https://doi.org/10.13140/RG.2.2.11472.71689

Dargo, H., Gabbiye, N., & Ayalew, A. (2015). Removal of Methylene Blue from Waste Water Using Activated Carbon Prepared from Rice Husk Removal of Methylene Blue from Waste Water Using Activated Carbon Prepared from. *International Journal of Innovation and Scientific Research*, *9*(January), 317–325.

Das, B., Dash, S. K., Mandal, D., Ghosh, T., Chattopadhyay, S., Tripathy, S., Das, S., Dey, S. K., Das, D., & Roy, S. (2017). Green synthesized silver nanoparticles destroy multidrug resistant bacteria via reactive oxygen species mediated membrane damage. *Arabian Journal of Chemistry*, *10*(6), 862–876. https://doi.org/10.1016/j.arabjc.2015.08.008

Daud, N. D., Puzi, S. M., & Rozi, S. K. M. (2019). *New Application of Pomegranate Peel Waste: The Decontamination of Toxic Methylene Blue Dye from Textile Wastewater*. *11*, 14.

dos Santos, A. B., Cervantes, F. J., & van Lier, J. B. (2007). Review paper on current technologies for decolourisation of textile wastewaters: Perspectives for anaerobic biotechnology. *Bioresource Technology*, *98*(12), 2369–2385. https://doi.org/10.1016/j.biortech.2006.11.013

Davarnejad, R., Azizi, A., Mohammadi, M., & Mansoori, S. (2020). A green technique for synthesising iron oxide nanoparticles by extract of centaurea cyanus plant: An optimised adsorption process for methylene blue. *International Journal of Environmental Analytical Chemistry*, 1–15. https://doi.org/10.1080/03067319.2020.1756273

Dave, P. N., & Chopda, L. V. (2014). Application of iron oxide nanomaterials for the removal of heavy metals. *Journal of Nanotechnology*, 1–15. https://doi.org/10.1155/2014/398569

Devi, H. S., & Singh, T. D. (2014). Synthesis of copper oxide nanoparticles by a novel method and its application in the degradation of methyl orange. *Advance in Electronic and Electric Engineering*, *4*(1), 83–88.

Dixit, S., & Hering, J. G. (2003). *Comparison of Arsenic (V) and Arsenic (III) Sorption onto Iron Oxide Minerals: Implications for Arsenic Mobility*. *37*(18), 4182–4189.

Dong, Y., Su, Y., Chen, W., Peng, J., Zhang, Y., & Jiang, Z. (2011). Ultrafiltration enhanced with activated carbon adsorption for efficient dye removal from aqueous solution. *Chinese Journal of Chemical Engineering*, *19*(5), 863–869. https://doi.org/10.1016/S1004-9541(11)60066-9

Dutta, S., Gupta, B., Srivastava, S. K., & Gupta, A. K. (2021). Recent advances on the removal of dyes from wastewater using various adsorbents: A critical review. *Materials Advances*, *2*(14), 4497–4531. https://doi.org/10.1039/d1ma00354.

Ehssan Nassef, N. S. Y. and R. F. (2020). Adsorption of Dye by Nano-zinc oxide. *J Am Sci*, *3*(16), 81–89. https://doi.org/10.7537/marsjas160320.10.

Farraji, H., Zaman, N. Q., Tajuddin, R. M., & Faraji, H. (2016). Advantages and Disadvantages of Advantages and Disadvantages of. *IMerit and Demerit of Phytoremediation Int J Env Tech Sci*, 1–75.

Fatiha, M., & Belkacem, B. (2016). *Adsorption of methylene blue from aqueous solutions using natural clay*. *7*(1), 285–292.

Gayathri, S., Manjunath, N. T., Nagarajappa, D. P., & Shetty, R. (2019). Batch studies on color removal potential by Zinc oxide nanoparticles. *July*, 2181–2185.

Getasew Nibreta, Shadab Ahmadb, Dubasi Govardhana Raoc, Imran Ahmadd, S. M. A. and Z. U. R. (2019). Removal of Methylene Blue Dye from Textile Wastewater Using Water Hyacinth Activated Carbon as Adsorbent: Synthesis, Characterization and Kinetic Studies. *International Conference on Sustainable Computing in Science*, 1959–1969.

Geetha.V (20173). *Green synthesis of silver nanoparticles from Azadirachta indica leaves and its antibacterial activity*. *International Journal of Applied Research*, 3(7), 313-316.

Ghalehkhondabi, V., Fazlali, A., & Ketabi, K. (2021). Synthesis and characterization of modified activated carbon (MgO/AC) for methylene blue adsorption: Optimization, equilibrium

isotherm and kinetic studies. *Water Science and Technology*, *83*(7), 1548–1565. https://doi.org/10.2166/wst.2021.016

Gopalakrishnan, K., Ramesh, C., Ragunathan, V., & Thamilselvan, M. (2012). Antibacterial activity of Cu2O nanoparticles on e.coli synthesized from tridax procumbens leaf extract and surface coating with polyaniline. *Digest Journal of Nanomaterials and Biostructures*, *7*(2), 833–839.

Gosavi, V. D., & Sharma, S. (2013). *A General Review on Various Treatment Methods for Textile Wastewater*. 12.

Goutam, S. P., Saxena, G., Roy, D., Yadav, A. K., & Bharagava, R. N. (2020). Green Synthesis of Nanoparticles and Their Applications in Water and Wastewater Treatment. In *Bioremediation of Industrial Waste for Environmental Safety* (Issue Dm). https://doi.org/10.1007/978-981-13-1891-7_16

Gu, M., Hao, L., Wang, Y., Li, X., Chen, Y., Li, W., & Jiang, L. (2020). The selective heavy metal ions adsorption of zinc oxide nanoparticles from dental wastewater. *Chemical Physics*, *534*(June), 110750. https://doi.org/10.1016/j.chemphys.2020.110750

Guncha Munjal, G. D. and A. N. B. (2015). Adsorption Studies of Methylene Blue on TiO2 Nanoparticles: Experimental and Mathematical Modeling Guncha. *International Proceedings of Chemical, Biological and Environmental Engineering*, *90*, 1–5. https://doi.org/10.7763/IPCBEE

H. Shokry Hassan, 1 M. F. Elkady, 2, 3 A. H. El-Shazly, 2 andHishamS.Bamufleh4 1. (2014). Formulation of Synthesized Zinc Oxide Nanopowder into Hybrid Beads for Dye Separation. *Journal of Nanomaterials*, *2014*.

Herlekar, M., Barve, S., & Kumar, R. (2014). Plant-Mediated Green Synthesis of Iron Nanoparticles. *Journal of Nanoparticles*, *2014*, 1–9. https://doi.org/10.1155/2014/140614

Hina, Khatoona & Jai Prakash, N. R. (2016). Agricultural Waste Materials as Biosorbents for the Removal of Heavy Metals and Synthetics Dyes. *Octa Journal of Environmental Research*, *4*(3), 208–229.

Homaeigohar, S. (2020). The Nanosized Dye Adsorbents for Water Treatment. *MDPI*, *10*(295), 1–43.

Iwuozor, K. O. (2019). Prospects and Challenges of Using Coagulation-Flocculation method in the treatment of Effluents. *Advanced Journal of Chemistry*, *2*(2), 105–127. https://doi.org/10.29088/sami/ajca.2019.2.105127

Jabbari, R., & Ghasemi, N. (2021). *Investigating Methylene Blue Dye Adsorption Isotherms Using Silver Nano Particles Provided by Aqueous Extract of Tragopogon Buphthalmoides*. *5*, 21–29.

Jadhav, A. C., & Jadhav, N. C. (2021). Treatment of textile wastewater using adsorption and adsorbents. In *Sustainable Technologies for Textile Wastewater Treatments* (Issue January). https://doi.org/10.1016/b978-0-323-85829-8.00008-0

Kahraman, O., Binzet, R., Turunc, E., Dogen, A., & Arslan, H. (2018). Synthesis, characterization, antimicrobial and electrochemical activities of zinc oxide nanoparticles obtained from sarcopoterium spinosum (L.) spach leaf extract. *Materials Research Express, 5*(11), 115017.

Kandisa, R. V., & Saibaba KV, N. (2016). Dye Removal by Adsorption: A Review. *Journal of Bioremediation & Biodegradation*, *07*(06), 1–4. https://doi.org/10.4172/2155-6199.1000371

Kannan, M., & Sivakumar, P. (2016). *An Overview on synthesis of metal oxide nanoparticles*. *March*.

Kecili, R., & Hussain, C. M. (2018). Mechanism of adsorption on nanomaterials. In *Nanomaterials in Chromatography: Current Trends in Chromatographic Research Technology and Techniques*. Elsevier Inc. https://doi.org/10.1016/B978-0-12-812792-6.00004-2

Khaing, M. M., Thu, M. K., Kyaw, T., Tin, T., & Lwin, T. (2018). *Green Synthesis of Zinc Oxide Nanoparticles Using Tropical Plants and Their Characterizations*. *9*(8), 6.

Khairunnisa, S., Wonoputri, V., & Samadhi, T. W. (2021). Effective Deagglomeration in Biosynthesized Nanoparticles: A Mini Review. *IOP Conference Series: Materials Science and Engineering*, *1143*(1), 012006. https://doi.org/10.1088/1757-899x/1143/1/012006

Khalil, K. A., Fouad, H., Elsarnagawy, T., & Almajhdi, F. N. (2013). Preparation and characterization of electrospun PLGA/silver composite nanofibers for biomedical applications. *International Journal of Electrochemical Science*, *8*(3), 3483–3493.

Khan, S. A., Khan, S. B., Khan, L. U., Farooq, A., Akhtar, K., & Asiri, A. M. (2018). Fourier Transform Infrared Spectroscopy: Fundamentals and Application in Functional Groups and Nanomaterials Characterization. In S. K. Sharma (Ed.), *Handbook of Materials Characterization* (pp. 317–344). Springer International Publishing. https://doi.org/10.1007/978-3-319-92955-2_9

Khoshhesab, Z. M., Gonbadi, K., & Behbehani, G. R. (2010). Removal of Reactive Red 74 Dye from Textile Industrial Waste using Zinc Oxide Nanoparticle. Journal of advances in chemistry, *6*(3), 1077–1084. https://doi.org/10.24297/jac.v6i3.2645

Khosravi, M., & Arabi, S. (2016). Application of response surface methodology (RSM) for the removal of methylene blue dye from water by nano zero-valent iron (NZVI). *Water Science and Technology*, *74*(2), 343–352. https://doi.org/10.2166/wst.2016.122

Kyzas, G. Z., & Kostoglou, M. (2014). Green adsorbents for wastewaters: A critical review. *Materials*, *7*(1), 333–364. https://doi.org/10.3390/ma7010333

Mahmoud, M., El-Latif, A., Abd El-Latif, M. M., Ibrahim, A. M., & El-Kady, M. F. (2010). Adsorption Equilibrium, Kinetics and Thermodynamics of Methylene Blue from Aqueous Solutions Using Biopolymer Oak Sawdust Composite Water desalination View project Construction of Magnetic Materials Laborstory View project Adsorption Equilibrium, kinetics. *Journal of American Science*, *6*(6), 1–18.

Manyangadze, M., Chikuruwo, N. H. M., Narsaiah, T. B., Chakra, C. S., Radhakumari, M., & Danha, G. (2020). Enhancing adsorption capacity of nano-adsorbents via surface modification: A review. *South African Journal of Chemical Engineering*, *31*, 25–32. https://doi.org/10.1016/j.sajce.2019.11.003

Marimón-Bolívar, W., & González, E. E. (2018). Study of agglomeration and magnetic sedimentation of glutathione@fe3o4 nanoparticles in water medium. *DYNA (Colombia)*, *85*(205), 19–26. https://doi.org/10.15446/dyna.v85n205.68245

Métivier-Pignon, H., Faur-Brasquet, C., & Le Cloirec, P. (2003). Adsorption of dyes onto activated carbon cloths: *Separation and Purification Technology*, *31*(1), 3–11. https://doi.org/10.1016/S1383-5866(02)00147-8

Miao, Y. (1992). Biological remediation of dyes in textile effluent: A review on current treatment technologies. *Water*, 1–10.

Mittal, A. K., Chisti, Y., & Banerjee, U. C. (2013). Synthesis of metallic nanoparticles using plant extracts. *Biotechnology Advances*, *31*(2), 346–356. https://doi.org/10.1016/j.biotechadv.2013.01.003

Moawed, E. A., Hegajy, T. A., Kosbar, T. R., & Eissa, M. S. (2019). *Removal of methylene blue dye from wastewater using ZnONPs in the dark and light*. *July*.

Mohammad Razi, M. A., Mohd Hishammudin, M. N. A., & Hamdan, R. (2017). Factor Affecting Textile Dye Removal Using Adsorbent from Activated Carbon: A Review. *MATEC Web of Conferences*, *103*(06015), 1–17. https://doi.org/10.1051/matecconf/201710306015

Mulushewa, Z., Dinbore, W. T., & Ayele, Y. (2021). Removal of methylene blue from textile waste water using kaolin and zeolite-x synthesized from Ethiopian kaolin. *Environmental Analysis Health and Toxicology*, *36*(1), e2021007. https://doi.org/10.5620/eaht.2021007

Muruganandam, L., Kumar, M. P. S., Jena, A., Gulla, S., & Godhwani, B. (2017). Treatment of waste water by coagulation and flocculation using biomaterials. *IOP Conference Series: Materials Science and Engineering*, *263*(3), 1–11. https://doi.org/10.1088/1757-899X/263/3/032006

Muruganandham, M., Zhang, Y., Suri, R., Lee, G., Chen, P., Hsieh, S., Sillanpää, M., & Wu, J. J. (2015). Environmental Applications of ZnO Materials. *Journal of Nanoscience and Nanotechnology*, *15*, 6900–6913. https://doi.org/10.1166/jnn.2015.10725

Myneni, V. R. (2020). Methylene Blue Adsorption by Magnesium Oxide Nanoparticles Immobilized with Chitosan (CS-MgONP): Response Surface Methodology, Isotherm, Kinetics and Thermodynamic Studies. *Iran. J. Chem. Chem. Eng.*, *39*(6), 1–46.

Nalwa, K., Thakur, A., & Sharma, N. (2017). *Synthesis of ZnO nanoparticles and its application in adsorption*. *2*(11), 696–703. https://doi.org/10.5185/amp/2017/696

Narjes Babadi, H. T. and M. A. (2018). Synthesis and characterization of nanocomposite NiFeO4@salensi and its application in efficent removal of Ni(II) from aqueous solution. *Bull. Chem. Soc. Ethiop*, *32*(1), 77–88. https://dx.doi.org/10.4314/bcse.v32i1.7

Nasuha, N., Hameed, B. H., & Din, A. T. M. (2010). Rejected tea as a potential low-cost adsorbent for the removal of methylene blue. *Journal of Hazardous Materials*, *175*(1–3), 126–132. https://doi.org/10.1016/j.jhazmat.2009.09.138

Nethavhanani, T. (2017). *Synthesis of zinc oxide nanoparticles by a green process and the investigation of their physical properties.*

Nharingo, T., Shoniwa, V., Hunga, O., & Shumba, M. (2013). Exploring the biosorption of Methylene Blue dye onto acid treated sugarcane bagasse. *International Journal of Current Research*, *5*(08), 2169–2175.

Nik Abdul Ghani, N., Jami, M., & Alam, M. (2021). The role of nanoadsorbents and nanocomposite adsorbents in the removal of heavy metals from wastewater: A review and prospect. *Pollution*, *7*(1), 153–179. https://doi.org/10.22059/poll.2020.307069.859

Nithya, K., & Kalyanasundharam, S. (2019). Effect of chemically synthesis compared to biosynthesized ZnO nanoparticles using aqueous extract of C. halicacabum and their antibacterial activity. *OpenNano*, *4*. https://doi.org/10.1016/j.onano.2018.10.001

N.K.Sankaranarayanan1, Dr. S. K. (2021). Journal of University of Shanghai for Science and Technology ISSN: 1007-6735. *Journal of University of Shanghai for Science and Technology*, *23*(1007–6735), 887.

Okafor, F., Janen, A., Kukhtareva, T., Edwards, V., & Curley, M. (2013). Green synthesis of silver nanoparticles, their characterization, application and antibacterial activity. *International Journal of Environmental Research and Public Health*, *10*(10).

Oyewo, O. A., Adeniyi, A., Sithole, B. B., & Onyango, M. S. (2020). Sawdust-Based Cellulose Nanocrystals Incorporated with ZnO Nanoparticles as Efficient Adsorption Media in the Removal of Methylene Blue Dye. *ACS Omega*, *5*(30), 18798–18807. https://doi.org/10.1021/acsomega.0c01924

Özer, A., & Dursun, G. (2007). Removal of methylene blue from aqueous solution by dehydrated wheat bran carbon. *Journal of Hazardous Materials*, *146*(1–2), 262–269. https://doi.org/10.1016/j.jhazmat.2006.12.016

Pal, S., Mondal, S., & Maity, J. (2018). Green synthesis of silver nanoparticles using Moringa oleifera leaf extract. *Investigation of Photocatalytic Activity. J Nanosci Nanoeng Appl*, *8*, 60–68.

Pankaj, S., Lokeshwar, T., Mukesh, B., & Vishnu, B. (2011). Review on neem (Azadirachta indica): Thousand problems one solution. *International Research Journal of Pharmacy*, *2*(12), 97-102.

Pirbazari, A. E., & Saberikhah, E. (2014). Fe 3 O 4 – wheat straw: Preparation , characterization and its application for methylene blue adsorption. *Water Resources and Industry*, *7–8*, 23–37. https://doi.org/10.1016/j.wri.2014.09.001

Rafatullah, M., Sulaiman, O., Hashim, R., & Ahmad, A. (2010). Adsorption of methylene blue on low-cost adsorbents: A review. *Journal of Hazardous Materials*, *177*(1–3), 70–80. https://doi.org/10.1016/j.jhazmat.2009.12.047

Raizada, A., Ganguly, D., Mankad, M., & Krishna, R. H. (2014). *A Highly Efficient Copper Oxide Nanopowder for Adsorption of Methylene Blue Dye from Aqueous Medium*. *6*(4), 287–291.

Raj, A., & Lawerence, R. (2018). Green synthesis and charcterization of ZnO nanoparticles from leafs extracts of Rosa indica and its antibacterial activity. *Rasayan Journal of Chemistry*, *11*(3), 1339–1348. https://doi.org/10.31788/RJC.2018.1132009

Rajabi, M., Mahanpoor, K., & Moradi, O. (2017). Removal of dye molecules from aqueous solution by carbon nanotubes and carbon nanotube functional groups: Critical review. *RSC Advances*, *7*(74), 47083–47090. https://doi.org/10.1039/c7ra09377b

Ramesh, M., Anbuvannan, M., & Viruthagiri, G. (2014). Spectrochimica Acta Part A : Molecular and Biomolecular Spectroscopy Green synthesis of ZnO nanoparticles using Solanum nigrum leaf extract and their antibacterial activity. https://doi.org/10.1016/j.saa.2014.09.105

Rath, P. P., Priyadarshini, B., Behera, S. S., Parhi, P. K., & Panda, S. R. (2019). *Adsorptive removal of Congo Red dye from aqueous solution using TiO2 nanoparticles: Kinetics , thermodynamics and isothermal insights Adsorptive removal of Congo Red Dye from aqueous solution using TiO2 nanoparticles: Kinetics, Thermodynamics and Isot. 030115*(July), 2–6.

Rathilal, E. O. E. and S. (2020). Membrane Technologies in Wastewater Treatment : *MDPI*, *10*(89), 1–28.

Rathilal, S. (2021). Coagulation Treatment of Wastewater: Kinetics and Natural. *MDPI*, *26*(698), 1–15.

Ravva, S. V., & Korn, A. (2015). Effect of Neem (Azadirachta indica) on the Survival of Escherichia coli O157: H7 in Dairy Manure. *International Journal of Environmental Research and Public Health*, *12*(7), 7794–7803.

Razali, S. Z., Aziz, M. Y., Edinur, H. A., & Razali Ishak, A. (2020). Adsorption of Methylene Blue onto Iron Oxide Magnetic Nanoparticles Coated with Sugarcane Bagasse. *IOP Conference Series: Earth and Environmental Science*, *596*, 012052. https://doi.org/10.1088/1755-1315/596/1/012052

Robinson, T., Marchant, R., & Nigam, P. (2001). Remediation of dyes in textile e,uent: A critical review on current treatment technologies with a proposed alternative. *Bioresource Technology*, 9.

Saif, S., Tahir, A., & Chen, Y. (2016). Green synthesis of iron nanoparticles and their environmental applications and implications. *Nanomaterials*, *6*(11), 1–26. https://doi.org/10.3390/nano6110209

Sajjad, S., Leghari, S. A. K., Ryma, N.-U.-A., & Farooqi, S. A. (2018). Green Synthesis of Metal-Based Nanoparticles and their applications, (23–77). https://doi.org/10.1002/9781119418900.ch2

Sala, M., & Gutiérrez-Bouzán, M. C. (2012). Electrochemical techniques in textile processes and wastewater treatment. *International Journal of Photoenergy*, *2012*, 1–12. https://doi.org/10.1155/2012/629103

Saleem, H., & Zaidi, S. J. (2020). Developments in the application of nanomaterials for water treatment and their impact on the environment. In *Nanomaterials* (Vol. 10, Issue 9). https://doi.org/10.3390/nano10091764

Sangeetha, G., Rajeshwari, S., & Venckatesh, R. (2011). Green synthesis of zinc oxide nanoparticles by aloe barbadensis miller leaf extract: Structure and optical properties. *Materials Research Bulletin*, *46*(12), 2560–2566. https://doi.org/10.1016/j.materresbull.2011.07.046

Sen, T. K., Afroze, S., & Ang, H. M. (2011). Equilibrium, kinetics and mechanism of removal of methylene blue from aqueous solution by adsorption onto pine cone biomass of Pinus radiata. *Water, Air, and Soil Pollution*, *218*(1–4), 499–515. https://doi.org/10.1007/s11270-010-0663-y

Senthilkumar, N., Nandhakumar, E., Priya, P., Soni, D., Vimalan, M., & Potheher, I. V. (2017). *Synthesis of ZnO nanoparticles using leaf extract of Tectona grandis (L.) and their anti-bacterial, anti-arthritic, anti-oxidant and in vitro cytotoxicity activities. New Journal of Chemistry, 41(18), 10347-10356.*

Senthil Kumar, P., Joshiba, G. J., Femina, C. C., Varshini, P., Priyadharshini, S., Arun Karthick, M. S., & Jothirani, R. (2019). A critical review on recent developments in the low-cost adsorption of dyes from wastewater. *Desalination and water treatment*, *172*, 395–416. https://doi.org/10.5004/dwt.2019.24613.

Senthilkumar, S. R., & Sivakumar, T. (2014). Green tea (Camellia sinensis) mediated synthesis of zinc oxide (ZnO) nanoparticles and studies on their antimicrobial activities. *Int J Pharm Pharm Sci*, *6*(6), 461-465.

Seyed Hassan Sharifi, H. S., & Wood. (2018). *J. Water Environ. Nanotechnol*, *2*(3), 157-172 Spring. https://doi.org/10.22090/jwent.2018.02.007

Shadmehri, A. A., & Namvar, F. (2020). *A Review on Green Synthesis , Cytotoxicity Mechanism and Antibacterial Activity of Zno-NPs*. *6*(1), 23–31.

Shafey, A. M. El. (2020). Green synthesis of metal and metal oxide nanoparticles from plant leaf extracts and their applications: A review. *Green Processing and Synthesis*, *9*(1), 304–339. https://doi.org/10.1515/gps-2020-0031

Sharifi, S. H., & Shoja, H. (2018). *Optimization of process variables by response surface methodology for methylene blue dye removal using Spruce sawdust/MgO nano-biocomposite*. *3*(2), 157–172. https://doi.org/10.22090/jwent.2018.02.007

Simeonidis, K., Mourdikoudis, S., Kaprara, E., Mitrakas, M., & Polavarapu, L. (2016). Inorganic engineered nanoparticles in drinking water treatment: A critical review. *Environmental Science: Water Research & Technology*, *2*(1), 43–70. https://doi.org/10.1039/C5EW00152H

Singh, J., Dutta, T., Kim, K. H., Rawat, M., Samddar, P., & Kumar, P. (2018). "Green" synthesis of metals and their oxide nanoparticles: Applications for environmental remediation. *Journal of Nanobiotechnology*, *16*(1), 1–24. https://doi.org/10.1186/s12951-018-0408-4

Singh, S., Sidhu, G. K., & Singh, H. (2017). Removal of methylene blue dye using activated carbon prepared from biowaste precursor. *Indian Chemical Engineer*, 1–12. https://doi.org/10.1080/00194506.2017.1408431

Slama, H. B., Chenari Bouket, A., Pourhassan, Z., Alenezi, F. N., Silini, A., Cherif-Silini, H., Oszako, T., Luptakova, L., Golińska, P., & Belbahri, L. (2021). Diversity of Synthetic Dyes from Textile Industries, Discharge Impacts and Treatment Methods. *Applied Sciences*, *11*(14), 6255. https://doi.org/10.3390/app11146255

S, M., N, H., & P.P, V. (2020). In Vitro Biocompatibility and Antimicrobial activities of Zinc Oxide Nanoparticles (ZnO NPs) Prepared by Chemical and Green Synthetic Route—A Comparative Study. *BioNanoScience*, *10*(1), 112–121. https://doi.org/10.1007/s12668-019-00698-w

S N A Mohamad Sukri, K Shameli, E D Mohamed Isa, N. A. I. (2021). Green Synthesis of Zinc Oxide-Based Nanomaterials for Photocatalytic Studies: A Mini Review Green Synthesis of Zinc Oxide-Based Nanomaterials for Photocatalytic Studies: A Mini Review. *ICATAS-MJJIC 2020 IOP Conf. Series: Materials Science and Engineering*. https://doi.org/10.1088/1757-899X/1051/1/012083

Soltani, A., Faramarzi, M., & Mousavi Parsa, S. A. (2021). A review on adsorbent parameters for removal of dye products from industrial wastewater. *Water Quality Research Journal*, *56*(4), 181–193. https://doi.org/10.2166/wqrj.2021.023.

S. Prathap Chandran, Minakshi Chaudhary, Renu Pasricha, Absar Ahmad, * and Murali Sastry*. (2006). ASynthesis of Gold Nanotriangles and Silver Nanoparticles Using Aloe vera Plant Extract. *Biotechnol. Prog.*, *22*(2), 577−583.

Sulekha. (2016). Nanotechnology for waste water treatment. *International Journal of Chemical Studies IJCS*, *4*(2), 22–24.

Sundaramurthy, N., & Parthiban, C. (2015). Biosynthesis of Copper Oxide Nanoparticles Using Pyrus Pyrifolia Leaf Extract and Evolve the Catalytic Activity. *International Research Journal of Engineering and Technology*, *02*(06), 332–338.

Suresh, D., Nethravathi, P. C., Rajanaika, H., Nagabhushana, H., & Sharma, S. C. (2015). Green synthesis of multifunctional zinc oxide (ZnO) nanoparticles using Cassia fistula plant extrac and their photodegradative , antioxidant and antibacterial activities Materials Science in Semiconductor Processing Green synthesis of multifunctional z. *Materials Science in*

Semiconductor Processing, *31*(April 2021), 446–454.
https://doi.org/10.1016/j.mssp.2014.12.023

Swamy, M. M., Nagabhushana, B. M., Krishna, R. H., Kottam, N., Raveendra, R. S., & Prashanth, P. A. (2017). Fast adsorptive removal of methylene blue dye from aqueous solution onto a wild carrot flower activated carbon: Isotherms and kinetics studies. *Desalination and Water Treatment*, *71*(January), 399–405.
https://doi.org/10.5004/dwt.2017.20520

Tan, K. A., Morad, N., Teng, T. T., Norli, I., & Panneerselvam, P. (2012). Removal of Cationic Dye by Magnetic Nanoparticle (Fe3O4) Impregnated onto Activated Maize Cob Powder and Kinetic Study of Dye Waste Adsorption. *APCBEE Procedia*, *1*, 83–89.
https://doi.org/10.1016/j.apcbee.2012.03.015

Tan, K. B., Reza, A. K., Abdullah, A. Z., Amini Horri, B., & Salamatinia, B. (2018). Development of self-assembled nanocrystalline cellulose as a promising practical adsorbent for methylene blue removal. *Carbohydrate Polymers*, *199*, 92–101.
https://doi.org/10.1016/j.carbpol.2018.07.006

Tara, N., Siddiqui, S. I., Rathi, G., Chaudhry, S. A., Inamuddin, & Asiri, A. M. (2019). Nano-engineered Adsorbent for the Removal of Dyes from Water: A Review. *Current Analytical Chemistry*, *16*(1), 14–40. https://doi.org/10.2174/1573411015666190117124344

Thema, F. T., Manikandan, E., Dhlamini, M. S., & Maaza, M. (2015). Green synthesis of ZnO nanoparticles via Agathosma betulina natural extract. *Materials Letters*, *161*, 124–127.
https://doi.org/10.1016/j.matlet.2015.08.052

Tsade Kara, H., Anshebo, S. T., Sabir, F. K., & Adam Workineh, G. (2021). Removal of Methylene Blue Dye from Wastewater Using Periodiated Modified Nanocellulose. *International Journal of Chemical Engineering*, *2021*, 1–16.
https://doi.org/10.1155/2021/9965452

Verma, R. K., Sankhla, M. S., Rathod, N. V., Sonone, S. S., Parihar, K., & Singh, G. K. (2021). Eradication of Fatal Textile Industrial Dyes by Wastewater Treatment.

Viswanathan, B. (2017). Photocatalytic Degradation of Dyes: An Overview. *Current Catalysis*, *7*(2), 99–121. https://doi.org/10.2174/2211544707666171219161846

Voutetaki Alexia, Gkouletsos Dimitrios, Papadopoulos Athanasios I., Seferlis Panos, Plakas Konstantinos, Bollas Dimitrios, & Parcharidis Symeon. (2020). Efficient Modeling of Electrodialysis Process for Waste Water Treatment through Systematic Parameter Estimation. *Chemical Engineering Transactions*, *81*, 841–846. https://doi.org/10.3303/CET2081141

Warade, A. R., Gaikwad, R. W., Sapkal, R. S., & Sapkal, V. S. (2016). Study of removal techniques for dyes by adsorption : Areview. *Www.Ijariie.Com*, *2*(3), 2687–3869.

Weldegebrieal, G. K. (2020). Synthesis method , antibacterial and photocatalytic activity of ZnO nanoparticles for azo dyes in wastewater treatment: A review. *Inorganic Chemistry Communications*, *120*(July), 108140. https://doi.org/10.1016/j.inoche.2020.108140

Yashni, G., Willy, K. B., Al-Gheethi, A. A., Mohamed, R. M. S. R., Mohd Salleh, S. N. A., & Amir Hashim, M. K. (2020). A Review on Green Synthesis of ZnO Nanoparticles Using Coriandrum Sativum Leaf Extract for Degrading Dyes in Textile Wastewater: A Prospect Towards Green Chemistry. *IOP Conference Series: Materials Science and Engineering*, *736*(4). https://doi.org/10.1088/1757-899X/736/4/042003

Yuzer, B., & Selcuk, H. (2021). Recovery of Biologically Treated Textile Wastewater by Ozonation and Subsequent Bipolar Membrane Electrodialysis Process. *Membranes*, *11*(11), 900. https://doi.org/10.3390/membranes11110900

Zaidi, R., Khan, S. U., Azam, A., & Farooqi, I. H. (2021). A study on effective adsorption of lead from an aqueous solution using Copper Oxide nanoparticles. *IOP Conference Series: Materials Science and Engineering*, *1058*(1), 012074. https://doi.org/10.1088/1757-899X/1058/1/012074

Zare, E. N., Motahari, A., & Sillanpää, M. (2018). Nanoadsorbents based on conducting polymer nanocomposites with main focus on polyaniline and its derivatives for removal of heavy metal ions/dyes: A review. *Environmental Research*, *162*, 173–195. https://doi.org/10.1016/j.envres.2017.12.025

Zekić, E., Vuković, Ž., Halkijević, I., Zelić, E., Hidrokon doo, M., & Ivan Halkijević, A. (2018). Application of nanotechnology in wastewater treatment Authors: Subject review. *Nano-Adsorbens*, *4*, 315–323.

Zhong, Y. H., Liang, X. L., Zhu, J. X., He, H. P., & Yuan, P. (2010). Adsorption of methylene blue onto vanadium-doped magnetite. *Huanjing Kexue/Environmental Science*, *31*(6), 1568–1574.

Zirehpour, A., & Rahimpour, A. (2016). Membranes for Wastewater Treatment. In *Nanostructured Polymer Membranes* (Vol. 2, Issue September). https://doi.org/10.1002/9781118831823.

APPENDIXES

Appendix A: Result of from Design Expert software and experimental value

Table 7.1: Experimental results for the removal of MBD

Std	Run	Factor 1 A:ZnO-TSA NPS dosage (g/L)	Factor 2 B:Contact time (min)	Factor 3 C:Initial conc.MBD (mg/L)	Factor 4 D:pH	Absorbance	Ce (mg/L)	Response 1 Removal (%)
7	1	0.3	60	50	8	0.013	0.979	98.042
17	2	0.3	60	50	14	0.226	17.218	65.565
5	3	0.3	60	50	8	0.007	0.538	98.923
21	4	0.4	40	70	11	0.138	10.532	84.955
8	5	0.2	40	70	11	0.134	10.200	85.428
18	6	0.4	80	30	5	0.035	2.704	90.987
13	7	0.4	40	30	11	0.069	5.233	82.556
28	8	0.4	40	70	5	0.090	6.850	90.215
10	9	0.2	80	70	11	0.071	5.401	92.285
2	10	0.3	60	90	8	0.017	1.274	98.585
30	11	0.3	60	50	2	0.147	11.189	77.622
29	12	0.4	80	70	11	0.091	6.920	90.115
14	13	0.2	40	30	11	0.054	4.113	86.289
1	14	0.3	60	50	8	0.007	0.539	98.921
25	15	0.3	100	50	8	0.011	0.839	98.321
15	16	0.1	60	50	8	0.032	2.419	95.162
12	17	0.4	40	30	5	0.028	2.167	92.778
26	18	0.3	60	50	8	0.008	0.638	98.724
27	19	0.2	40	30	5	0.012	0.923	96.922
16	20	0.3	60	10	8	0.002	0.144	98.557
11	21	0.3	60	50	8	0.007	0.527	98.946

20	22	0.3	60	50	8	0.011	0.859	98.281
3	23	0.2	80	30	11	0.047	3.567	88.111
23	24	0.3	20	50	8	0.038	2.910	94.181
9	25	0.5	60	50	8	0.063	4.818	90.364
22	26	0.2	40	70	5	0.066	5.000	92.857
24	27	0.4	80	30	11	0.065	4.967	83.444
19	28	0.4	80	70	5	0.074	5.643	91.938
6	29	0.2	80	70	5	0.054	4.113	94.124
4	30	0.2	80	30	5	0.026	2.000	93.333

Appendix B: Values of MBD removal studies

Table 7.2: predicted value Vs actual value of Methylene blue dye removal Efficiency

Std	Run	Factor 1	Factor 2	Factor 3	Factor 4	Removal (%)	
		A:ZnO-TSA NPS dosage g/L	B:Contact time Min	C:Initial conc.MBD mg/L	D:pH	Actual Value	Predicted Value
7	1	0.3	60	50	8	98.042	98.64
17	2	0.3	60	50	14	65.565	65.40
5	3	0.3	60	50	8	98.923	98.64
21	4	0.4	40	70	11	84.955	84.23
8	5	0.2	40	70	11	85.428	85.88
18	6	0.4	80	30	5	90.987	90.48
13	7	0.4	40	30	11	82.556	82.72
28	8	0.4	40	70	5	90.215	90.35
10	9	0.2	80	70	11	92.285	91.99
2	10	0.3	60	90	8	98.585	99.18
30	11	0.3	60	50	2	77.622	77.75
29	12	0.4	80	70	11	90.115	90.25
14	13	0.2	40	30	11	86.289	86.23

1	14	0.3	60	50	8	98.921	98.64
25	15	0.3	100	50	8	98.321	97.95
15	16	0.1	60	50	8	95.162	95.41
12	17	0.4	40	30	5	92.778	93.16
26	18	0.3	60	50	8	98.724	98.64
27	19	0.2	40	30	5	96.922	96.73
16	20	0.3	60	10	8	98.557	97.93
11	21	0.3	60	50	8	98.946	98.64
20	22	0.3	60	50	8	98.281	98.64
3	23	0.2	80	30	11	88.111	87.92
23	24	0.3	20	50	8	94.181	94.52
9	25	0.5	60	50	8	90.364	90.08
22	26	0.2	40	70	5	92.857	92.07
24	27	0.4	80	30	11	83.444	84.32
19	28	0.4	80	70	5	91.938	92.09
6	29	0.2	80	70	5	94.124	93.90
4	30	0.2	80	30	5	93.333	94.15

Table 7.3: Calibration curve data

Number	Conc. of MBD std (x)	Absorbance (y)	Ce
1	0	0	0.000
2	10	0.08	1.246
3	30	0.22	3.427
4	50	0.34	5.296
5	70	0.47	7.321

6	90	0.58	9.034
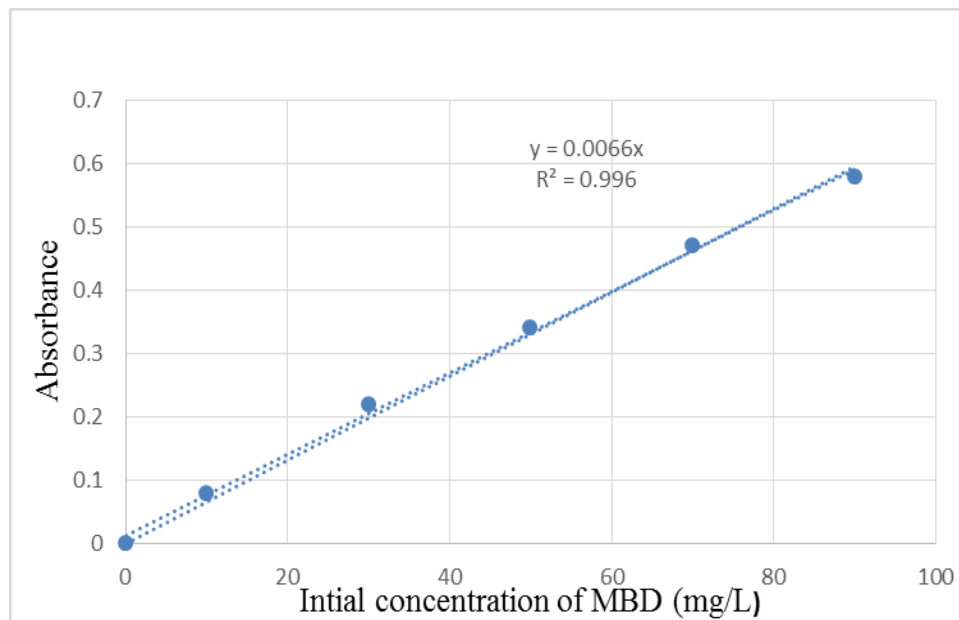
Figure 7.1: Concentration vs absorbance calibration curve

Table 7.4: Effect of pH on MBD removal

pH	Test 1 A1	Test 2 A2	Test 3 A3	Av. Absorbance (A)	Ce (mg/L)	Adsorption capacity (qe) (mg/g)	Efficiency (%)
2	0.156	0.154	0.158	0.156	8.95	7.76	77.622
5	0.070	0.071	0.069	0.70	5.77	8.55	85.565
8	0.026	0.028	0.027	0.027	2.35	9.41	94.124
11	0.071	0.072	0.076	0.073	2.42	9.39	93.946
14	0.087	0.086	0.090	0.088	3.086	9.23	92. 285

Constant parameters used Zno-TSA dose = 0.4 g, Initial concentration = 40 mg/L, Contact time
= 40 min

Table 7.5: Effect of ZnO-TSA adsorbent dosage on MBD removal

Adsorbent dosage (g/l)	Test 1 A1	Test 2 A2	Test 3 A3	Av. Absorbance (A)	Ce (mg/L)	Adsorption capacity (qe) (mg/g)	Efficiency (%)
0.1	10.103	10.095	10.117	10.105	2.73	9.32	93.162
0.2	9.080	9.07	9.12	9.090	1.63	9.59	95.922
0.3	1.426	1.438	1.447	1.437	1.13	9.72	97.164
0.4	0.786	0.783	0.785	0.785	1.17	9.70	97.063
0.5	0.780	0.779	0.784	0.781	1.16	9.71	97.078

Constant parameters used: pH = 8, Initial concentration = 40 mg/L, Contact time = 40 min

Table 7.6: Effect of contact time on MBD removal

Contact time (min)	Test 1 A1	Test 2 A2	Test 3 A3	Av. Absorbance (A)	Ce (mg/L)	Adsorption capacity (qe) (mg/g)	Efficiency (%)
20	10.104	10.086	10.105	10.105	2.33	9.42	94.181
40	0.061	0.060	0.065	0.062	1.91	9.52	95.222
60	0.048	0.042	0.046	0.050	0.87	9.78	97.821
80	0.041	0.042	0.046	0.043	0.894	9.76	97.764
100	0.027	0.027	0.031	0.028	0.890	9.77	97.774

Constant parameters used: pH = 8, Initial concentration = 40 mg/L, Zno-TSA dose = 0.4 g

Table 7.7: Effect of initial concentration on MBD removal

Initial concentration (Mg/l)	Test 1 A1	Test 2 A2	Test 3 A3	Av. Absorbance (A)	Ce (mg/L)	Adsorption capacity (qe) (mg/g)	Efficiency (%)
10	0.098	0.096	0.103	0.099	0.18	9.95	99.54
30	0.025	0.023	0.03	0.026	0.22	9.94	99.45
50	0.030	0.032	0,037	0.033	1.52	9.96	99.62
70	0.076	0.077	0.081	0.078	5.54	8.61	86.15
90	0.017	0.018	0.022	0.019	7.28	8.18	81.79

Constant parameters used: pH = 8, Zno-TSA dose = 0.2 g, Contact time = 40 min

Appendix C: Results of Adsorption isotherm study

Table 7.8: Data for adsorption isotherm studies

No	Co	Absorbance	Ce	1/Ce	LogCe	lnCe	Qe	1/qe	Logqe	ce/qe	lnqe
1	10	0.08	1.2461	0.8025	0.0956	0.2200	2.9180	0.3427	0.4651	0.4270	1.0709
2	30	0.22	3.4268	0.2918	0.5349	1.2316	8.8577	0.1129	0.9473	0.3869	2.1813
3	50	0.34	5.2960	0.1888	0.7239	1.6669	14.9013	0.0671	1.1732	0.3554	2.7015
4	70	0.47	7.3209	0.1366	0.8646	1.9907	20.8930	0.0479	1.3200	0.3504	3.0394
5	90	0.58	9.0343	0.1107	0.9559	2.2010	26.9886	0.0371	1.4312	0.3347	3.2954

Constant parameters used: pH=6.904, ZnO-TSA NPs dose=0.265 g , and Contact time =77.873 min

Table 7.9: Average size calculation from XRD data analysis of produced ZnO-TSA nanoparticles

Peak Pos.2theta (^{0})	Miller indexes			FWHM in 2theta	Crystalline size(nm)	Av.crystalline size (nm)
	H	K	L			
28.87	2	3	3	0.15	24.320	
31.25	3	6	1	0.16	28.902	
32.03	1	0	0	0.19	29.875	
32.90	1	4	2	0.17	26.352	
34.68	0	0	2	0.21	36.875	
36.507	1	0	1	0.29	28.312	
42.95	0	2	0	0.16	25.345	
47.79	0	1	2	0.23	29.493	
50.93	1	0	2	0.14	24.632	
56.86	1	1	0	0.26	25.697	27.196
61.07	0	1	3	0.53	26.013	
63.14	1	0	3	0.28	28.032	
66.66	2	0	0	0.26	29.632	
68.24	1	1	2	0.32	24.127	
69.38	2	0	1	0.30	25.094	

| 72.82 | 0 | 0 | 4 | 0.14 | 26.092 |
| 77.23 | 2 | 0 | 2 | 0.09 | 23.546 |

Table 7.10: Average size calculation from XRD data analysis of produced ZnO nanoparticles

Peak Pos.2theta (^{0})	Miller indexes			FWHM in 2theta	Crystalline size(nm)	Av.crystalline size (nm)
	H	K	L			
32.09	1	0	0	0.19	29.875	
34.68	0	0	2	0.21	36.875	
36.507	1	0	1	0.29	28.312	
50.93	1	0	2	0.14	24.632	
56.86	1	1	0	0.26	25.697	24.619 nm
63.14	1	0	3	0.28	28.032	
66.66	2	0	0	0.26	29.632	
68.24	1	1	2	0.32	24.127	
69.38	2	0	1	0.30	25.094	
77.23	2	0	2	0.09	23.546	

Appendix D: Functional groups wave numbers range and point of zero charge

Table 7.11: Range in wavenumber (cm^{-1}) of various functional groups (Khan et al., 2018).

Range (cm^{-1})	Functional group
3200–3550	O-H stretching
2500–3000	Carboxylic O-H
3300–3500	N-H stretch, primary amine gives two, a secondary one, while tertiary amine gives no peak
3500–3500	O=C-N-H stretch
2260–2220	Nitrile (CN)
2950–2850	C-H stretch
3010–3100	=C-H stretch
1620–1680	C=C stretch
1740–1690	Aldehyde C= O
1750–1680	Ketone C = O
1750–1735	Ester C = O
1780–1710	Carboxylic acid C=O
1690–1630	Amide C=O
2800–2700	Aldehyde C-H stretch

Table 7.12: FT-IR spectrum of ZnO-TSA NPs

Groups	Stretching and bending	Peaks
O-H	O-H stretching and phenols	3546 and 3581
N-H	N-H stretch	3363- 3241
C-H	C-H asymmetric stretch	2820

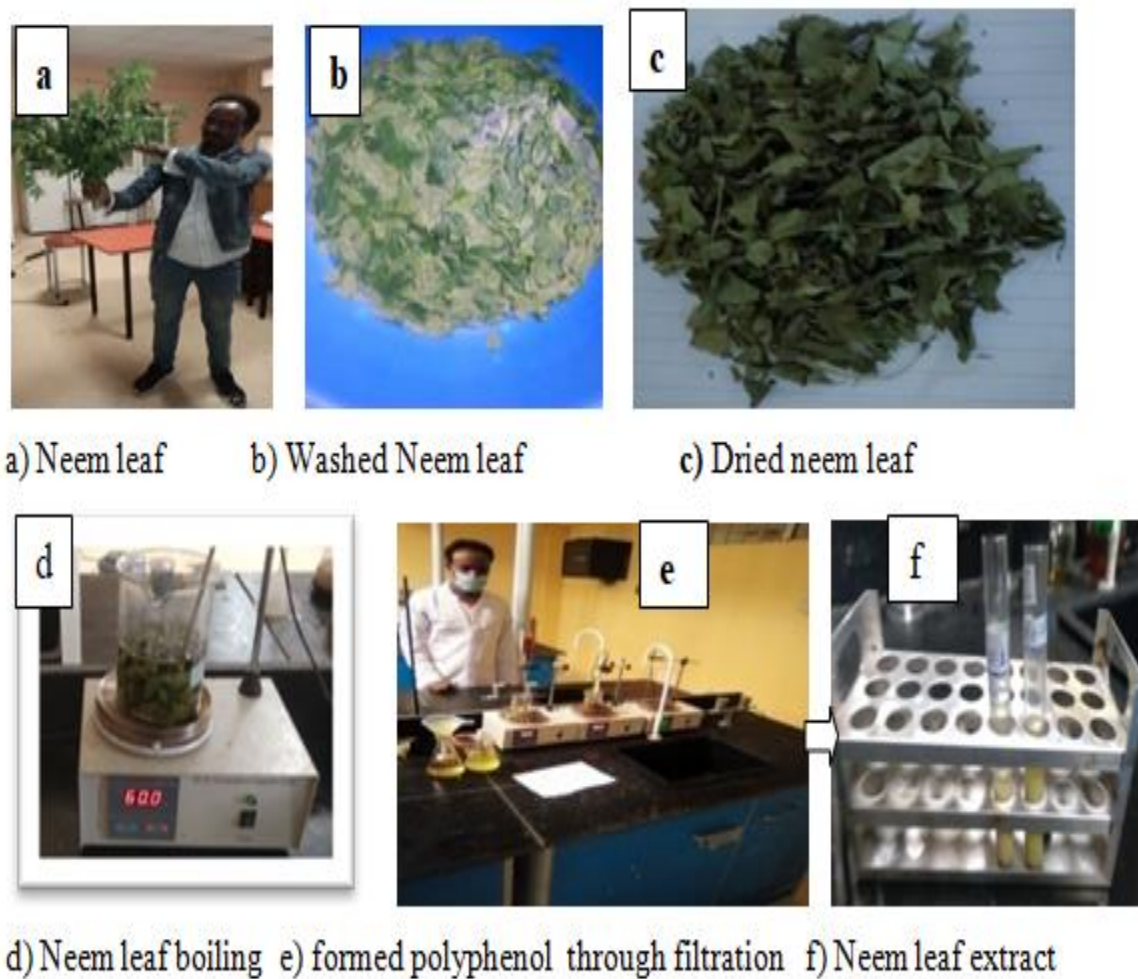| C=O | Amide C=O | 1639 |
C=C	Aromatic C=C stretching of lignin	1591
C-O	C-O Strech	1380
C-H ,O-H, C=O, and C-O	Presence of Zn-O,bending	559 cm^{-1} and 613 cm^{-1}
C-O and C-C	C-O and C-C bending vibrations	1089 and 1095

Table 7.13: Point of zero charge

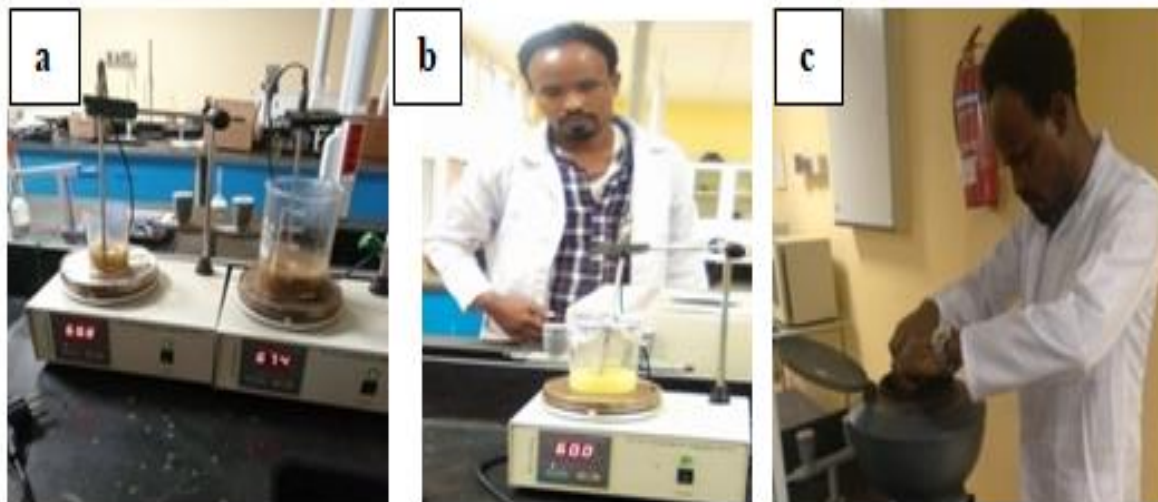| pH$_i$	2	3	4	5	6	7	8	9	10
pH$_f$	1.56	2.62	3.76	5.62	7.73	8.85	9.94	10.85	11.97
ΔpH	0.44	0.38	0.25	-0.62	-1.73	-1.85	-1.94	-1.85	-1.97

Appendix E: Some listed pictures of laboratory work
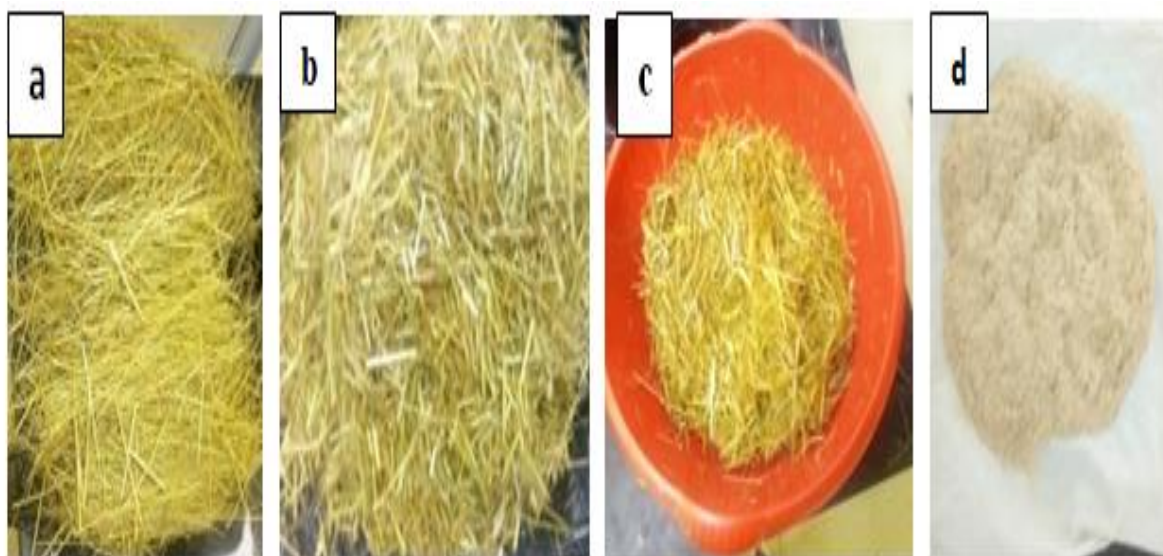
a) Collected Teff straw b) Cut and air dried Teff straw c) Washed Teff straw d) TSP

Figure 7.2: Collection and Porous powedered teff straw preparation

a) Neem leaf   b) Washed Neem leaf   c) Dried neem leaf

d) Neem leaf boiling e) formed polyphenol through filtration f) Neem leaf extract

Figure 7.3: Polyphenol preparation

a) ZnO-TSA synthesis b) precipitated ZnO-TSA   c) Centerifugation
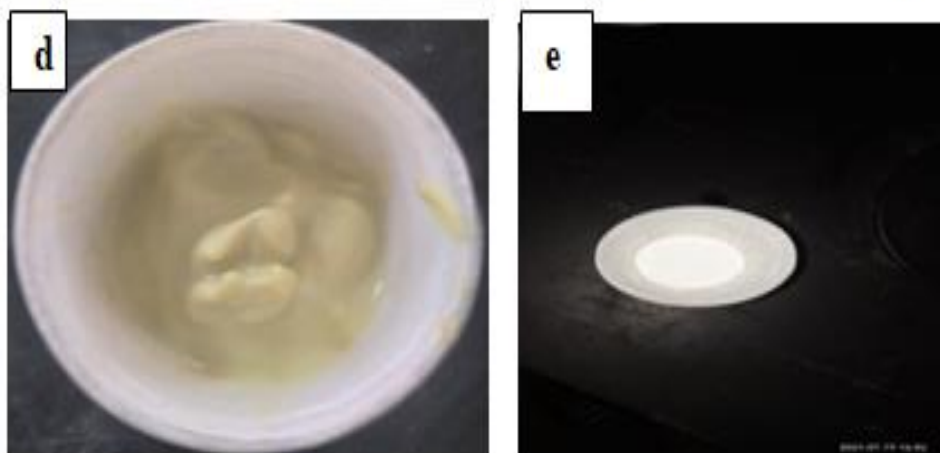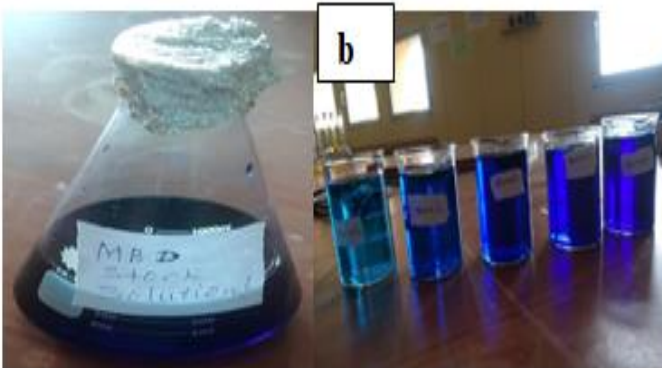
d) Formed paste of ZnO-TSA   e) ZnO-TSA NPs

Figure 7.4: Synthesis of ZnO Nps and ZnO-TSA NPs

a) Uv-visible spectroscopy test for neem leaf extract   b) Prepared MBD stock solution

pH test for MBD

MBD before adsorption

Adsorbent- adsorbate contact

Setup for adsorption Experiments

Vacuum filtration | Supernatant left | Residue left

uv-absorbance test of MBD

Textile waste water

Stock solutions preparations for TWW testing

Chloride testing

TDS determination

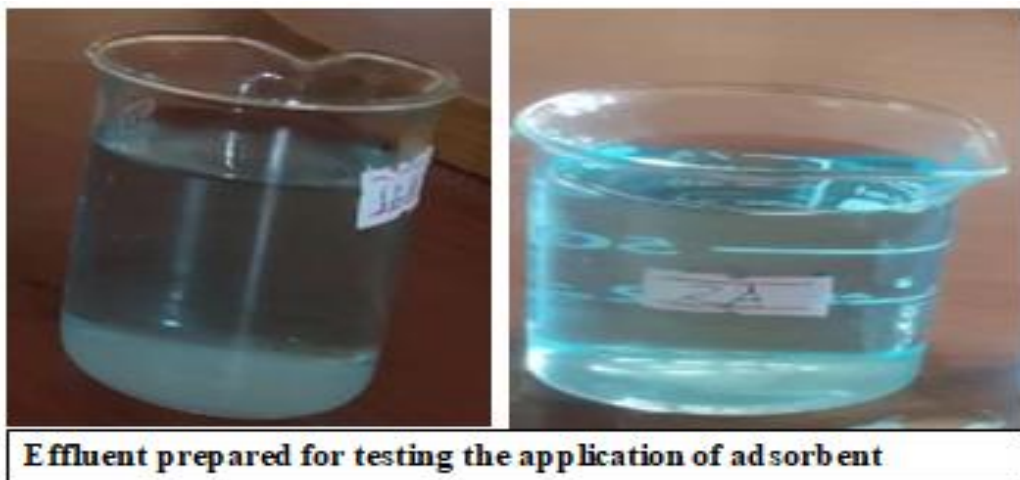COD determination

pH determination of TWW

Turbidity determination

TS determination

Figure 7.5: Image throughout lab work